ISSN 1173-5996

SMOKE EXPLOSIONS

BY

B J Sutherland

Supervised by

Dr Charley Fleischmann

Fire Engineering Research Report 99/15
March 1999

This report was presented as a project report
as part of the M.E. (Fire) degree at the University of Canterbury

School of Engineering
University of Canterbury
Private Bag 4800
Christchurch, New Zealand

Phone 643 364-2250
Fax 643 364-2758

Abstract

Eleven experiments were conducted at the University of Canterbury using a 1.0 metre by 1.0 metre by 1.5 metre compartment and wooden crib fires. The main objective of these experiments was to produce smoke explosions, and to develop a mechanism that explains their occurrence.

Spontaneous smoke explosions were produced in four experiments. The largest of these explosions produced pressures in excess of 2.5 kPa. All the smoke explosions produced were the result of smouldering fires, all of which started out as under-ventilated fires. Of the six smoke explosions produced, investigation of the results indicates that a single process was responsible for the occurrence of each explosion.

A mechanism was developed for the smoke explosions. Oxygen concentration is suspected as the trigger that determines when the explosion occurs.

Acknowledgments

I would like to thank the following people for there assistance in this project.

I would first like to thank my supervisor, Dr Charley Fleischmann without his encouragement and guidance this project would not have been as successful as it was.

Frank Greenslade whose assistance in the laboratory was invaluable.

Trevor Berry who taught me the finer points of gas chromatography.

Grant Dunlop for the fantastic wielding job on the compartment.

Angus Bain, Jackie Van Asch and John Cuthbert for their much appreciated assistance in the final stages of this report.

I would also like to acknowledge the New Zealand Fire Service Commission for their financial support of the fire engineering program. Without their support the fire engineering program and this research would not have been possible.

Contents

List of Figures

List of Tables

Chapter 1.0 Introduction

On the eighth of November 1974 an explosion from a warehouse fire at the Chatham Dockyards claimed the lives of two fire fighters and injured four others. The incident was unusual because the conditions prior to the explosion gave no indication of what was to follow. When the Kent Fire Brigade arrived at the scene they found that the fire was contained to two storerooms on the ground floor of a three-story building. The main store where smoke had been seen emerging from a window contained 178 foam mattresses and cleaning equipment. The second store was empty. A thorough search of the fire-area failed to find any flames, but it was found that cool, dense smoke had formed a layer half-a-metre deep above the floor. After the search that was initiated to investigate the source of the fire had concluded, doors and windows were opened to ventilate the smoke. It was at this point that an explosion occurred, large enough to shatter windows in the building, yet not large enough to cause structural damage (Woolley and Ames, 1975).

The Chatham Dockyards incident is thought to be an example of what is termed a 'smoke explosion', and although not widely documented there have been other similar incidents (Croft, 1980; Russel, 1983). The major concern with this phenomenon is that the explosions are never anticipated, ironically the initial fires are generally thought to be safe.

Smoke explosions generally occur as a result of incomplete combustion. Incomplete combustion provides the energy source; primarily, partially oxidized combustion products. An explosion occurs when enough flammable material and oxygen accumulates in the presence of an ignition source.

The aim of this research is to investigate smoke explosions with the intention of developing a mechanism that can explain their occurrence. Under examination also is the question of whether the explosions are the result of a single gaseous component, or a number of components (for example, methane as opposed to a mixture of hydrocarbons). Lastly, it is hoped that a better understanding of the phenomenon shall yield criteria that may be utilized to predict the occurrence of smoke explosions.

One of the first hurdles of this research topic is that very few answers can be found from analysing previous smoke explosions, this is due to several factors:

- Most of what is documented on actual smoke explosions has been gathered from eyewitness accounts of fire fighters and onlookers, the majority of whom have a very limited education in fire science.
- Furthermore, documented smoke explosions are usually only noted after the injury of a fire fighter. This creates a further problem in that documented cases might be bound to certain types of fires, typically those fires that a fire fighter would enter. This possible misjudgment is evident in an article by Croft (1980), when he refers to smoke explosions as "... a phenomenon normally, but not exclusively associated with smouldering fires..."

This report is based primarily on experimental research of smoke explosions. Experiments were conducted in a fireproof compartment measuring approximately one metre in width, 0.95 metres in height, and 1.48 metres in depth (refer to Figure 3.1). It is anticipated that through the combustion of wooden cribs in under-ventilated conditions it will be possible to produce smoke explosions.

Chapter 2.0 Background

The purpose of this chapter is to provide the reader with a very basic understanding of incomplete combustion, and how it can lead to a smoke explosion.

2.1 Requirements for a smoke explosion

There are three basic requirements that must be met before a smoke explosion can occur; they are:

1. A contained smoke layer that consists of enough unburned pyrolyzates that places the mixture within its limits of flammability. For example, the flammability limits for carbon monoxide are 12.5% and 74%, for methane the range is between 5% and 15%, (SFPE, 1995, 3-16).
2. To ignite the flammable mixture an ignition source is needed; there is a minimum amount of energy that will ignite the layer.
3. The last requirement is enough oxygen to support combustion.

2.2 Combustion Chemistry

Combustion may be explained simply as a series of oxidation reduction reactions. During the process fuel molecules are oxidised and oxygen molecules are reduced. However even the simplest of combustion processes can involve more than one hundred individual reactions. Analysis of a combustion process is complicated even further by the formation of radical intermediates, whose existence may be as short as a few microseconds (Solomons, 1992). This is compounded further because many of the important reactions in the combustion process occur via a radical mechanism.

The combustion process can be broken down into three significant steps with many different reactions occurring during each step.

1. For combustion to occur a fuel molecule must be present as a gas. Pyrolysis is the process of chemical decomposition where fuel molecules are vaporized; usually the heat source is feedback from the combustion zone.
2. The second step involves the oxidation of the fuel to carbon monoxide, accompanied by the production of water.
3. The last step in the combustion process is the oxidation of the carbon monoxide to carbon dioxide, accompanied by the production of more water.

In an under-ventilated compartment fire, many of the reactions in steps 2 and 3 may occur in the upper layer. An upper layer is a layer of hot gases or smoke confined by a physical boundary, usually a ceiling.

In most combustion situations, the growth of a fire is controlled largely by only two variables, the concentration of the reactants and the temperature. In the following reaction

$$aA + bB \longrightarrow cC + dD \tag{2.1}$$

the conversion of reactants a and b to products c and d is given by the expression;

$$K = \frac{[C]^c [D]^d}{[A]^a [B]^b} \tag{2.2}$$

where K is the equilibrium constant, A, B, C and D are the concentrations of a, b, c and d, respectively (Chang, 1998).

Although Equation 2.2 will calculate the conversion of the reactants into products, this is not an instantaneous process, and for some reactions it may occur very slowly. The rate of the reaction can be determined from the expression

$$\text{rate} = k[A]^x [B]^y \tag{2.3}$$

where A and B are the concentrations of a and b, and x and y are numbers that must be determined experimentally. k is the rate constant and is temperature dependent according to Arrhenius equation

$$k = Ae^{\frac{-E_a}{RT}} \qquad (2.4)$$

where A is a constant; R is the universal gas constant, and E_a is the activation energy (Chang, 1998).

2.3 Production of Combustion Intermediates

The following section summarizes the relevant literature that was reviewed concerning the production of combustion intermediates. It is hoped that this information will provide a basis for the production of a smoke explosion, whilst also acting as an invaluable reference for the analysis of a smoke explosion.

2.3.1 Carbon Monoxide

The last decade has seen a considerable amount of research investigating carbon monoxide production from under-ventilated fires. Interest in this area has been fuelled largely because carbon monoxide asphyxiation is one of the primary causes of death in residential fires in the United States (Pitts, 1997). Carbon monoxide (CO) production is examined thoroughly in this report due to speculation that smoke explosions might actually be carbon monoxide explosions, or at least one of the dominant gas species before an explosion. It also occurs that the types of fires that produce carbon monoxide are likely to be similar to those that would produce other combustion intermediates, such as hydrocarbons.

One of the theories common in the literature is that high concentrations of carbon monoxide are obtained when the upper layer reactions of CO to CO_2 are slowed or frozen. Gottuk (1992) reports that this reaction is essentially frozen at layer temperatures below 875 K. In a latter study Gottuk and Roby (1995) concluded that the transition from a very slow reaction to

a very fast reaction occurs over the temperature range of 800 K to 900 K. Therefore, large amounts of carbon monoxide could be produced when the plume is short and there is a cool upper layer to quench the plume reactions. Thereby freezing any layer reactions that would occur at higher temperatures.

A possible connection between the global equivalence ratio and carbon monoxide production is a theory that is commonly referred to in the literature. The global equivalence ratio, ϕ is defined in this study as the ratio of the fuel volatilization rate to the air entrainment rate into the plume, normalized by the stoichiometric fuel-to-air ratio (mass basis) (Gottuk, 1995). Other definitions exist where the air entrainment rate is of the layer and not the plume (Gottuk, 1992). Basically at a ϕ of less than one there is an excess of fuel over air; this is reversed for a ϕ greater than one. Many authors have attempted to use empirical correlations between CO and ϕ as a means for predicting CO concentrations in under-ventilated conditions. However as Pitts (1997) mentions there are a number of other mechanisms for CO production that need to be accounted for. Gottuk et al., (1995) reports that CO production increases rapidly after a ϕ of 1 and plateaus at approximately a ϕ of 1.4. This is based upon experiments conducted in a 2.2 m^3 compartment. To explain this Pitts (1994) states that CO is formed in preference to CO_2 at $\phi>1$, because fuel molecules are more reactive than CO with the important free radicals, $\cdot OH$, $\cdot HO_2$, and H atoms. Major CO_2 production can only begin when the majority of fuel molecules have been oxidized to CO.

Another factor that has shown to contribute to the production of CO is the composition of the fuel. Beyler (1984) asserts that, "...under fuel rich conditions the carbon monoxide production ranks according to: oxygenated hydrocarbons > hydrocarbons > aromatics". Although dependent on the conditions, additional CO can be produced when burning an oxygenated fuel in a fuel rich environment because oxygen can be sourced directly from the fuel. Therefore, the system is less reliant on the ventilation.

Although highly dependent on the conditions, increasing the residence time of the upper layer can cause additional CO to be produced. This is dependent on the availability of oxygen in the upper layer and temperature. If there is no available oxygen the layer will effectively be unreactive below 1400 K (Pitts, 1997). If there is O_2 available but the temperature is low,

then CO production will be time dependent, as the process slows considerably at lower temperatures (refer equation 2.3).

A fire known as the 'Sharon Townhouse Fire' in 1987 triggered some interesting research on the direct pyrolysis of fuel in the upper layer and its affect on CO production. Pitts (1997) reports CO levels as high as 14% in the upper layer when he lined a reduced scale enclosure with plywood.

2.3.2 Hydrocarbons

Of the energy released during the combustion process approximately one quarter is released when carbon monoxide is formed, the other three quarters is liberated when carbon dioxide is formed (Chang, 1998). These figures neglect the formation of water during the combustion process, as it is unknown exactly when water is formed. Therefore, freezing the combustion process before the formation of CO is of significance to this study as it could lead to a smoke explosion with a larger energy release. Only a small amount of indirect research was identified that discussed low temperature oxidation of CO, it is summarized below.

> 'The appearance of luminescence as well of "cold flames" in fuel vapour-air mixtures was first discovered by Perkin in hydrocarbons, ethers, fatty acids (also, carbon disulphide) at temperatures of about 200° to 250° upwards' (Jost, 1946).

Jost (1946) defines these phenomena as oxidation processes. Theoretically then, a fire environment at a very low temperature (below 200°C) should be capable of producing an atmosphere of mainly pyrolysis products with the formation of very little CO and CO_2. This is dependent on the efficiency of the fire at the fuel.

2.4 Smouldering Fires

It is a general perception of those in the field that smoke explosions occur from smouldering fires (Croft, 1980; Woolley and Ames, 1975). It is for this reason that it is important to clarify exactly what a smouldering fire is. Dosanjh et al. (1987) defines smouldering as "combustion

without flame". In the average flaming fire, the majority of the combustion occurs in the flame. In a smouldering fire the O_2 has to diffuse to the fuel surface where it is absorbed. At this time combustion occurs at the surface of the fuel, and the products of this combustion then desorb and disperse (Dosanjh et al, 1987)

High concentrations of pyrolyzates and carbon monoxide can be produced from a smouldering fire because:

1. There is no flame, which would usually act as a high temperature reaction zone, oxidising the most of the pyrolyzates. In a smouldering fire, only the surface of the fuel is available for combustion, which may not be able to oxidise the pyrolyzates at the same rate as they are produced.
2. Secondly, because of the lower temperatures the layer and the plume will not be hot to support post-flame oxidation.

2.5 Smoke Explosions

After the explosion that occurred during the fire at the Chatham Dockyards (refer Chapter 1.0) the Fire Research Station, FRS in Borehamwood England investigated the burning behaviour of mattress foam. Their intent was to explain why the explosion occurred (Wooley and Ames, 1975). The main conclusions from the study were:

- The combustion products from a smouldering foam mattress fire are flammable.
- The products of a contained smouldering fire are explosive; a small external flame was used as the ignition source. The experiments were conducted in a 1.4 m^3 explosion chamber and the mattress foam was allowed to smoulder for 32 minutes before the flame was introduced.
- Before the explosion, the smoke was noted as cool, grey and dense. Analysis of the smoke reported an O_2 content of 20%, and a CO concentration of 1000-2000 ppm. The flammable content of filtered smoke was found to be 20% of the lower explosive limit. It was concluded that it was the combination of gases and condensed matter accumulated in the chamber that fueled the explosion.

The FRS concluded that a smouldering mattress was probably responsible for filling the store at the Chatham Dockyards with the cool dense smoke reported by the fire fighters. The layer would have mixed due to the recently opened windows and the movement of the fire fighters. The ignition source is thought to have been the development of the smouldering fire into a flaming fire, possibly a result of the action of the fire fighters.

2.6 Propagation of an Explosion

An explosion is defined in this study as the rapid propagation of a flame front with an accompanying pressure wave (Croft, 1980). Croft (1980) suggests that pressures as high as 5-10 kPa could be produced during a smoke explosion. Pressures this high are large enough to break windows. It is the velocity of the flame front that determines the magnitude of the pressure wave. If the pressure wave is not formed or is negligible, then the phenomenon is known as a flash fire, and not an explosion (Wiekema, 1984).

Wiekema's (1984) study of sixty-eight fire incidents found that the presence of obstacles in a vapour cloud promotes the formation of an explosion and not a flash fire. Wiekema declares that obstacles cause turbulence, and turbulence is known to enhance flame speeds; thus, a pressure wave is generated.

Chapter 3.0 Apparatus

The following list is a list of all the apparatus and instruments used in this research:

- Test compartment.
- MTI Micro Gas Chromatograph.
- Type K thermocouples.
- Pressure transducers (Setra 264 and MKS Instruments 223)
- Mettler Toledo load-cell.
- Servomex and Ultramat analysers for O_2, CO_2, CO.

The following sub-sections provide the specifics on the apparatus listed above.

3.1 The Compartment

3.1.1 Construction

For stability and durability, the original compartment built in 1994 was retrofitted in 1998, keeping only the original 50 x 50 x 5 mm steel angle frame. To the outside of the frame, one layer of 1.25 mm stainless 430 was added, all the seams were wielded together. Stainless 430 was used because it is dimensionally stable up to 700°C. On the internal walls and ceilings two layers of 25 mm thick blanket Kaowool were added, covering this was one layer of 25 mm Kaowool vacuum board (refer Figure 3.2). On the door and the floor two layers of the 25 mm Kaowool vacuum board were attached without the blankets (refer to Figure 3.2). The addition of the insulation reduces the internal dimensions of the compartment to 1.48 x 1.0 x 0.95 m. This is approximately two fifths the size of the standard full scale room proposed by ISO and ASTM for full scale fire tests (Bryner and Johnsson, 1994). Both the vacuum board and the Kaowool blankets were fastened to the frame using 100 mm steel studs and 100 mm screws.

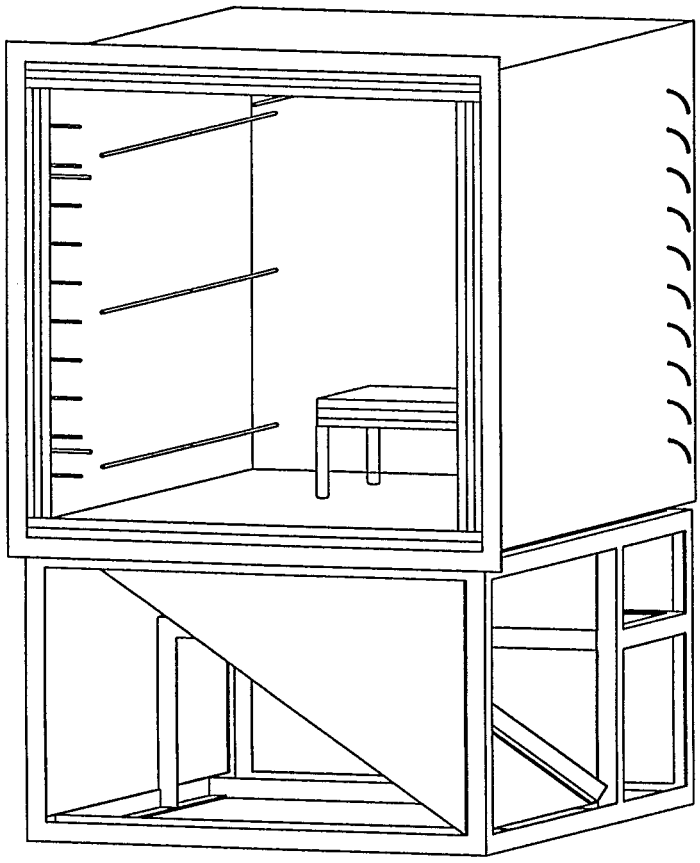

Figure 3.1 – Isometric View of the Compartment

The compartment is elevated approximately 800 mm off the ground by a base constructed of 50 mm angle-steel as used in the compartment frame (refer Figure 3.1). The base sits on wheels, allowing the compartment to be moved. Four leveling feet are attached to the base, allowing the compartment to be leveled.

The compartment has a 1215 mm square door with a horizontal swing. To achieve a tight seal when the compartment door is closed, 30 mm Kaowool rope was glued around the edge of the doorframe. This compresses when the door is closed. RTV Silicon Rubber was used to fasten the rope to the compartment and although it melts at 200°C, only a small portion of the RTV is exposed to the high temperatures. Its strength is regained when cooled. Four clamps, one wielded to each corner of the doorframe, allow the door to be securely shut.

Due to the possibility of an explosion in the compartment, a pressure relief panel is located in the floor of the compartment. In case of a large explosion, the pressure relief panel will open,

allowing the force of the explosion to be directed towards a safe area. The panel is 0.76 m square and is hinged on one edge. It has a spring activated latch on the opposite edge; the latch was calibrated to open the panel when exposed to a gauge pressure of 2 kPa or more.

3.1.2 Ventilation

Historically, ventilation for most compartment fire experiments has been provided using a single rectangular opening to replicate the conditions in a real compartment fire. However, the quality of any results using a single opening for inflow and outflow is compromised. The reasoning being that the air entry rate is not measured directly, but rather estimated from a ventilation factor $Ah^{1/2}$.

Ventilation in the compartment is provided via two circular openings, one for air inflow (lower opening) and the other for the smoke outflow (upper opening). Openings are situated on the centreline of the door, the lower opening is approximately 145 mm from the floor and the upper opening is approximately 190 mm from the ceiling. Both measurements were measured from the centre of the openings.

Table 3.1 – Orifice Plate Sizes

Orifice Plate	**Diameter**	**Area**
	(mm)	**(mm^2)**
No orifice plate	100	7850
1	71	3960
2	50	1960
3	35.8	990
4	25.5	511

Both openings have a diameter of 100 mm; bolting steel orifice plates over the openings reduces this. The orifice plates were constructed out of stainless 430 sheeting. They were designed so the area of each opening is reduced by half from the previous plate (refer Table

3.1). Four 6 mm bolts, one in each corner of the plate are used to secure the plates over the openings.

3.1.3 Gas-Sampling

Gas Chromatograph

Combustion gases are sampled for analysis by the gas chromatograph (GC) from a single location within the upper layer. A sample probe was constructed from ¼ inch 316 stainless tubing with holes every 100 mm; holes were only drilled through a single side of the tube. A hole size of 1.5 mm was selected to avoid blockage by particulate matter. The sample probe runs the length of the compartment; from the back wall to the door, equally spaced from either side wall and at a height of 975 mm from the floor (refer Figures 3.4 and 3.5). The door-end of the sample probe was crimped and wielded, preventing the majority of the sample being drawn through this opening. To avoid unnecessary leakage from the compartment, the hole through which the probe enters the compartment was sealed with high temperature gasket-maker.

Between the compartment and the gas chromatograph the sample line is filtered through a glass tube packed with glass fibres. The tube is 57 mm long with an internal diameter of 32 mm.

Servomex and Ultramat Analysers

Due to the need for continuous sampling, a further three sampling probes were installed in the compartment for use by the Servomex 540 A and Ultramat 6 analysers. One-quarter inch 316 stainless tubing was used to construct the probes with 1.5 mm holes spaced 100 mm apart. To allow sampling from the upper and lower layers the probes run horizontally, at heights of 100, 500 and 900 mm (refer Figure 3.5). All three probes run parallel with left-hand side wall, situated at a distance of 150 mm from the wall (refer Figure 3.4). Each probe is 1300 mm long and positioned to provide a 100 mm gap between the end of a probe and the front and back walls (refer Figure 3.5). The probes were originally constructed from brass tees; these

were replaced with stainless steel tees after the brass buckled during the high temperatures produced in the first few experiments.

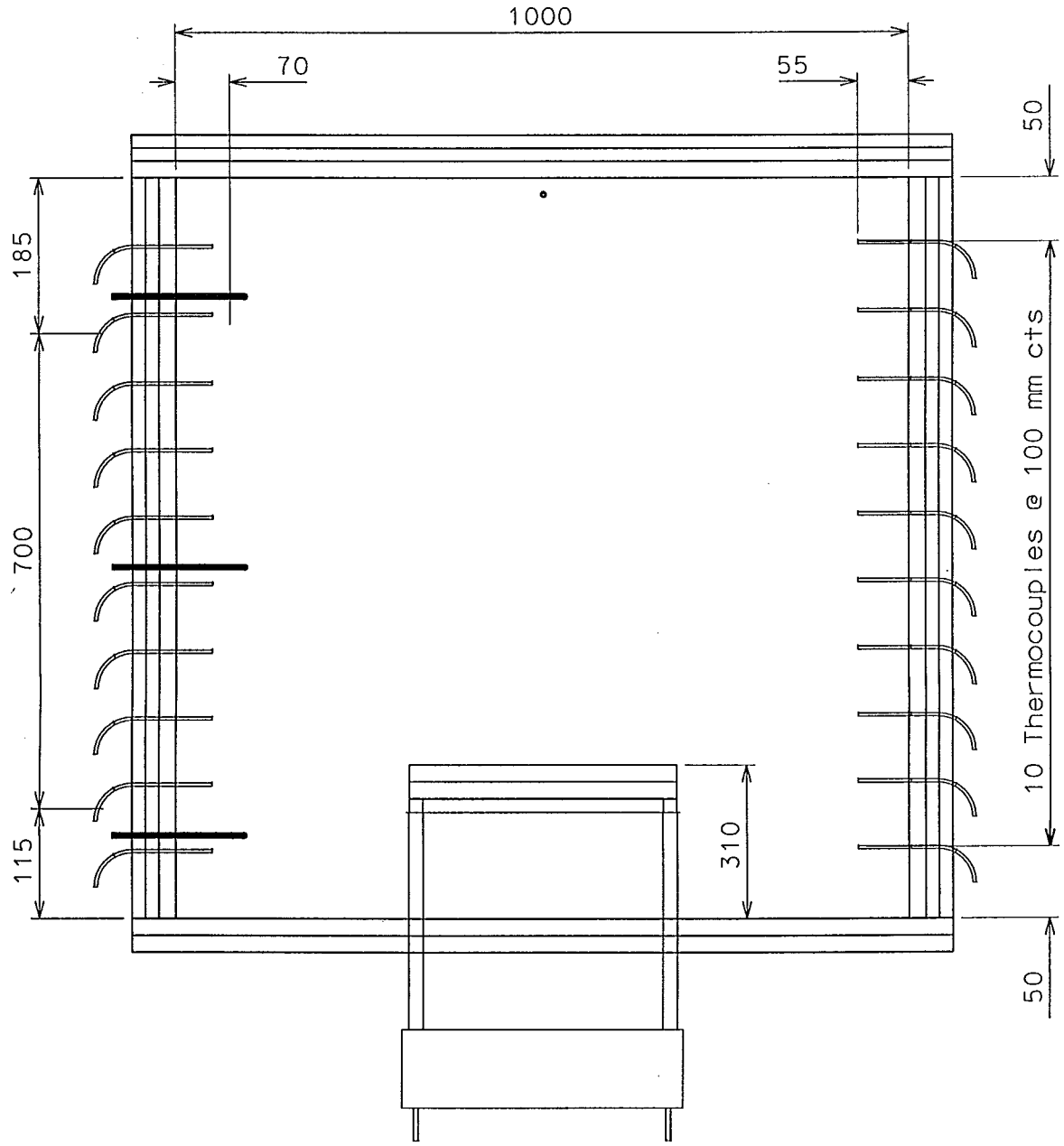

Figure 3.2 – Front Elevation, Dimensions of the Pressure Transducers, Thermocouples, and the Fuel Table Height (mm).

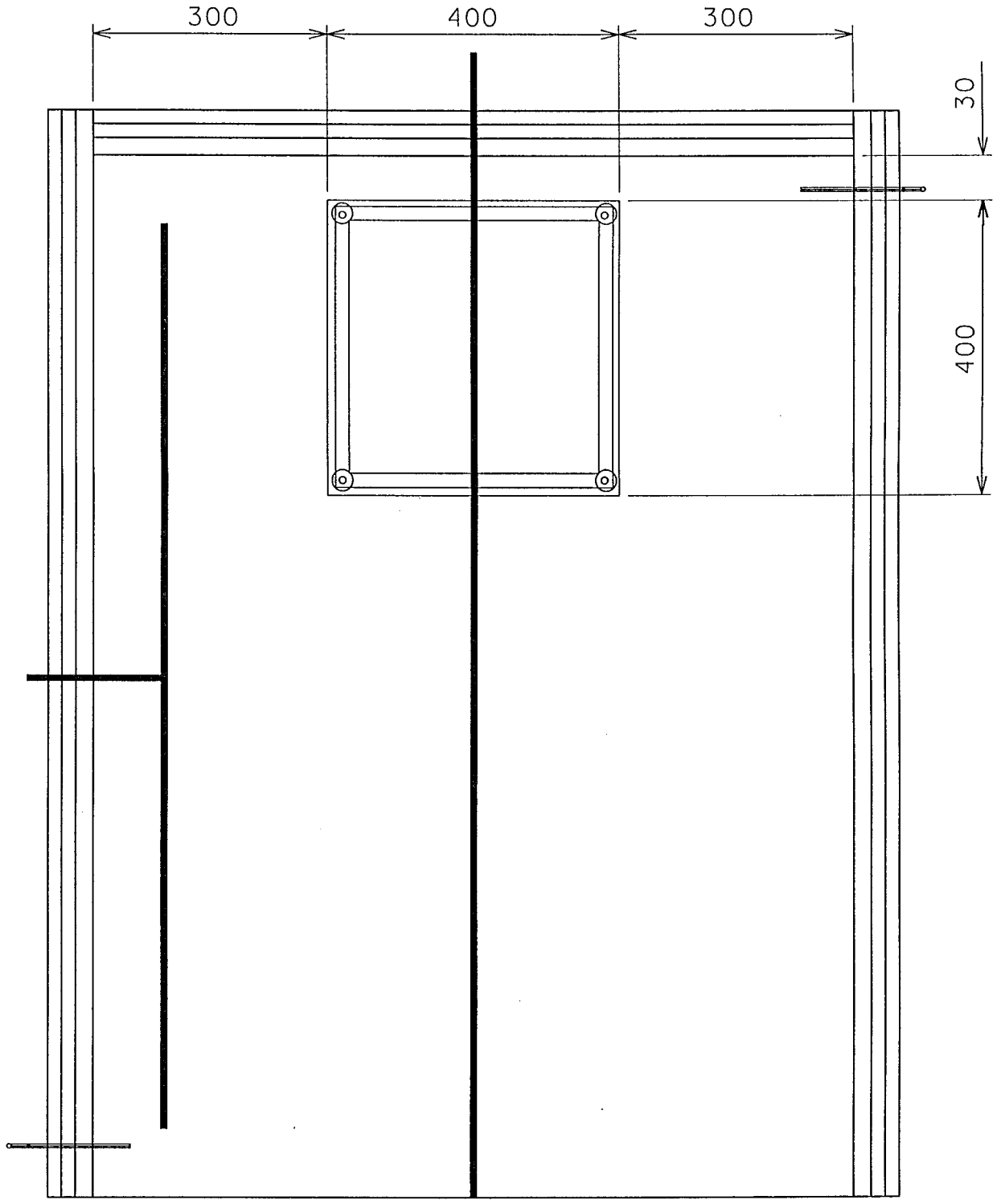

Figure 3.3 – Plan, Dimensions of the Fuel Table (mm).

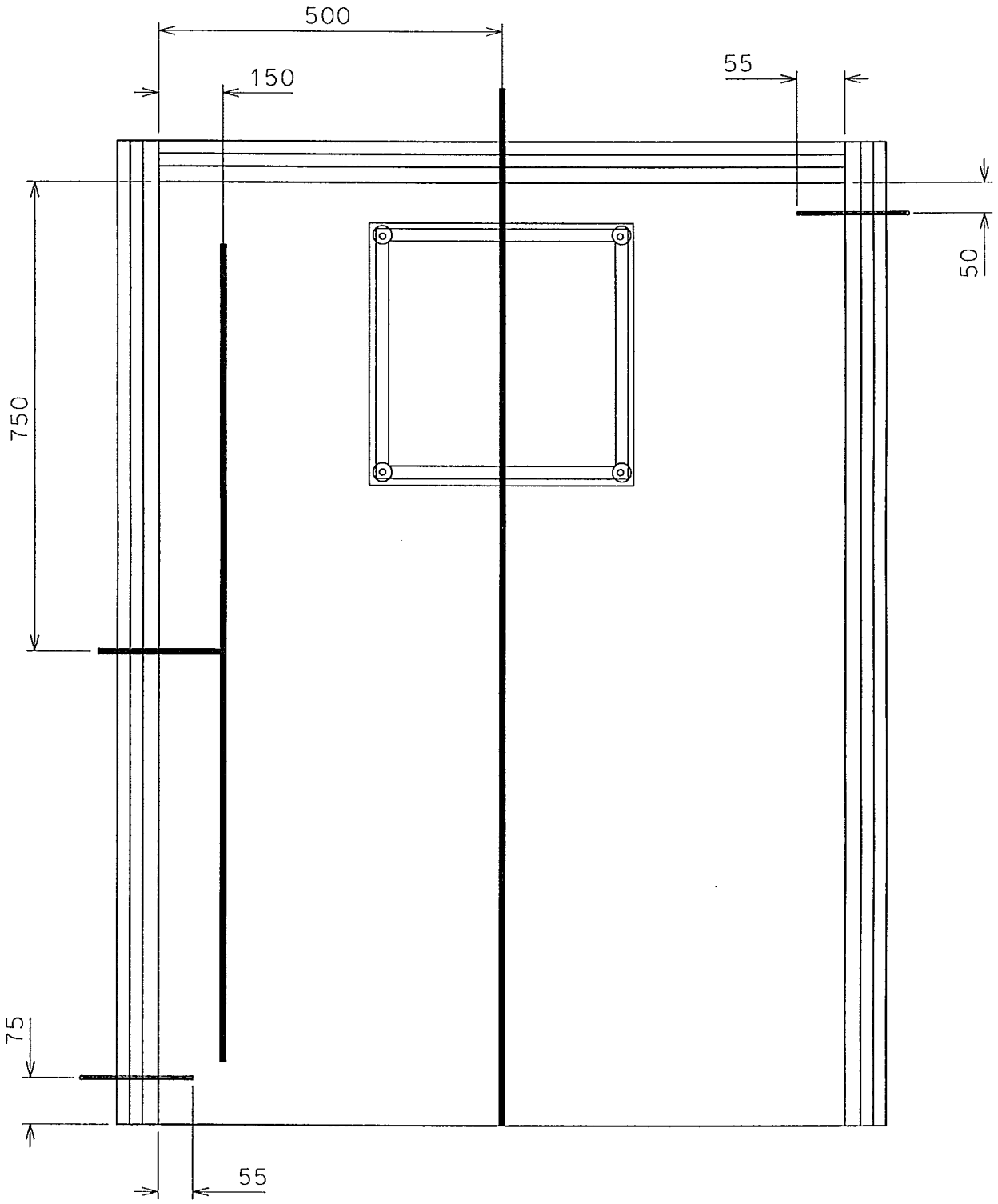

Figure 3.4 - Plan – Dimensions of the Gas Sampling Probes and the Thermocouples (mm).

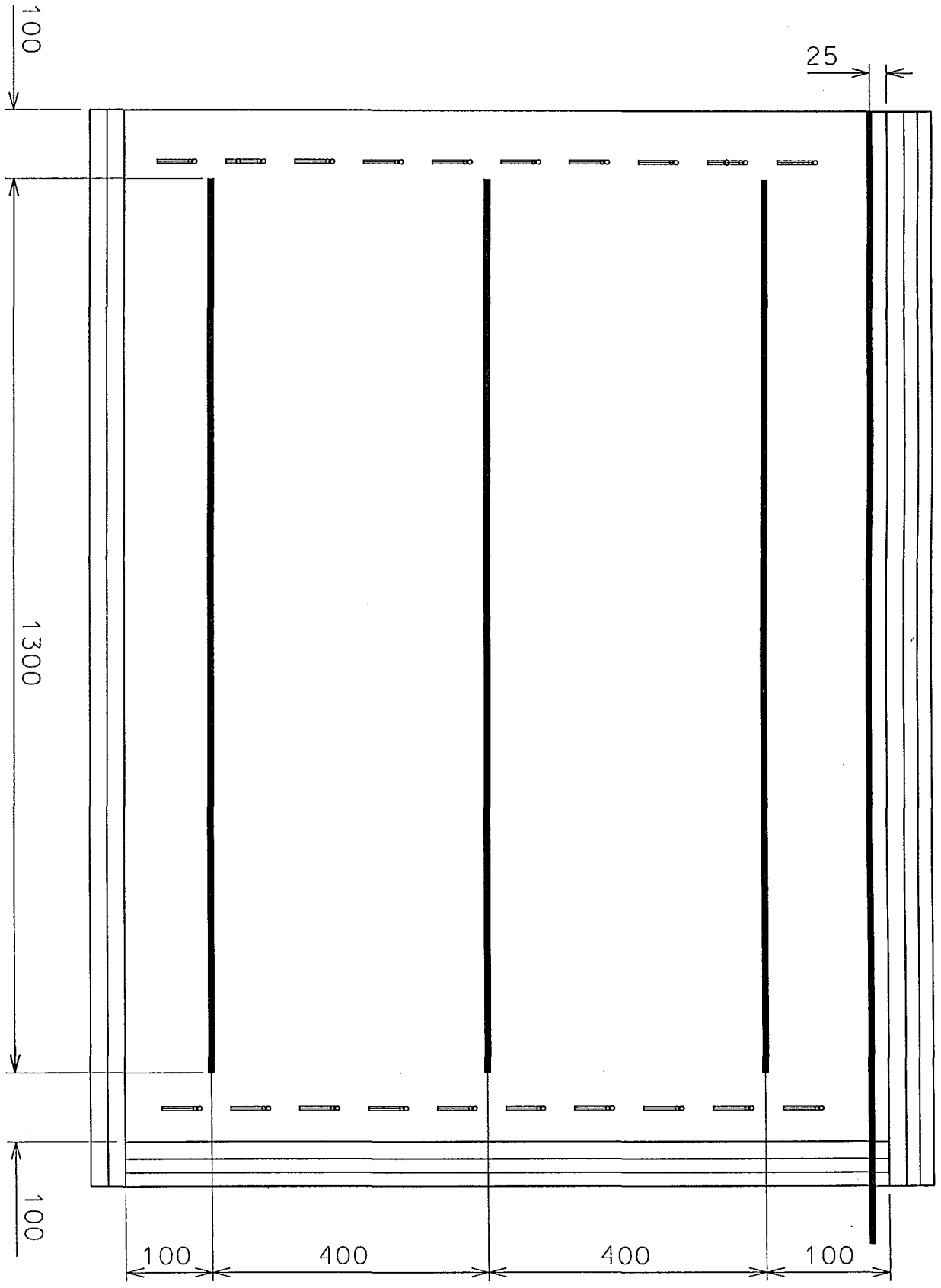

Figure 3.5 – Side Elevation, Dimensions of the Gas Sampling Probes (mm).

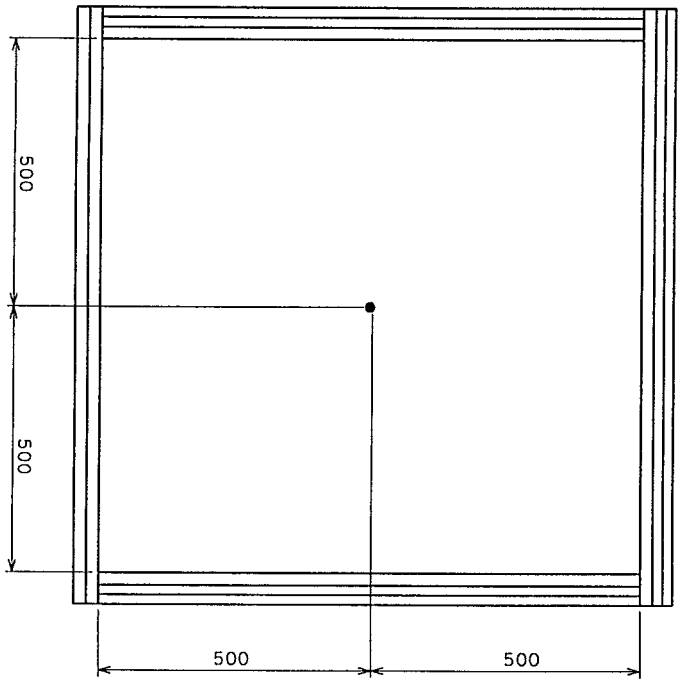

Figure 3.6 – End Elevation, Placement of the Internal Thermocouples in the End Wall (mm).

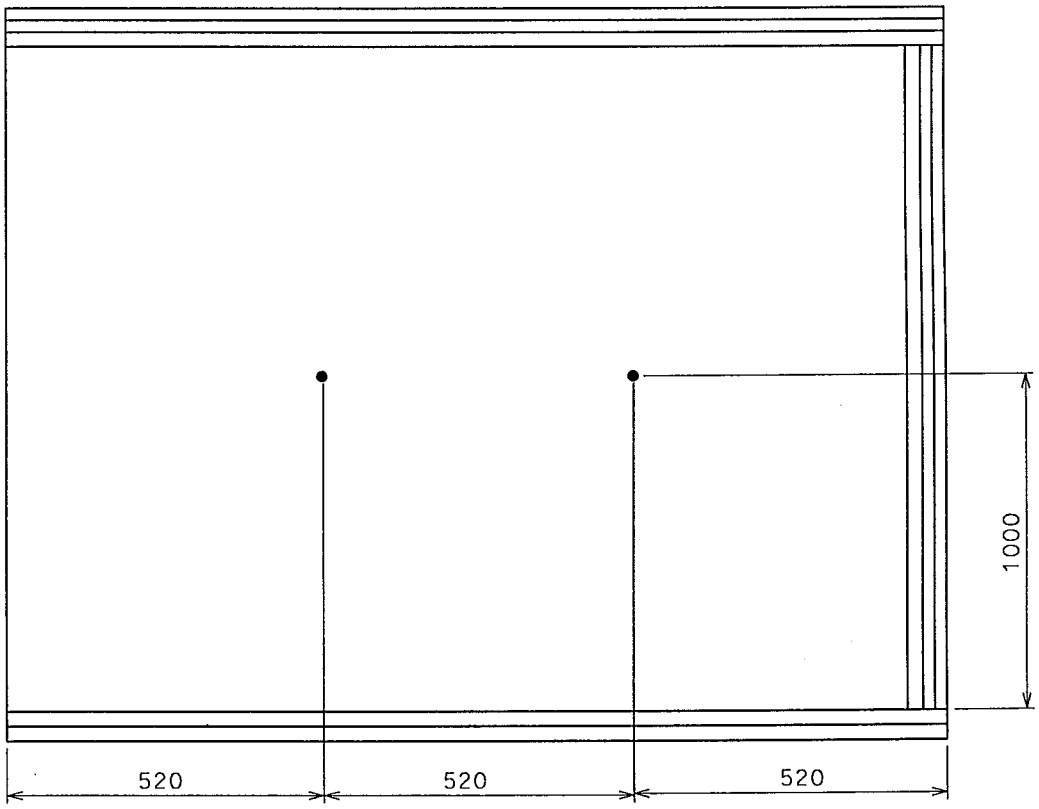

Figure 3.7 – Side Elevation, Placement of the Internal Thermocouples in the Sidewalls and the Ceiling (mm).

3.2 Instrumentation

3.2.1 Pressures

To calculate the flow rates from an orifice plate, a measurement of the pressure drop across the plate is required (refer section 5.2). Two Setra 264 pressure transducers are located at heights corresponding to the middle of each opening. One side of each transducer is exposed to ambient conditions, while the other side is located inside the compartment, 75mm from the wall and 50 mm from the door, on the left-hand sidewall (refer Figures 3.2 and 3.4). To avoid ambient fluctuations from drafts, opened and closed doors etc., a glass-wool-fibre filter was added before the transducer on the ambient side. The transducers have an output of 0-5 VDC, which corresponds to +/- 0.1 inches of water.

Because the output data of the Setra pressure transducers was logged on a time averaged basis, a MKS Instruments 223 BD-00010AAB pressure transducer was installed to measure the instantaneous pressures produced during an explosion. It is setup to sample from the same location in the upper layer as the transducer described in the previous paragraph. The MKS transducer has a 0-1 V output, which corresponds to 0-10 torr. A Tektronix TDS 520 oscilloscope was used to log the output, and was setup to only recorded pressures greater than 50 Pa of the baseline pressure.

3.2.2 Temperatures

Two thermocouple trees were utilized to measure internal compartment temperatures; one tree was located in the front corner and one in the back corner. Each tree consists of ten thermocouples located at 50 mm, 150 mm, 250 mm, 350 mm, 450 mm, 550 mm, 650 mm, 750 mm, 850 mm and 950mm above the floor (refer Figure 3.2). To avoid dead-air spots and boundary layers the front thermocouple tree was located 75 mm from the door and 55 mm from the wall. The rear tree is located 50 mm from the back wall and 55 mm from the side wall (refer Figures 3.2 and 3.4). Each thermocouple wire is encased in ¼ inch stainless pipe, with the tip of each thermocouple extending 5 mm beyond the end of each pipe. Attached to

through two more filters to remove water vapour, and finally through a Jeanne filter to remove particulate matter greater than 2 microns.

Servomex and Ultramat Analysers

Continuous sampling of CO_2, CO and O_2 is achieved with the use of a Servomex 540 A and Ultramat 6 analysers.

3.2.4 Fuel Vaporisation

A Mettler Toledo load cell is used to monitor the rate of fuel volatilization. The load cell was located under the rear of the compartment and was connected to the fuel-table inside the compartment via four steel columns (refer Figures 3.2 and 3.3). The columns are adjustable allowing the table to be raised or lowered. The fuel-table was constructed from a square steel frame onto which one layer of stainless 430 was wielded and covered by two layers of 25 mm Kaowool Vacuum Board.

The load cell was calibrated with a 15 kg weight (compartment door shut), theoretically allowing an accuracy of $\pm$ 0.0005 kg. Due to the dependence on the configuration of the compartment, the load cell was found to be accurate too only $\pm$ 0.3 kg (visually observed). However, it is the rate of change that is of interest during the experiments, this was found to be accurate to 0.05 kg (refer Appendix A1).

3.2.5 Data Acquisition

Output data from the thirty-six thermocouples, two pressure transducers and the load cell were monitored and collected using an i-tec Pentium Pro computer running at 200 MHz.

each pipe is a flange; each thermocouple is fastened to the compartment by screwing this flange to the compartment. The external end of each pipe was sealed with high temperature gasket-maker to avoid leaks.

Individual thermocouples were placed inside the two sidewalls, the ceiling, and the back wall to allow a heat transfer analysis of the compartment if required. Temperatures were monitored at seven different locations around the compartment (refer Figures 3.6 and 3.7). At each location two temperatures were recorded, one between the stainless and the insulation, and one between the Kaowool blankets and the Kaowool Vacuum Board. Thermocouples were glued into place with high temperature gasket-maker to stop them moving during contraction and expansion of the insulation. All holes through the compartment were filled with high temperature gasket-maker to reduce the leakage area of the compartment.

Type K, 24 gauge thermocouple wire was used in both the walls and the trees. Thermocouple wire with thicker insulation was used in the trees because of the exposure to higher temperatures and the need for durability. Each thermocouple was made by wielding the chromel alumel wires together. Wielding was accomplished by placing a large voltage between the wires while immersed in mercury.

Two thermocouples were utilized to measure the ambient air temperature during each experiment.

3.2.3 Gas Analysis

Gas Chromatograph

CO, CO_2, O_2, He, and N_2 concentrations were measured with a MTI Analytical Instruments Micro Gas Chromatograph, which also gave an indication of the presence of other gaseous species. A chromatograph can only analyse on a grab sample basis; the period between each sample is dependent on the set-up of the instrument. All gas concentrations are given on a dry basis. Prior to analysis, the gas was cooled and filtered through two glass-fibre filters, then

3.3 Fuel

Wood was chosen as the fuel type for all of the experiments. This choice was based on the following points:

1. Wood is one of the major construction materials in New Zealand. It is also widely used in packaging, stationary and furniture. Therefore, it is expected that it would be present in most fires in New Zealand. The author feels that the results will be more relevant and applicable if the fuel and fire conditions are similar to those that could be expected in a real fire.
2. The only previous research on smoke explosions found in the literature used mattress foam as the fuel (refer section 2.5). Yet a literature study by Croft (1988) found that of the 77 fires studied involving explosions, cellulose materials were responsible for 74% of the explosions.
3. Research has found that the combustion of wood in an under-ventilated environment can lead to the production of large amounts of carbon monoxide (refer section 2.3.1). This finding may substantiate claims that CO might be a dominant species before a smoke explosion.

Medium density fibre board (MDF) was chosen as the wood type because of its uniformity in relation to density and composition. This may allow better replication of experimental conditions than if unprocessed timbers, such as Pinus Radiata, had been used. The wood was arranged as cribs to allow further replication.

Eighteen millimetre square sticks were spaced at 18 mm intervals so that ventilation to the crib controlled the burning rate (refer Appendix B1). Thus hopefully producing a high level of unburned pyrolyzates. Cribs were constructed in two sizes, a large crib 300 x 300 x 300 mm, weighing approximately 8 kg and a smaller crib 300 x 300 x 150 mm, weighing approximately 4 kg. Sticks were held in a crib arrangement by nailing them together with 30 mm nails.

The cribs were kept in a conditioning room for a minimum of a month before burning to ensure that the moisture content of each crib was the same. The conditioning room had a relative humidity of 50% at a temperature of 30°C.

3.4 Extinguishing System

A water extinguishing system was installed in the compartment; it consisted of a ¼ inch stainless pipe with an agricultural sprinkler nozzle. The sprinkler was directed towards the side of the crib, at a distance of approximately 150 mm. Due to the protection a crib offers a fire this arrangement was found ineffective at extinguishing the fires. An improved method was devised where the sprinkler pipe is hand held, allowing water to be sprayed in every direction as required.

4.0 Experimental Procedure

The following Table summarizes the setup of each experiment conducted.

Table 4.1 – Experimental Setups

Experiment	Crib Weight	Orifice Diameters
	(kg)	(mm)
1	4.4	50
2	4.3	35
3	4.4	71
4	4.4	25
5	4.2	100
6	4.0	100
7	4.4	100
8	4.3	100
9	4.7	100
10	8.0	100
11	7.5	100

4.1 Gas Chromatograph

Refer to M200/M200H Micro Gas Chromatograph User's Manual (1994) for instructions on the setup procedure and operating method for the MTI Micro Gas Chromatograph.

The MTI Micro Gas Chromatograph uses two columns (Molecular Sieve and a Poraplot Q) to analysis a gas sample, contained in the following table is operating conditions that were used for each column.

Table 4.2 – Operating Conditions of the GC

Column	A	B
Column temperature (°C)	46	59
Run time (sec)	90	90
Sample time (sec)	20	20
Inject time (msec)	50	30
Detector sensitivity	medium	low

The gas chromatograph was calibrated with the following range of gases.

Table 4.3 – GC Calibration

Calibration Gas	Carbon monoxide	Oxygen	Nitrogen	Carbon dioxide	Helium
	(vol %)	(vol %)	(vol %)	(vol %)	(vol %)
1		20.9	78.1	0.033	
2	20		20	20	20
3		16.02	83.98		
4	5.0		64.7	30.3	
5	2.42		97.07	0.408	

Before each experiment the accuracy of the gas chromatograph was checked with at least one of the known gases, there should be no more than a 5% discrepancy. The glass wool in the first filter should also be changed as a highly pungent liquid residue accumulates there.

Due to the volume of the filtering system in line before the chromatograph, at least three minutes of sample should be sucked through the system before the sample is analysed. The first sample was usually analysed at 10 minutes, and then at 5 to 10 minute intervals throughout the course of the experiment.

4.2 External Ventilation

A 3 x 3 m hood above the compartment was used to exhaust the smoke. The hood was set to exhaust at its maximum rate of 4 m^3/sec.

4.3 Arrangement of the Fuel

The top of the fuel table was elevated 310 mm off the floor of the compartment in all experiments. The cribs were positioned in the centre of the fuel table. Cribs were elevated 25 mm off the fuel table, supported underneath by a steel baking-tray (190 x 285 x 24 mm) and ceramic tiles (height 25 mm) stacked around the baking tray.

4.4 Servomex and Ultramat Analysers

Servomex and Ultramat analysers were utilized in experiments 6 and 11. Samples were drawn from the top probe in both experiments. The analysers were zeroed with 100% N_2 and spanned with ambient air, 30.3% CO_2 and 5.0% CO. The instruction manual for the Ultramat analyser (Siemens, 1997) should be referred to for the setup of the Ultramat 6 analyser. The 540A Oxygen analyser Instruction Manual should be consulted for the correct operating procedure of the Servomex analyser (Servomex, 1994).

If using these instruments in the future for similar work, the instruments should be started during the experiment as their filter become blocked 20 to 30 minutes into the experiment, after which accurate analysis cannot be achieved.

4.5 Data Logging

Before commencing an experiment, two minutes of data was logged for calibration purposes. Data was read every second with the average of every ten readings logged. Although the

output data is slightly smoothed, logging extra data only made analysing and interpreting more difficult (refer Appendix A, Experiment Six).

4.6 Ignition of the Fuel

All experiments were conducted using 200 ml of white sprits to start the crib fires. The sprits were contained in the baking tray positioned under crib. A gas torch was used to ignite the white sprits. Once the white sprits had been consumed (observed visually), the compartment door was shut. On average the white sprits burned for 4 to 5 minutes.

4.7 Extinguishment

The cribs were extinguished with approximately 5 to 10 litres of water applied to every surface. To ensure the cribs would not re-ignite after the water was applied they were then placed in a bucket of water.

Chapter 5.0 Data Analysis

5.1 Gas Concentrations

The outputs of the gas chromatograph and of the Servomex and Ultramat analysers were gas concentrations on a dry basis; water was removed before the gas samples were analysed. To allow comparison with other studies and for easier interpretation, dry-basis concentrations are converted to wet basis concentrations through use of the following assumption:

$$CH_2O + 2O_2 \longrightarrow CO_2 + H_2O \qquad (5.1)$$

CH_2O, formaldehyde is assumed to be the chemical composition of the pyrolyzates produced from the combustion of medium density fibre board (refer SFPE, 1995, Table 3-4.10). Ambient water vapour is also accounted for by assuming that at all times the air in the lab had a water vapour concentration of 1.25 volume percent.

Wet basis gas concentrations were derived by calculating the amount of water produced, then the total number of moles were recalculated and ambient water vapour was added. The molar percentages on a wet basis were then recalculated. This conversion is only approximate. It does not allow for any water that might be produced from carbon monoxide formation or any of the hydrocarbon material that condenses in-line before the analysers.

Quantitatively the gas chromatograph only measures the concentrations of N_2, O_2, CO_2, CO, and CH_4 (the only gases that were available for calibration). The concentration of other species, for example hydrocarbons other than CH_4 were calculated by summing N_2, O_2, CO_2, CO and CH_4 and subtracting the total from one hundred percent. These others species are referred to in the rest of the report as the 'residual hydrocarbon content'.

5.2 Vent Flowrates

Inlet and outlet flowrates were calculated from the following equation for flow through an orifice plate. Flow is the mass flowrate in kg^3/sec (refer de Nevers, 1991).

$$m = A_2 C_v \rho \left[\frac{2(P_1 - P_2)}{\rho(1 - A_2^2/A_1^2)} \right]^{1/2} \qquad (5.2)$$

A_1 and A_2 are the areas in square metres of the inlet before the orifice and the area of the orifice opening respectively. P_1 and P_2 are the pressures at the orifice inlet and of the ambient respectively, measured in Pascals. C_v is the discharge coefficient of the orifice plate, and ρ is the density of the flow before it passes through the orifice in kg/m^3.

Because the inlet before each opening is so much larger than the actual area of the opening, the term A_2^2/A_1^2 was neglected, simplifying equation 5.2 to

$$m = A_2 C_v \rho \left[\frac{2(P_1 - P_2)}{\rho} \right]^{1/2} \qquad (5.3)$$

The ideal gas law (equation 5.4) was used to calculate the density of the outlet flows.

$$\rho = \frac{PMr}{RT} \qquad (5.4)$$

Where Mr is the molar mass of the flow in g/mol; R is the universal gas constant of 8.314 $m^3 \cdot Pa/mol \cdot K$, and T is the temperature in Kelvin.

No correction was made for non-ideality, but density values were checked against those for dry air given in Rogers and Mayhew (1992), and were found to agree within 2% on average.

Discharge coefficient values for the inlet were estimated from a correlation between C_v and Reynolds number (refer Figure 5.12 in de Nevers, 1991). Reynolds numbers were calculated from equation 5.5. Viscosity values were derived from a table in Rogers and Mayhew (1992), assuming dry air. The C_v value for the outlet was calculated from a mass balance around the

compartment. The mass flows in and out of the compartment were calculated from equation 5.3, and the generation of the combustion products were obtained from the load cell. Both C_v values (inlet and outlet orifices) cannot be calculated from the mass balance alone, as there is only one equation and two unknowns, although they should be similar.

$$Re = \frac{VD\rho}{\mu} \tag{5.5}$$

C_v values were only calculated from periods of inactivity, where the mass loss was constant and there were no large pressure fluctuations. Over each period the pressures and mass loss were averaged and the difference between the mass in and out was calculated. Solver in Excel was used to optimize the outlet C_v value by minimizing the absolute sum of all the differences. For all the orifice plates, the inlet C_v value was set at 0.6 to enable the outlet to be calculated. Table 6.3 lists the inlet and outlet C_v values for each orifice plate.

Chapter 6.0 Results & Observations

The purpose of this chapter is to present and discuss the main results and observations from the eleven experiments conducted in this research (refer Table 4.1).

6.1 Flame Structure

In experiments 1 through 9, the fires were often noted as being very lazy, usually a single elongated flame extended from the crib to the ceiling. Smouldering fires were produced in experiments 5, 7, 10 and 11, all of which had 100 mm openings, the largest size opening used in any of the experiments. Visual observations were conducted randomly during each experiment, but were constrained by time and safety.

In experiments 10 and 11, very lazy flaming was noted at the base of the crib, often at distances exceeding 200 mm from the crib. This phenomenon was only noted at the beginning of both experiments, before the transition of the flaming fire to a smouldering fire. A photograph taken through the lower inlet during experiment 11 depicts this phenomenon (refer Figure 6.1). The right-hand side of the fuel table can be seen at the bottom of the photo, the crib is visible on the left-hand side of the photo. In experiment 11, these flames were periodically observed to burn all the way to the lower inlet, a distance of approximately one metre. The result of this phenomenon is seen externally as a small puff of smoke from the lower inlet, this is occasionally accompanied by a small flame.

Completely detached and stable burning was observed in experiment 10 while the compartment door was still open. This burning occurred on the ceiling directly above the crib, it lasted for approximately one minute and covered an area 300 x 300 x 50 mm thick. At the time, it was the only source of burning in the compartment, the crib fire had not yet taken hold, and no white spirits remained in the baking tray. A similar phenomenon was observed at the beginning of experiment 11, although it was not as stable as seen in experiment 10.

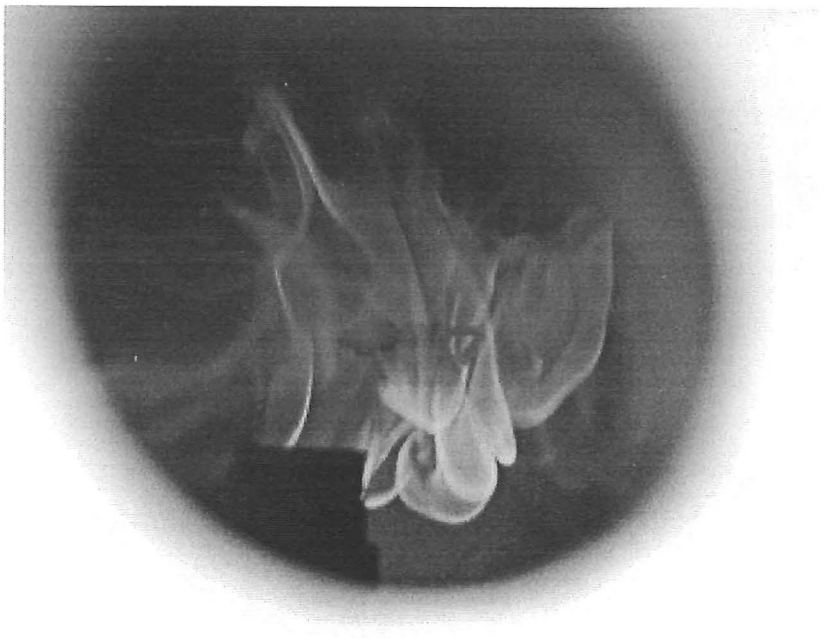

Figure 6.1 – Burning at the Side of the Crib, Experiment 11

6.2 Experimental Results

Included in this section are the results from experiments 1, 2, 4, 6, 8 and 9. Results and observations from experiments 3, 5, 7, 10 and 11 will be presented in section 6.3, which covers the experiments that produced smoke explosions.

6.2.1 Experiments 1, 2, and 4

Shown on the following chart is the fuel volatilization rate (load-cell output), temperature and pressure profiles for experiment 2, which burnt a 4 kg crib with 35 mm openings. Charts for experiments 1, 4, 6, and 9 can be found in Appendix A1. All the profiles were constructed from time averaged readings; one reading was taken every second and then every ten readings were averaged (refer section 4.4). The two pressure profiles refer to the gauge pressures in the front left-hand corner of the compartment, measured at the same elevation as each of the respective openings (refer section 3.2.1). The temperature profile shown on the chart is the temperature in the rear of the compartment, at an elevation of 950 mm. The readings from the other nineteen thermocouples can be found in Appendix A2 and A3. The load-cell output depicts the rate of fuel vapourisation; this should be treated with caution as it was found that

the physical configuration of the compartment affected the output. For example, whether the door was opened or closed changed the reading by approximately half a kilogram.

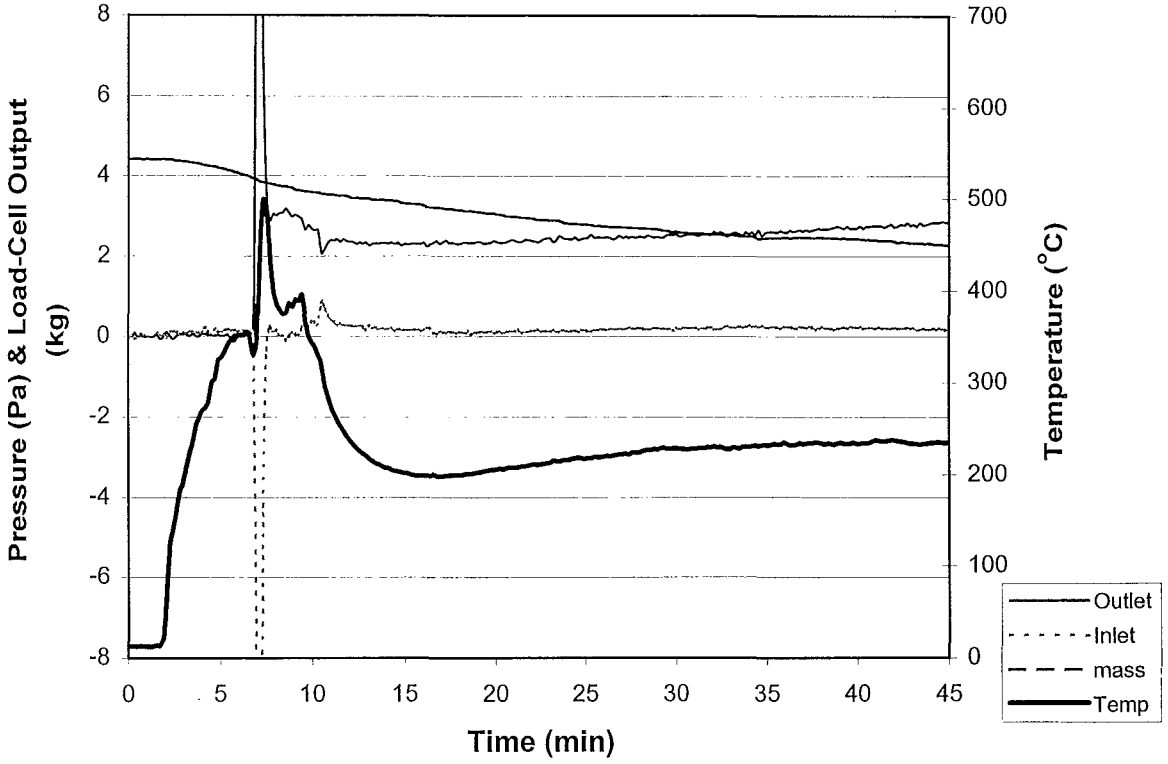

Figure 6.2 – Pressures, Temperature and Fuel Vaporization Profiles, Experiment 2

Between 2 minutes and 7 minutes, it appears from the output of the load-cell that there was a greater rate of fuel vaporization than during the rest of the experiment (refer Figure 6.2). Mass was lost at a greater rate during this period because both the crib and the white sprits were burning, as compared with just the crib during the rest of the experiment.

Table 6.1 – GC Readings, Experiment 2

Time	**O_2**	**N_2**	**CH_4**	**CO**	**CO_2**	**H_2O**
(min)	vol (%)	vol (%)	vol (%)	vol (%)	vol (%)	vol (%)
10.3	6.7	66.0	0.3	2.8	12.0	12.0
24.0	6.3	62.4	0.8	4.5	14.5	14.5
36.3	4.4	62.0	0.7	4.7	14.6	14.6
49.0	4.9	64.2	0.6	4.5	12.6	12.6
65.1	5.2	66.9	0.6	4.4	12.1	12.1

Shown in Table 6.1 is the composition of the atmosphere in the compartment during experiment 2. These measurements were made with the gas chromatograph, at an elevation of 975 mm (refer section 3.1.3). Only those gases that were available to calibrate the gas chromatograph are shown in the table. The residual hydrocarbon content is not shown, as it could not be accurately calculated. The smaller errors of the individual components when added together introduced a significant error into the residual hydrocarbon value (refer section 5.1). Gas chromatograph results for the other 10 experiments are located in Appendix A5.

The following graph displaying height versus temperature (rear) can be used to estimate the position of the upper layer in the compartment during experiment 2.

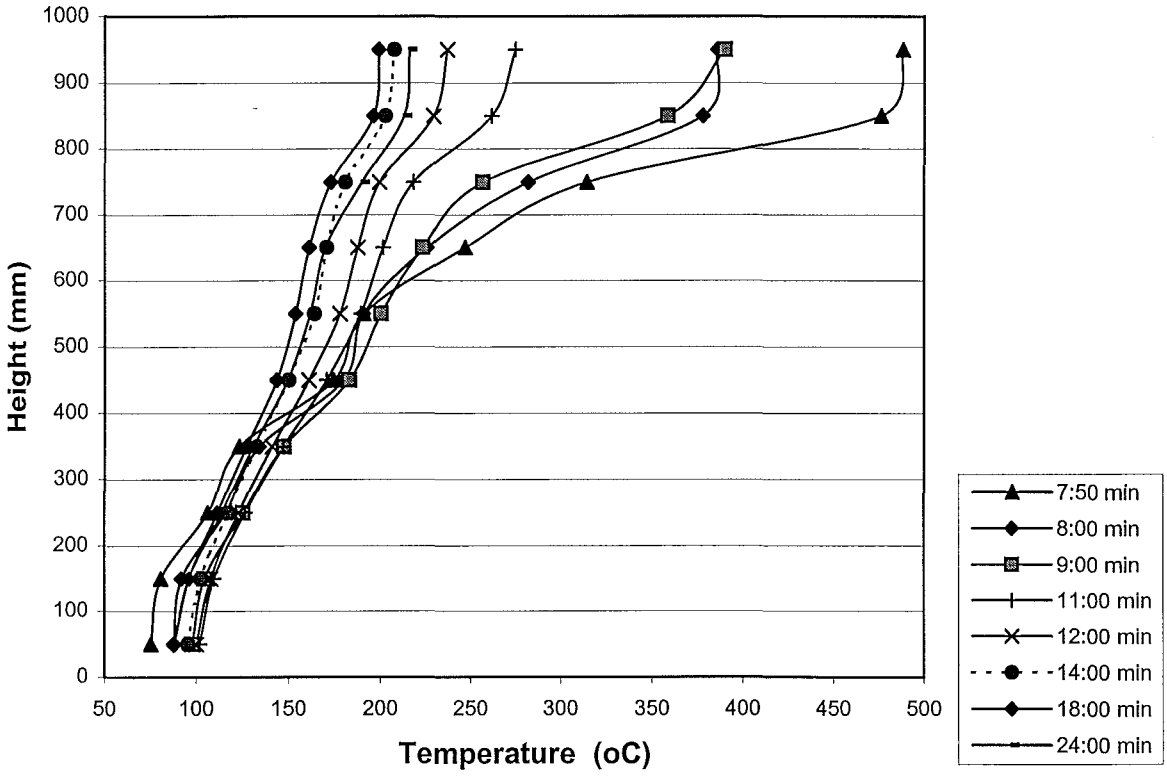

Figure 6.3 Upper Layer Position, Experiment 2

Once the door was shut at 7 minutes the layer started to deepen in the compartment. It reached a constant depth at 18 minutes (refer Figure 6.3). 498°C was the maximum temperature recorded during the experiment, it was measured in the rear of the compartment at an elevation of 950 mm. The maximum temperature occurred at 7:30 min, 20 seconds after the door was closed, after which the layer temperature steadily dropped for the next 12

minutes (refer Figure 6.3). When the layer reached a constant depth at 18 to 20 minutes the layer temperature began to increase, and kept increasing for the duration of the experiment (refer Figures 6.2 and 6.3). O_2, CO and CO_2 concentrations were fairly constant throughout the experiment; once the layer had formed (refer Table 6.1). The initial temperature decline is thought to be due to a lack of energy; there was not enough energy to support both an expanding layer and a temperature increase. This also explains the temperature increase observed after the layer reached a constant depth at 18 to 20 minutes.

The process of the deepening layer accompanied with a temperature decrease and followed by a gradual temperature increase described above for experiment 2, also occurred during experiments 1 and 4. Both of these experiments burnt a 4 kg crib, experiment 1 had 50 mm openings and experiment 4 had 25 mm openings (refer Appendix A).

6.2.2 Experiments 6, 8 and 9

Experiments 5, 6, 7, 8, 9, 10 and 11 were all setup with 100 mm openings. Experiments 5, 7, 10 and 11 are discussed in section 6.3 because smoke explosions were produced in these experiments. Experiments 6, 8 and 9 were not discussed in section 6.2.1, as in these experiments there was not the initial temperature decrease associated with the decreasing layer. Shown on the following chart is the fuel volatilization rate (load-cell output), temperature and pressure profiles for experiment 8. In experiment 8, a 4 kg crib was burnt with 100 mm openings. The accuracy of the load-cell output should be treated with caution (refer section 6.2.1). The two pressure profiles shown on the chart refer to the gauge pressures in the front-left-hand corner of the compartment, measured at the same elevation as each of the respective openings. The temperature profile was constructed from the temperature at rear of the compartment (elevation 950 mm). Temperature readings from the other thermocouples can be found in Appendix A2 and A3.

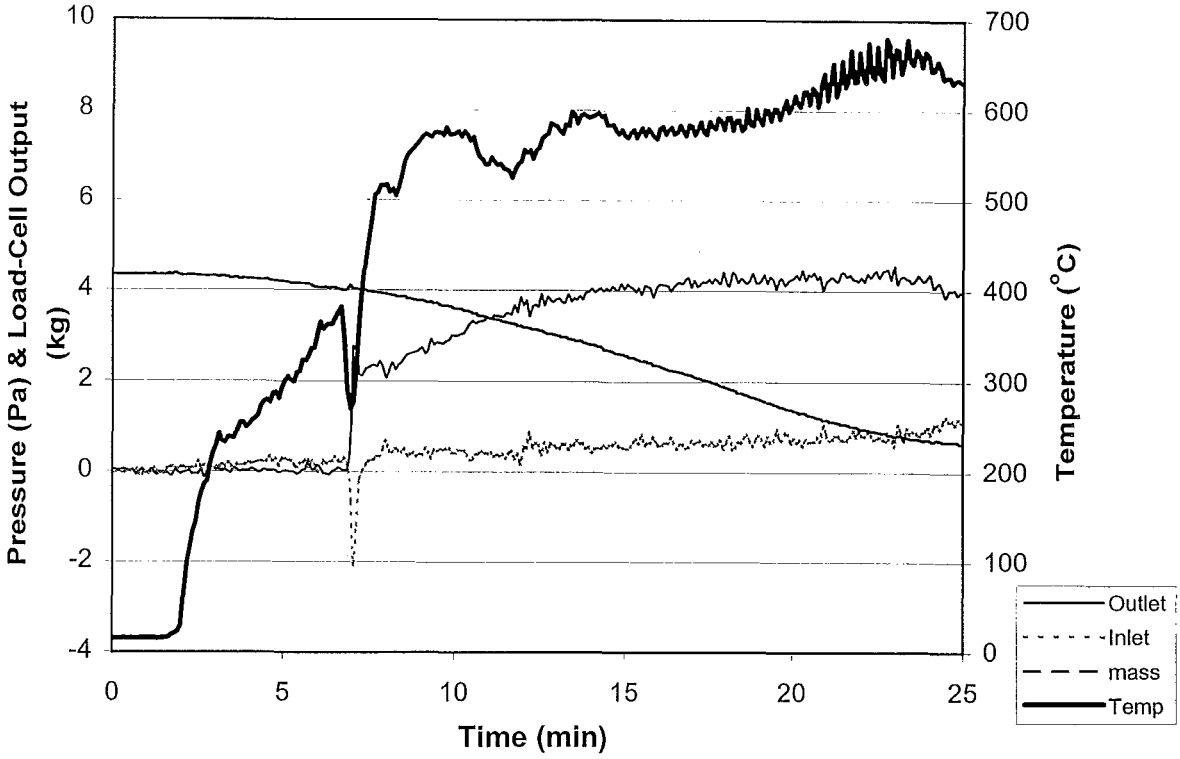

Figure 6.4 – Pressures, Temperature and Fuel Vaporization Profiles, Experiment 8

Shown in the following table is the composition of the atmosphere in the compartment (elevation 975 mm) during experiment 8, measured with the gas chromatograph (refer section 3.1.3). Only those gases that were available to calibrate the gas chromatograph are shown in the table. Gas Chromatograph results for the other 10 experiments are displayed in Appendix A5.

Table 6.2 - GC Results, Experiment 8

Time	**O_2**	**N_2**	**CH_4**	**CO**	**CO_2**	**H_2O**
(min)	vol (%)	vol (%)	vol (%)	vol (%)	vol (%)	vol (%)
11.0	0.6	55.9	0.7	4.5	15.7	15.7
19.0	7.2	62.5	0.6	2.8	12.8	12.8

The following graph displaying height versus temperature (rear) can be used to estimate the position of the upper layer in the compartment during experiment 8.

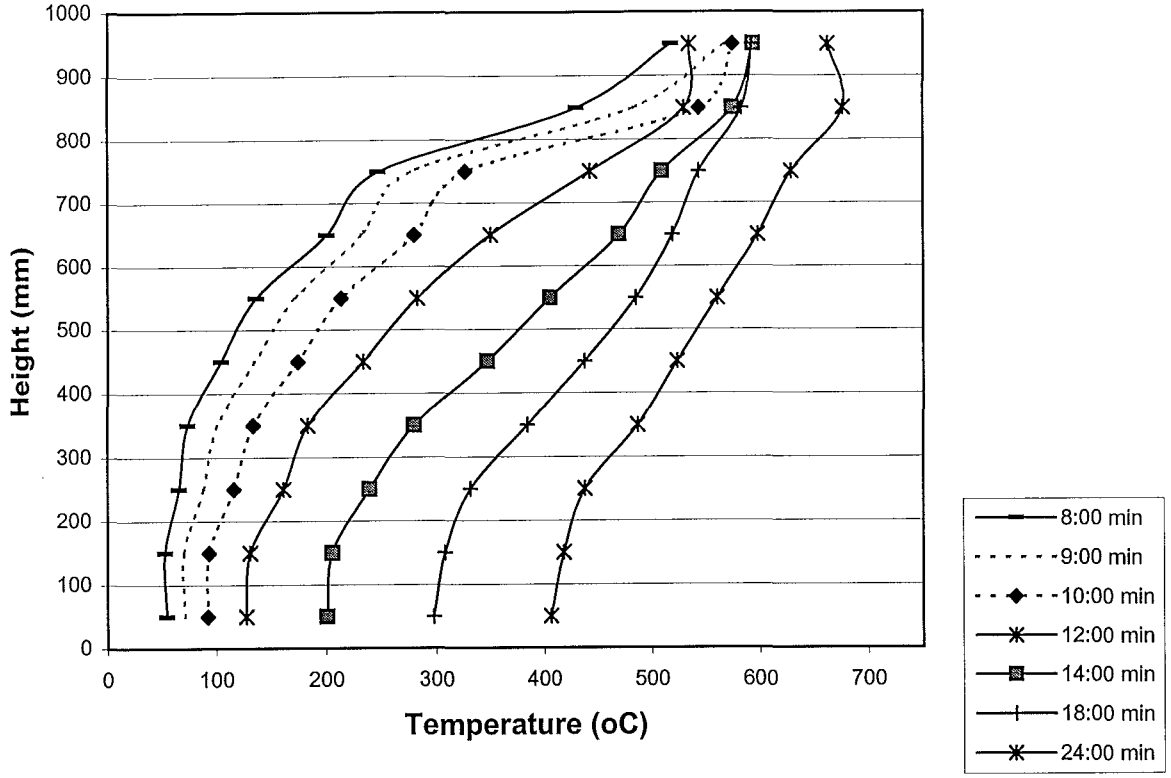

Figure 6.5 - Upper Layer Position, Experiment 8

It can been seen in Figure 6.5 that once the door was shut at 7 minutes the layer deepened, and the temperature increased. The reason for the initial temperature increase and not a decrease as observed in experiments 1, 2 and 4 is due to the larger openings used in experiment 8. An initial temperature increase was observed in experiments 6 and 9 (refer Appendix A), both of which had 100 mm openings; the same sized openings as used in experiment 8. Larger openings allow more air into the compartment. A larger airflow allows more combustion to occur, releasing more energy, which allows the layer to form at a greater rate and at higher temperatures.

During the layer formation (7–12 minutes) the O_2 concentration dropped to almost 0% and the CO and CO_2 concentrations increased to 4.5% and 16% respectively (refer Table 6.2). Approximately seven minutes later the O_2 concentration had increased to 7%, and the CO and CO_2 concentrations had decreased to 2.8% and 13% respectively (refer Table 6.2). This trend was also observed during experiments 5, 6, 7 and 8, but not during experiment 9 (refer Appendix A). All five experiments burnt a 4 kg crib with 100 mm openings. It is suspected

that the oxygen concentration increased after approximately 20 minutes because the combustion process was almost complete. This can be seen in the output from the load cell in Figure 6.4. At 19 minutes (the same time as the second GC measurement) the mass of the crib has dropped from its initial weight of 4.3 kg to 1.5 kg. Very little combustible fuel would have been left at this stage.

Comparison of experiments 8, 3, 1, 2 and 4, which had openings of 100, 75, 50, 35 and 25 mm respectively, shows that a larger opening produces higher temperatures during the experiment. Higher temperatures correspond to more combustion, which is expected when the ventilation is increased (refer Figures 6.4 and 6.2 and Appendix A1).

6.2.3 Volumetric and Mass Flowrates

Originally, it was intended that the flowrates in and out of the compartment would be calculated. However, accurate calculation of the flowrates was found to be particularly difficult as the orifice discharge coefficient (C_v) values could not be determined accurately (refer section 5.2 for the method of calculation).

The two main problems with current setup for measuring the flows in and out of the compartment are:

1. The pressures are very low, commonly 1 to 5 Pa below and above ambient, error and noise can be significant.
2. At very low flows, C_v cannot be assumed a constant (refer Figure 5.12, de Nevers, 1991).

Shown in the following table are the calculated C_v values for the five orifice plates used in experiments 1 through 11.

Table 6.3 – Discharge Coefficient Values for the Orifice Plates

Orifice Plate (mm)	Area (mm^2)	Inlet	Outlet
100	7850	0.6	0.53
71	3960	0.6	0.4
50	1960	0.6	0.5
35.8	990	0.6	0.3
25.5	511	0.6	0.5

The C_v values for the lower orifices are always 0.6 because they were set at this value to enable the outlet values to be calculated. The calculated values for the outlet range between 0.3 and 0.53 (refer Table 6.1). It was expected that the C_v values for the inlet and the outlet orifices would be similar, as Table 6.3 depicts this is not the case

6.3 Smoke Explosions

Smoke explosions were observed in experiments 5, 7, 10, and 11, all of which had 100 mm openings. The smoke explosions were easily recognized during the experiments as high velocity smoke would simultaneously flow from both openings; hitting the window of the control room three metres away (refer Figure 6.18). Experiments 5 and 7 burnt a 4 kg crib and produced only one explosion each. An 8 kg crib was burnt in experiments 10 and 11, and in both of these experiments two smoke explosions were produced.

A smoke explosion is thought to have occurred during experiment 3, although at the time it was noted as a flashover (refer section 6.3.3). A review of the temperature and pressure profiles after the experiment indicates that it could have been an explosion. As in all of the experiments that produced explosions there is a definite pattern that occurs before the explosion. This pattern is present in the experimental results of experiment 3 (refer Figures 6.6). Experiment 3 burnt a 4 kg crib with 75 mm openings.

6.3.1 Experiments that Produced Smoke Explosions

Figures 6.6 to 6.10 display the fuel volatilization rate (load-cell output), temperature and pressure profiles for the five experiments that produced smoke explosions. The profiles are not constructed from instantaneous readings, but from time averaged values (refer section 4.4). The two pressure profiles in these figures are constructed from the gauge pressures in the front left-hand corner of the compartment. These are measured at the same elevation as the centre of each respective opening (refer section 3.2.1). The Temperature shown on the chart is from the rear of the compartment, at an elevation of 950 mm (refer Appendix A2 and A3 for the readings of the other thermocouple readings). The output from the load-cell should be treated with caution, as it was found that the physical configuration of the compartment affected the reading. For example, whether the door was opened or closed could change the output by up to 15% (refer Figure 6.10, at 6 minutes).

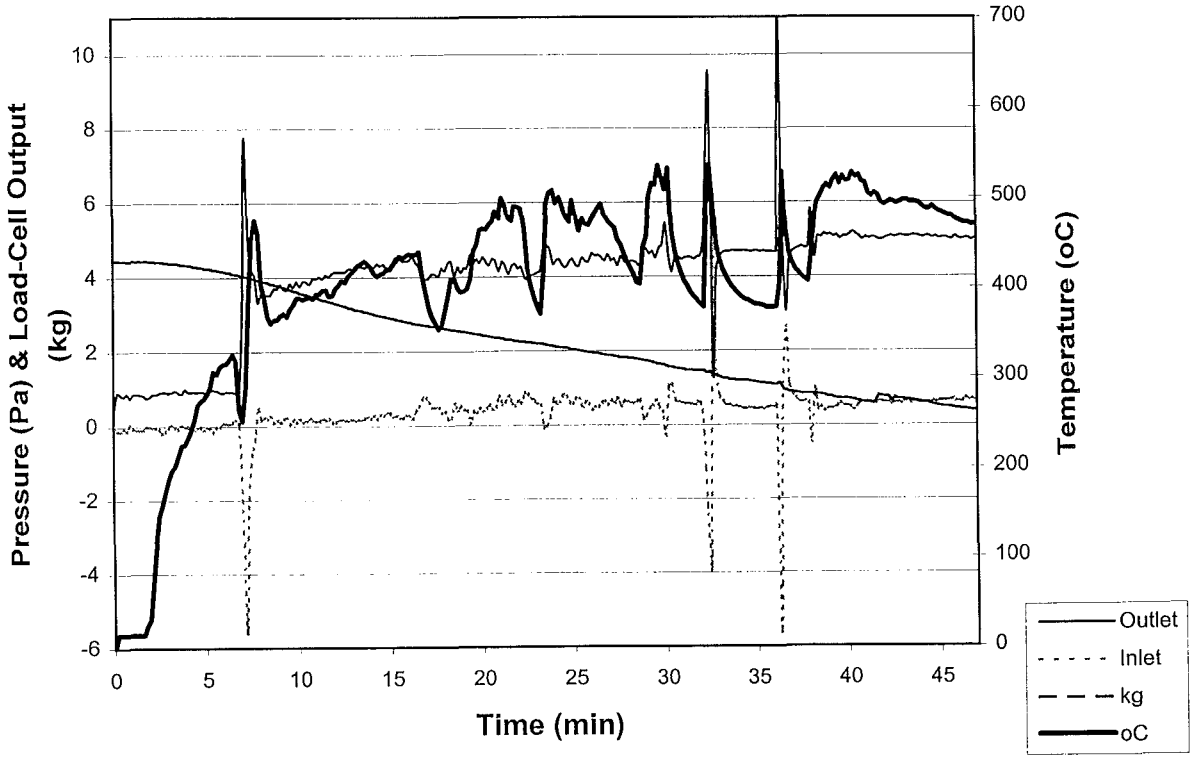

Figure 6.6 – Pressures, Temperature and Fuel Vaporization Profiles, Experiment 3

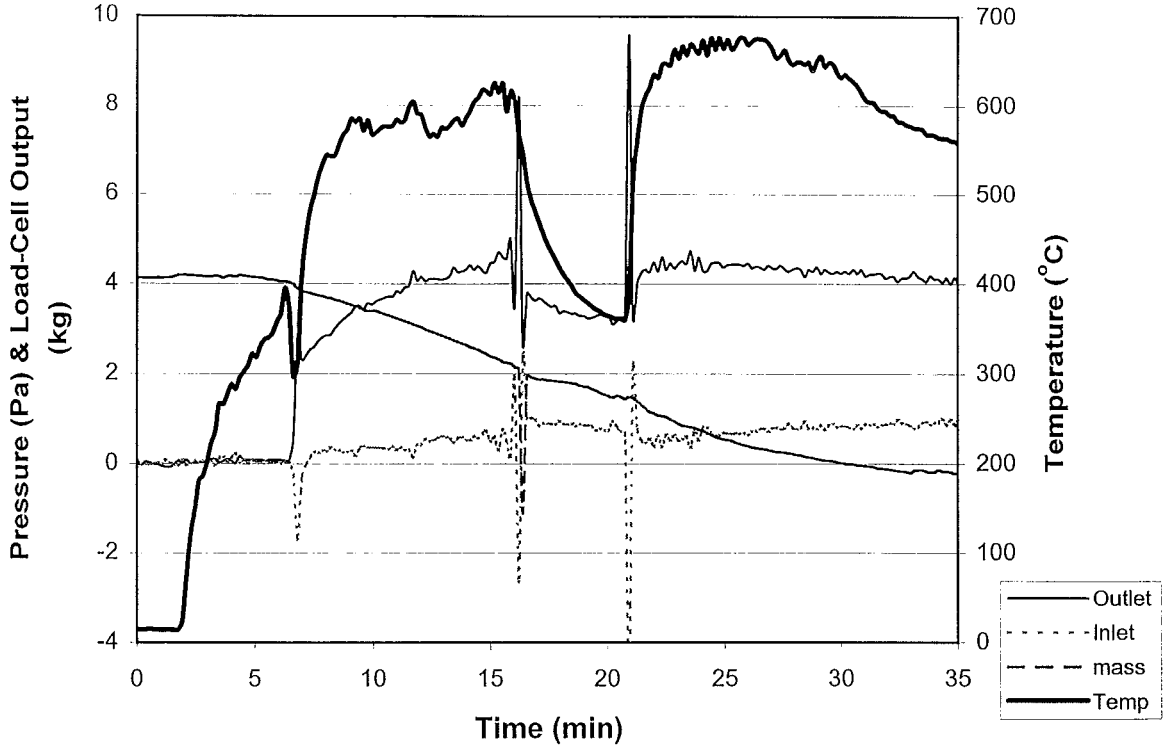

Figure 6.7 – Pressures, Temperature and Fuel Vaporization Profiles, Experiment 5

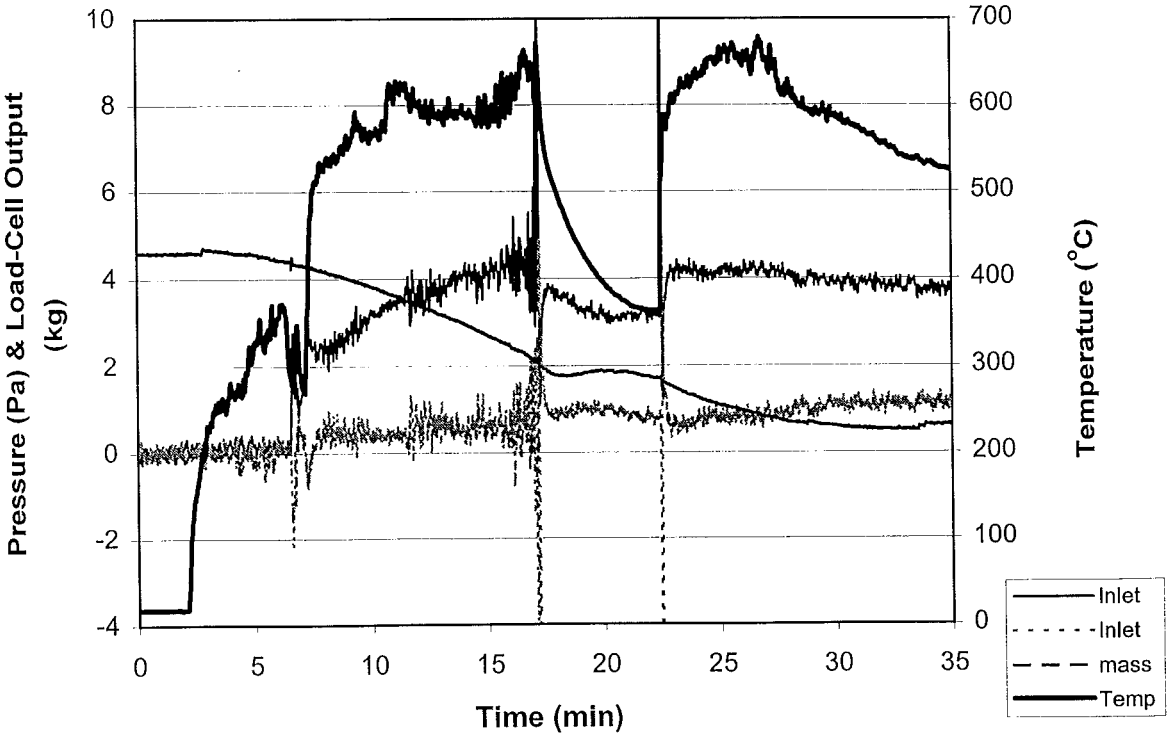

Figure 6.8 – Pressures, Temperature and Fuel Vaporization Profiles, Experiment 7

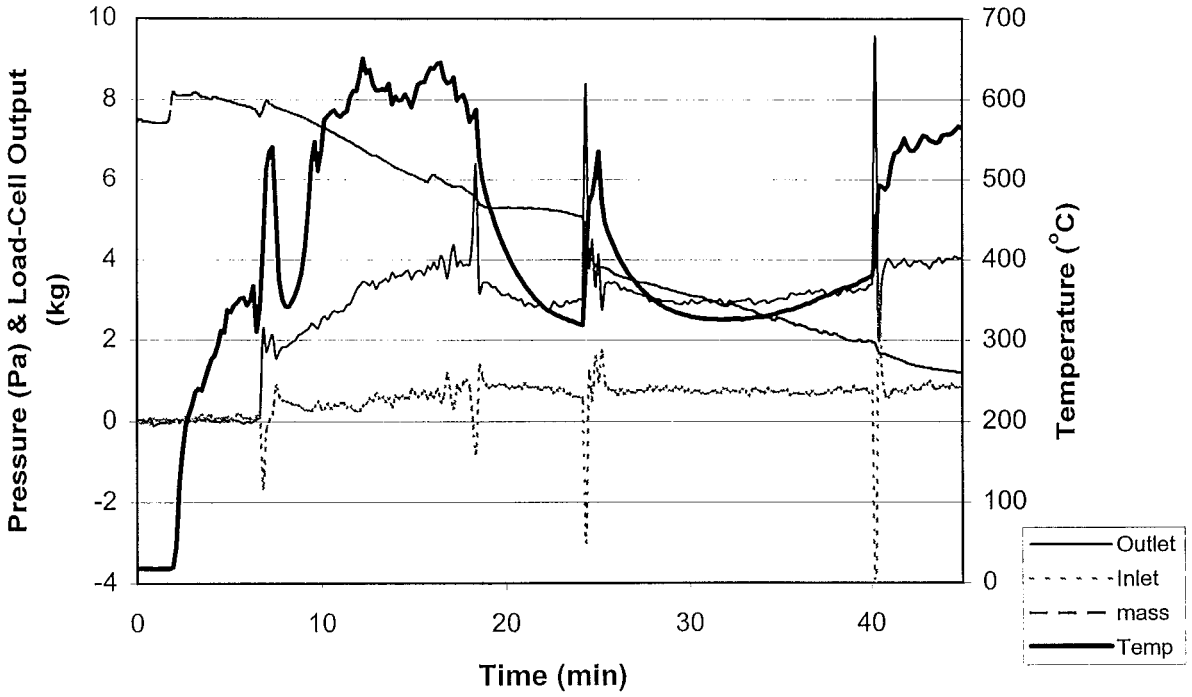

Figure 6.9 – Pressures, Temperature and Fuel Vaporization Profiles, Experiment 10

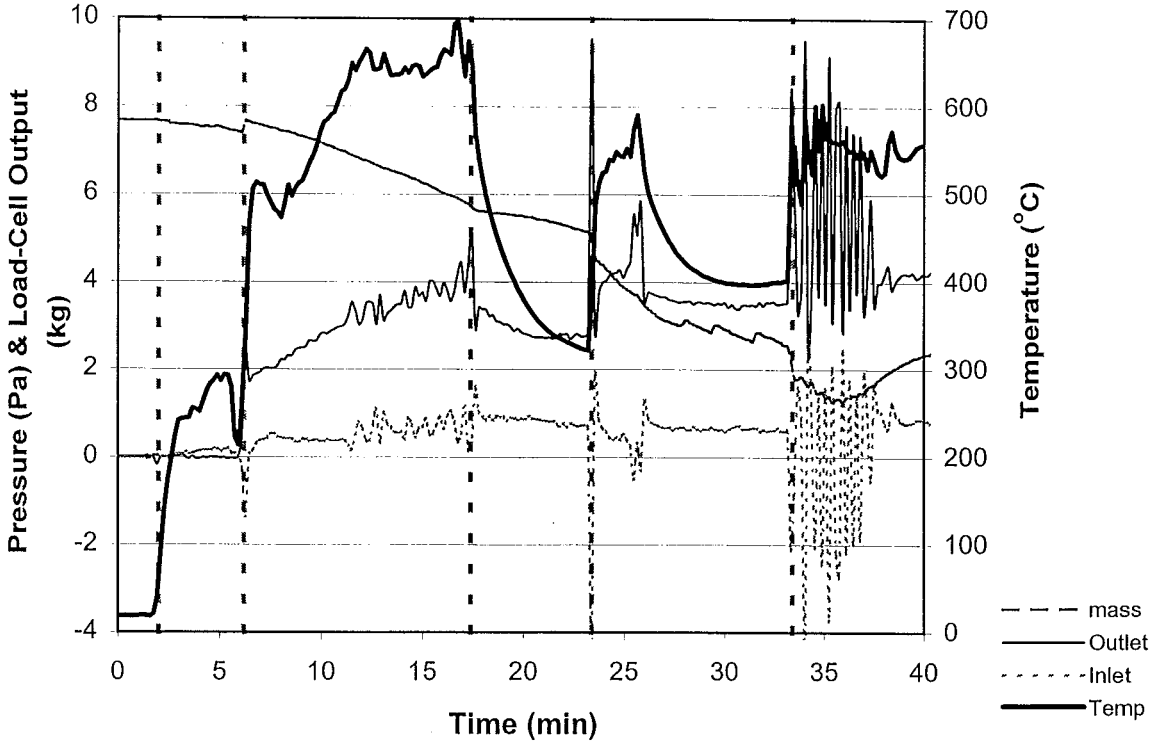

Figure 6.10 – Pressure, Temperature and Fuel Vaporization Profiles, Experiment 11

In experiments 3, 5 and 7 (refer Figures 6.6, 6.7, and 6.8) only one smoke explosion was produced per experiment. It is represented as the large pressure spike after the temperature drop. All three experiments burnt a 4 kg crib. Experiment 3 had 71 mm openings, and experiments 5 and 7 had 100 mm openings. Experiments 10 and 11, depicted in Figures 6.9 and 6.10, both burnt 8 kg cribs with 100 mm openings. In experiments 10 and 11, two smoke explosions were produced.

6.3.2 Experiment 11

Because of the very similar temperature and pressure profiles between experiments 5, 7, 10, and 11 (refer Figures 6.6 to 6.10), only experiment 11 will be described in detail. The main reason for using experiment 11 as the norm is that nearly all the important findings were made during this experiment. However, any results or observations from other experiments that were not observed during experiment 11, or add weight to suggested theories will also be included.

Referring to Figure 6.10, experiment 11 can be broken down into seven separate stages:

Table 6.4 – Breakdown of Experiment 11

Stage	Description	Time (min)
I	Fire Started – Door Closed	2:00 – 6:20
II	Door Closed – Smouldering Period	6:20 – 17:4
III	Smouldering Period – 1st Smoke Explosion	17.4 – 23.4
IV	1st Smoke Explosion	23.4
V	1st Smoke Explosion – 2nd Smoke Explosion	23.4 – 33.3
VI	2nd Smoke Explosion	33.3
VII	2nd Smoke Explosion – Decay Period	33.4 – Extinguishment

Each stage will be described in detail later in this section. Experiments 5, 7, 10 and 11 can be broken down as experiment 11 is in Table 6.4. However, in experiments 5 and 7 only the first four stages apply after which the fire started to decay.

The CO, CO_2, and O_2 concentrations in the compartment (elevation 900 mm) during experiment 11 are shown in Figure 6.11. These were measured with the Servomex and Ultramat analysers (refer section 3.1.3 – for sampling location). The analysers have a 20 to 30 second lag time behind the output of the thermocouples and pressure transducers.

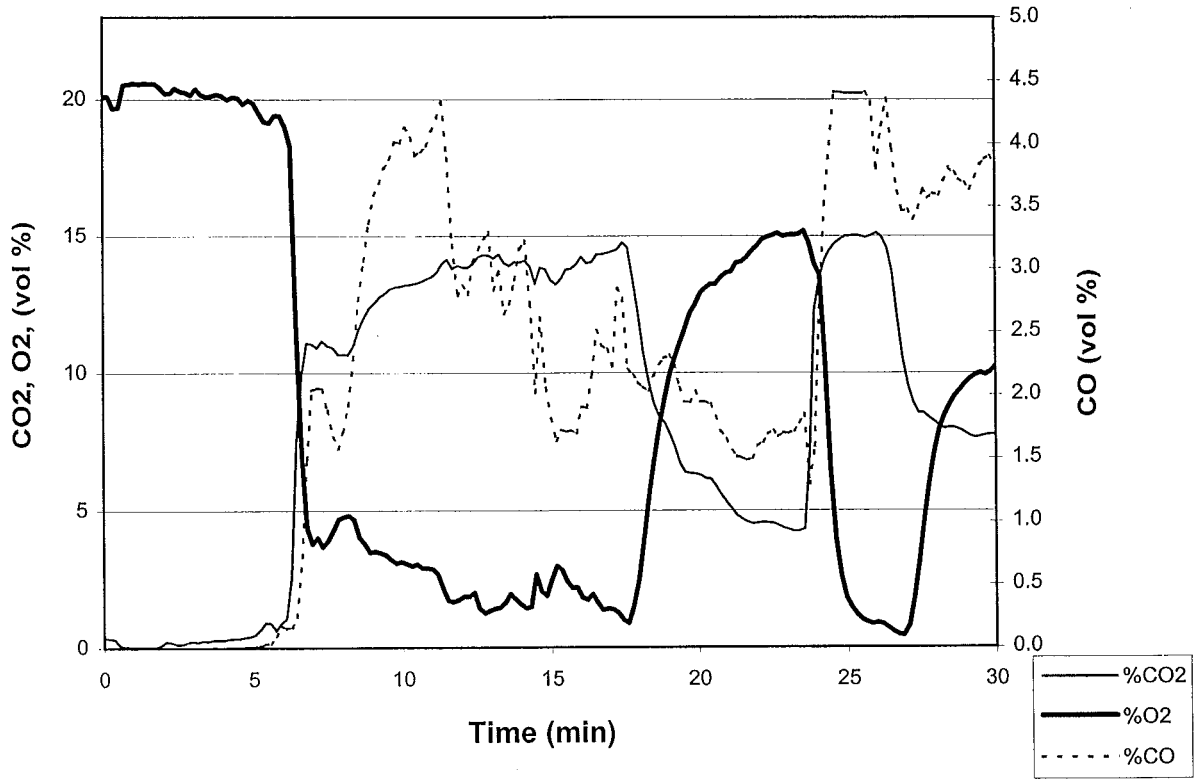

Figure 6.11 Upper Layer Concentrations, Experiment 11

Table 6.5 – GC Readings, Experiment 11

Time	**O_2**	**N_2**	**CH_4**	**CO**	**CO_2**	**H_2O**
(min)	vol (%)	vol (%)	vol (%)	vol (%)	vol (%)	vol (%)
12.2	0.5	58.8	0.41	2.9	16.3	16.3
16.9	3.4	58.6	0.2	2.2	13.4	13.4
31.1	9.7	57.3	0.84	3.6	8.7	8.7

Shown in Table 6.5 is the composition of the atmosphere in the compartment during experiment 11 (elevation 975 mm), measured with the gas chromatograph (refer section 3.1.3). Only those gases that were available to calibrate the gas chromatograph are shown in the table.

It is suspected that the results from the Servomex and Ultramat analysers are more accurate than the results from the gas chromatograph (refer Table 6.5 and Figure 6.11). Occasionally it was found that the results differed by up to 2 or 3 vol %. When the concentrations are as low as 1 vol % an extra 2 or 3 vol % introduces an error of 100 or 200 percent. The results from the Servomex and Ultramat analysers will be used in preference to the gas chromatograph results where possible because of this discrepancy, but mainly because they are a continuous reading.

Stage I: Fire Started – Door Closed (2:00 min – 6:20 min)

Stage I starts when the white sprits are ignited (approximately 2 minutes after the data logger is started), and ends when the door is closed. On average, stage I lasts for approximately four minutes. During this stage, 200 ml of white sprits are burnt under the crib to initiate the crib fire. The door is open during this stage and consequently the upper layer never increases to more than 50 mm thickness.

It was during this stage in experiment 11 that detached and stable burning was observed on the ceiling (refer section 6.1).

Stage II: Door Closed – Smouldering Period (6:20 min – 17:4 min)

This stage starts when the compartment door is closed, and ends when the fire changes from a flaming to a smouldering fire. This transition period is seen externally as the smoke changes from a light grey smoke to a thick white smoke (refer Figures 6.12 and 6.15).

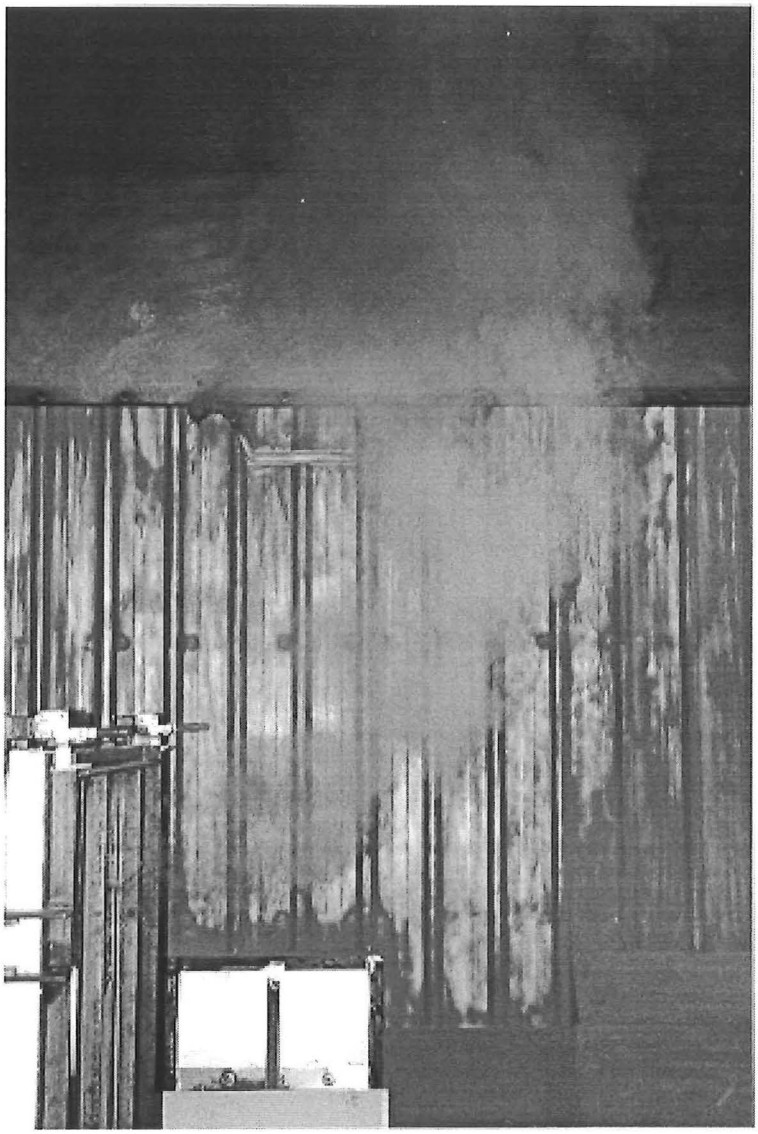

Figure 6.12 - Grey Smoke Production, Experiment 11

It can be observed in Figure 6.11 that immediately after the door was closed the oxygen content in the compartment dropped from 20% to 4% (elevation 900 mm). The fall in oxygen concentration was accompanied by a carbon dioxide increase from 1% to 11%. Carbon monoxide concentration also increased, but only to 2%, which was less than half the maximum concentration reached of 4%, four minutes later. During the next thirteen minutes the oxygen concentration progressively decreased to its lowest level of 1% at 17.4 minutes (end of stage II), the carbon dioxide stayed steady at approximately 14%. However as soon as the carbon monoxide reached its maximum concentration at 11 minutes, it began to decrease

rapidly, reaching a low of 1.3% at 16 minutes. The cause of this decrease is thought to be the increase in the upper layer temperature, as the decrease starts when the upper layer temperature reaches 600°C. This corresponds to the temperature suggested by Gottuk (1992), as the transition between a slow and a fast CO to CO_2 conversion (refer section 2.3.1).

The following chart displaying height versus temperature (rear) can be used to estimate the position of the upper layer in the compartment.

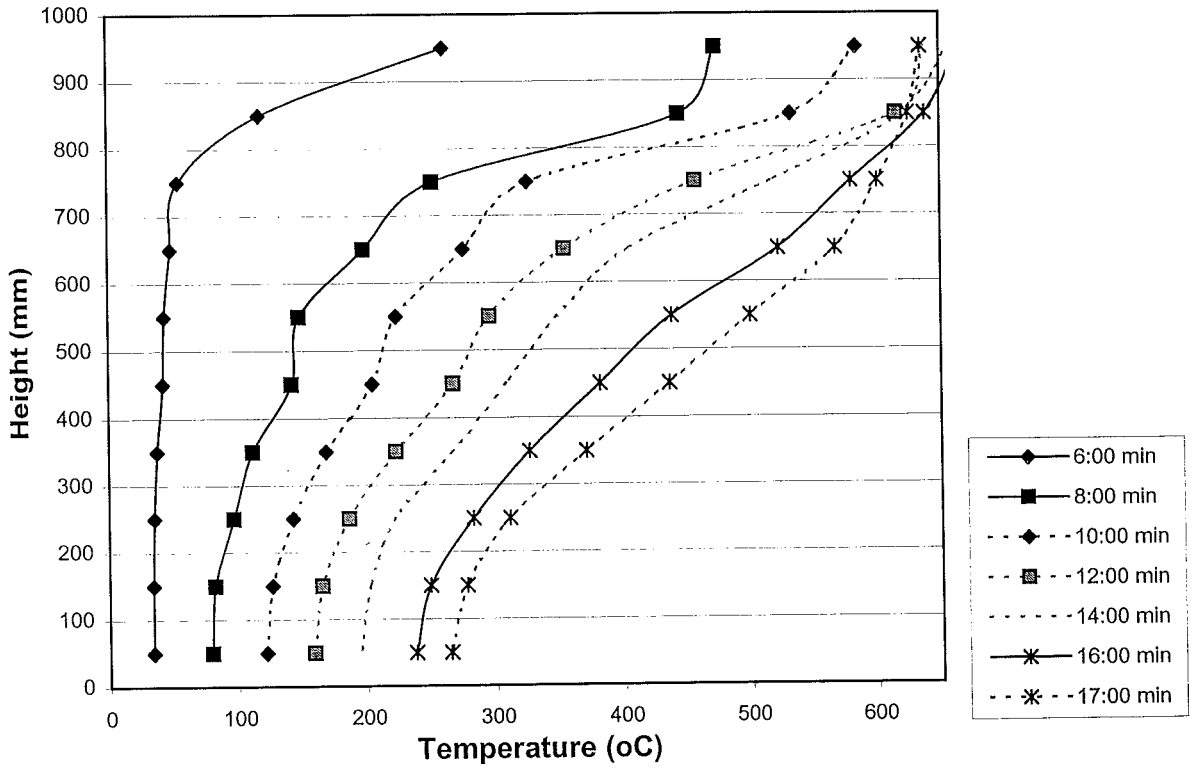

Figure 6.13 Upper Layer Position, Experiment 11- Stage II

As depicted in Figure 6.13 a layer of hot gases deepens in the compartment and reaches a constant depth at approximately 14 minutes, 8 minutes after was door was closed.

At the beginning of this stage, a light grey smoke was discharged from the outlet. The volume of this smoke gradually increased and reached approximately the rate depicted in Figure 6.12. After approximately 5 minutes the grey smoke production stoped, and smoke was not visible from the outlet. This was also noted during the same period in experiment 10. However, the upper and lower compartment pressures (refer Figure 6.10) indicate that there was still approximately the same flow in and out of the compartment. It is likely that the soot

content was so low that the smoke was transparent. Grey smoke was also noted during this stage in experiments, 5, 7 and 10.

It was during the last five minutes of this stage that detached burning at the side of the crib was observed (refer section 6.1). Towards the end of this stage, small puffs of smoke would flow periodically from the lower inlet every 30 seconds. These puffs were found to be caused by detached flaming at the side of the crib burning all the way to the lower inlet (refer section 6.1). Puffing was also noted in experiments 5, 7, and 10 before the start of the smouldering stage. The puffs usually started out moderately small and then became progressively larger towards the end of the stage. During experiment 11, the inflow after a large puff was observed to extinguish the fire. It is also interesting to note that no smoke layer was visible within the compartment during this period of puffing, substantiating the observation of the transparent smoke discussed in the previous paragraph.

Stage III: Smouldering Period – First Smoke Explosion (17:4 min – 23:4 min)

Stage III begins when the fire is extinguished (smouldering), and it ends when the first smoke explosion occurs. Smouldering is seen externally as the production of a thick white smoke (Refer Figure 6.15).

The output from the load-cell indicates that during the smouldering period the rate of fuel vaporization (pyrolysis) slows (refer Figure 6.10). This is expected from a smouldering fire. This decline is noted on the chart as a plateau and is seen before the first smoke explosion in experiments 5, 7, 10 and 11 (refer Figures 6.6 to 6.10). However, two points question the accuracy of the load-cell data during this stage. Firstly, this plateau is not seen before the second explosions in experiments 10 and 11 when the fire is again smouldering. Secondly, at the end of all the plateaus (the smoke explosions), the weight of the cribs drop suddenly, approximately 1 – 1.5 kg. Possible reasons for this are:

1. The explosion might have knocked some of the crib off the fuel table, this was visually observed during the second explosion in experiment 11.

2. Investigation of the plateau region shows that if the plateau is neglected and the load-cell output line is continued at the same slope as before the plateau region, then the two ends connect (refer Figures 6.7 to 6.10). It is possible that the plateau region is caused by the movement of the compartment, which is known to alter the load-cell output (refer section 6.2.1). The start of the plateau region corresponds to the puffing phenomena. The force of the puffing could cause the compartment to move and alter the output of the load cell. The end of the plateau corresponds to a smoke explosion, which could also move the compartment and possibly reset the output on its former path.

The following graph of height versus temperature (rear) can be used to estimate the position of the upper layer in the compartment.

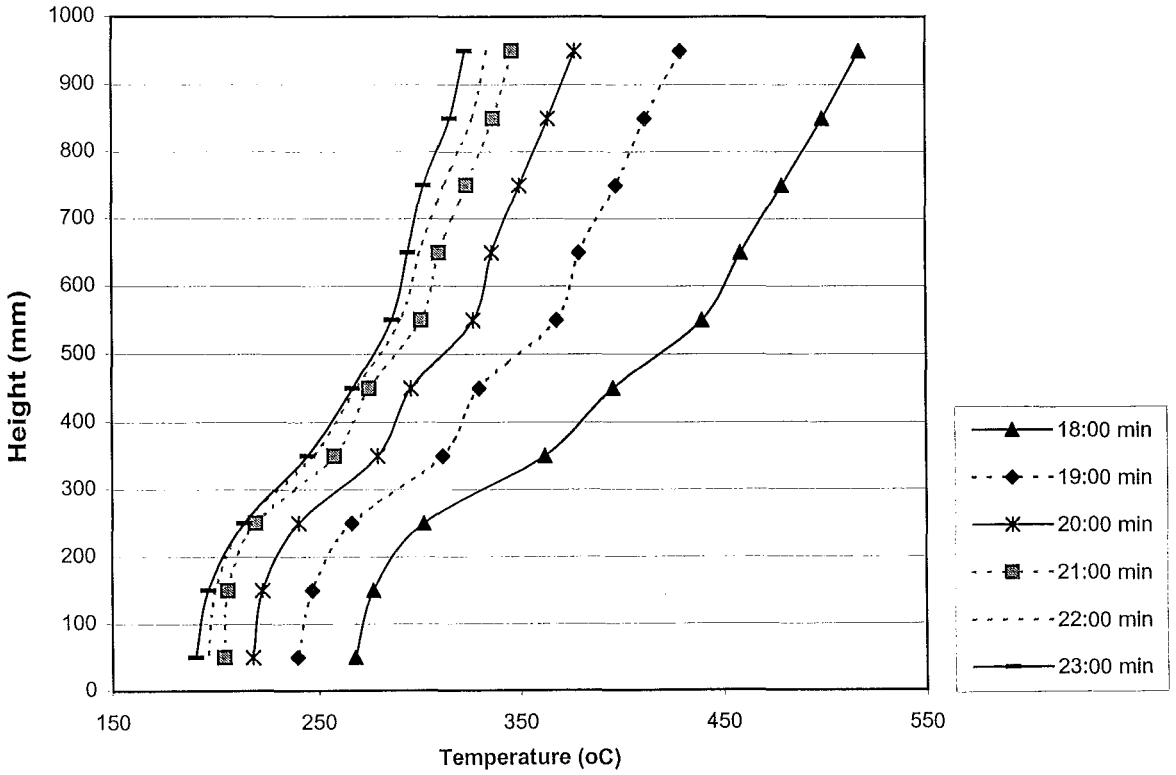

Figure 6.14 Upper Layer Position, Experiment 11- Stage III

As depicted in Figure 6.14 the upper layer in the compartment appears to reach a constant depth at approximately 21 minutes. Before 21 minutes the layer deepens and cools (refer Figure 6.14).

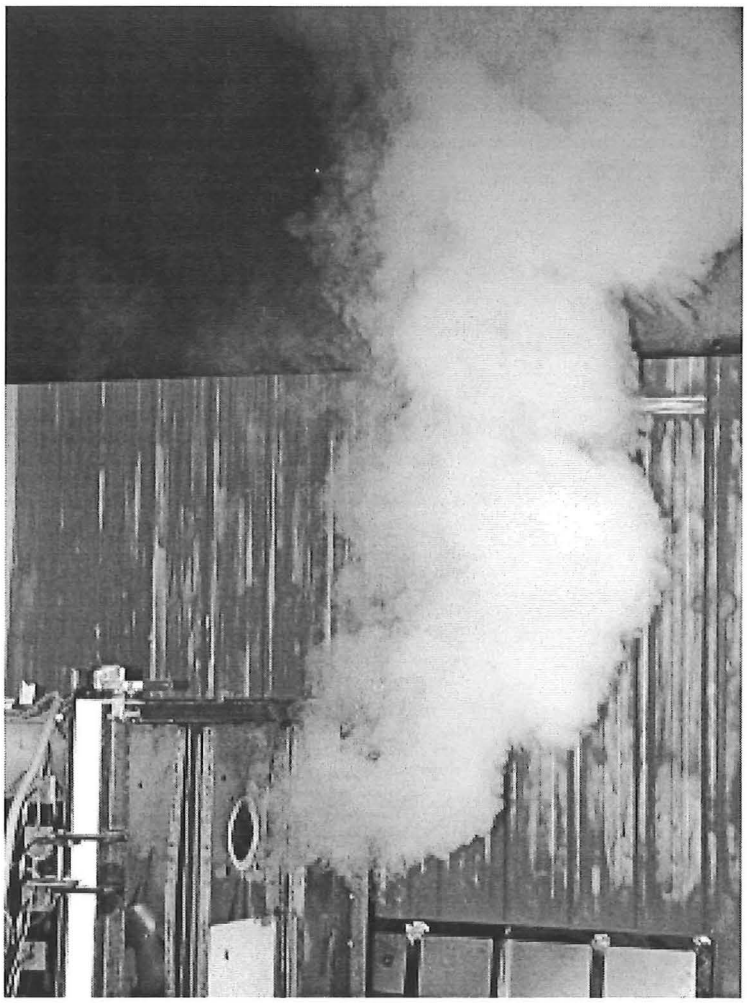

Figure 6.15- White Smoke Production during the Smouldering Period, Experiment 11

It can be seen in Figure 6.10 that there is a very consistent temperature drop during this stage, this is also evident in the other experiments (refer Figure 6.6 to 6.10). Accompanying the temperature drop are a decrease in CO_2 and CO and an increase in O_2 (refer Figure 6.11). Prior to the explosion, the layer in the compartment contained 15% O_2, 4% CO_2, and 1.5% CO.

The most logical reason for the decrease in CO_2 and CO and the increase in O_2 was that the hydrocarbon to CO reaction and the CO to CO_2 reaction were slowed or frozen due to the lower layer temperatures and the absence of a flame (refer section 2.3). If this were the case then the flow in and out of the compartment would effectively flush the contents of the compartment. This would explain the rapid increase in O_2 whilst also accounting for the decrease in CO_2 and CO.

The following two charts depict the volumetric and mass flowrates from both the upper and lower openings during experiment 11. As discussed in section 6.2.3 flowrate data should be treated with caution.

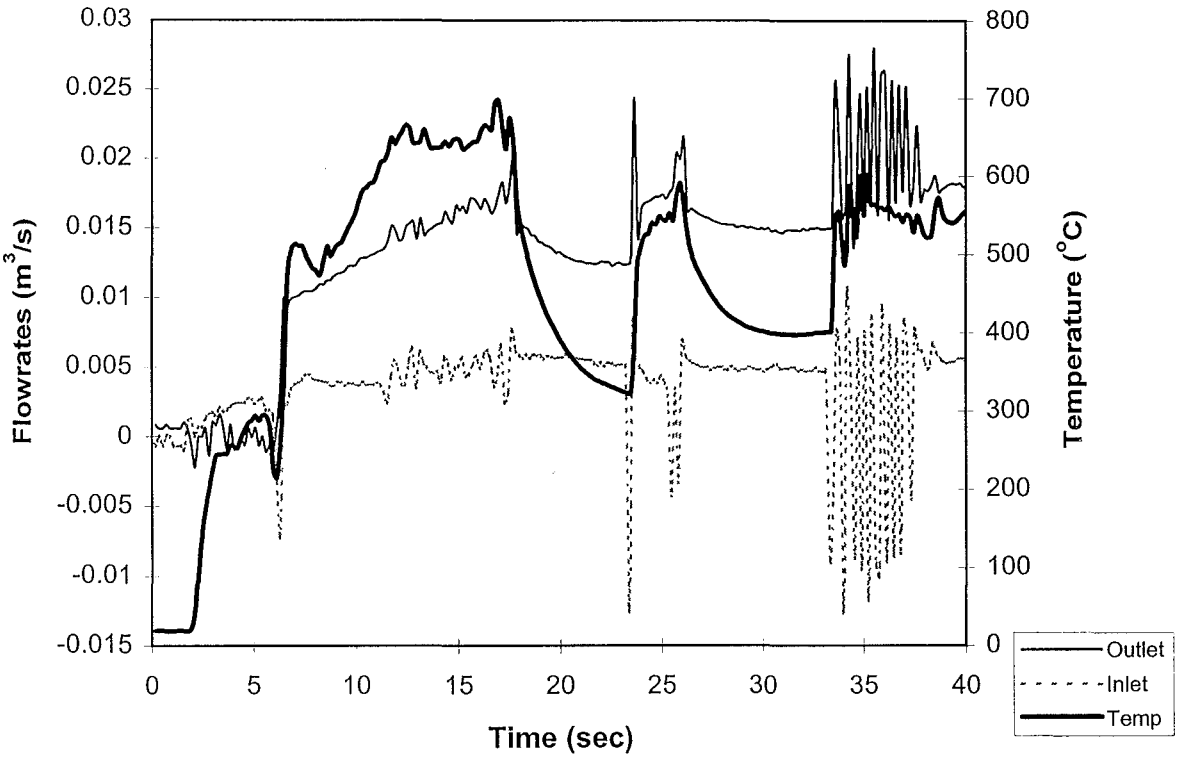

Figure 6.16 Volumetric Flowrates, Experiment 11

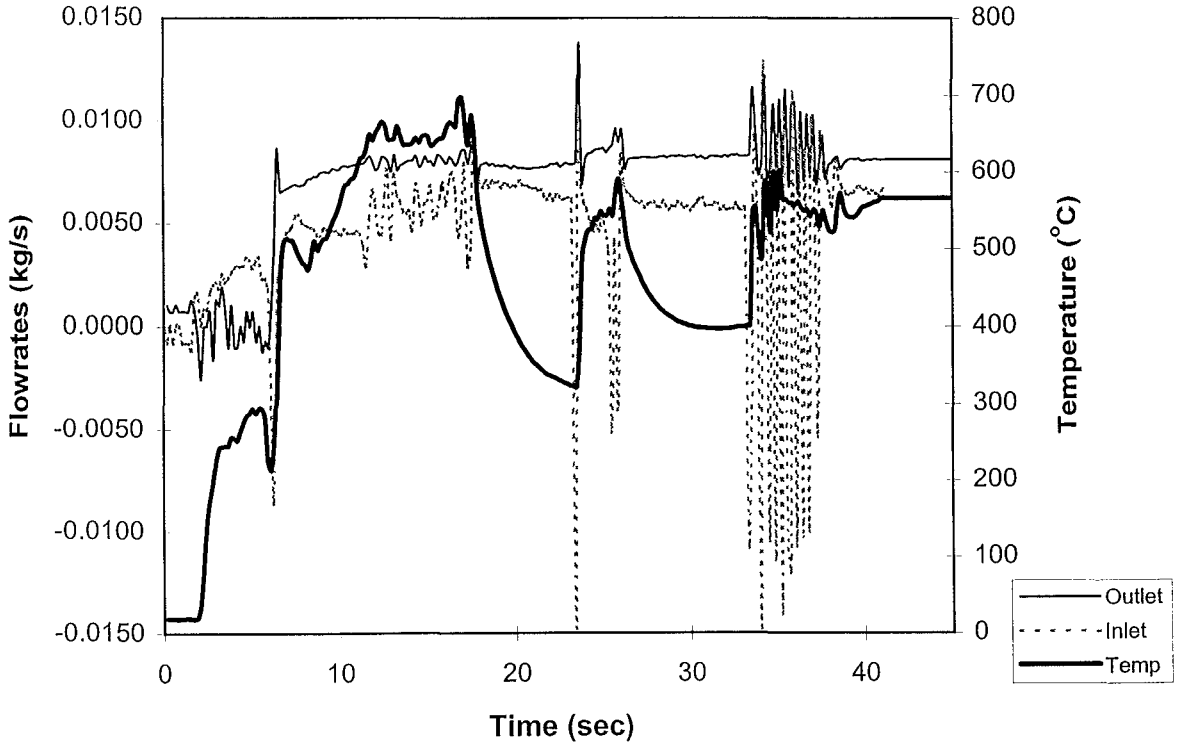

Figure 6.17 Mass Flowrates, Experiment 11

Twenty seconds after the large puff was observed to extinguish the fire, white smoke began to flow from the upper opening; it took only a further two minutes to reach a steady volumetric rate (refer Figure 6.15). Visually the velocity of the white smoke from the opening looked to be higher than that of the grey smoke in stage II. This also compares with what looks to be an increased volume of smoke (refer Figures and 6.12 and 6.15). However, the pressure readings in the compartment indicate that the internal pressure actually decreases during this stage. Figure 6.16 depicts volumetric flows during experiment 11, this chart indicates that the flowrates in and out of the compartment during stage III do indeed drop. However, because there was also a corresponding increase in density the mass flowrates do not differ from those in the previous stage (refer Figure 6.17). Although, both the mass and volumetric flowrates cannot be calculated accurately, because of difficulties in calculating C_v values, changes in flowrates with time are comparable (refer section 2.2.3).

Stage IV: First Smoke Explosion (23:4 min)

Smoke explosions are seen externally as the discharge of high velocity smoke and flames from both the lower and upper openings. In the four experiments where smoke explosions were noted, smoke struck the window of the control room three metres away. This was followed by the ejection of metre-long flames from both openings. The flames (refer Figure 6.20) were noted in all experiments as being conical and tapered, similar to the pre-mixed flame of a jet engine.

Shown in the following chart is the pressure spike produced during the first explosion in experiment 11. This was measured with a MKS Instruments pressure transducer and recorded on a Tektronix oscilloscope (refer section 3.2.1). It is an instantaneous reading unlike the other pressure transducers, for which the outputs are time averaged. The vertical scale on this chart is in units of 500 mV, which represents 5 torr or 660 Pa. From the chart it can be seen that the pressure peaked at approximately 900 Pa during the explosion. The pressure was measured in the top left-hand corner of the compartment, at the same elevation as the upper opening (refer section 3.2.1).

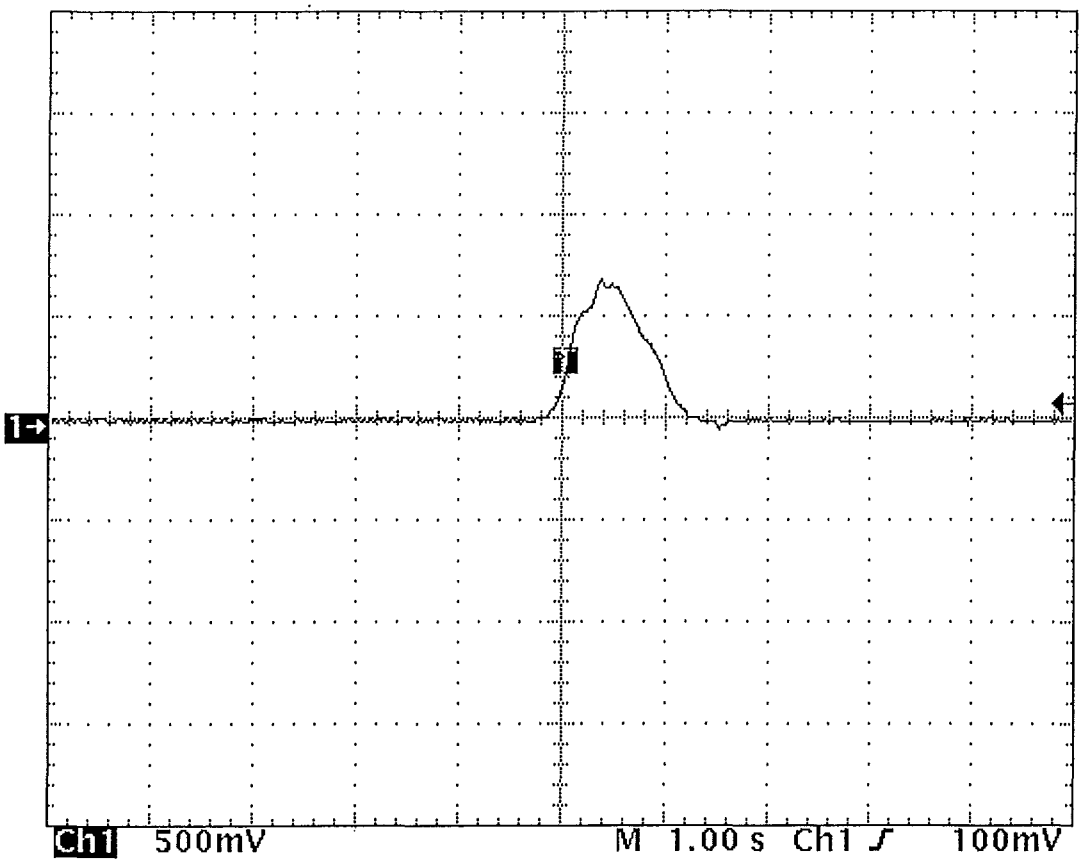

Figure 6.18 – Pressure in the Compartment (Elevation 850 mm, Front Corner) during the first Smoke Explosion, Experiment 11

During the smoke explosion the O_2 concentration dropped from 16% to 1%; the CO_2 concentration increased from 5% to 17.5%; and the CO concentration increased from 1.4% to greater than 5%. Five percent was the maximum measurable concentration of the analyser.

Stage V: First Smoke Explosion – Second Smoke Explosion (23:4 min – 33:3 min)

This stage begins after the first smoke explosion and ends at the start of the second explosion. In the experiments that burnt a 4 kg crib (5 and 7), the fire entered a decay phase directly after the first explosion (refer Figures 6.6 and 6.7).

The following graph of height versus temperature (rear) can be used to estimate the position of the upper layer in the compartment.

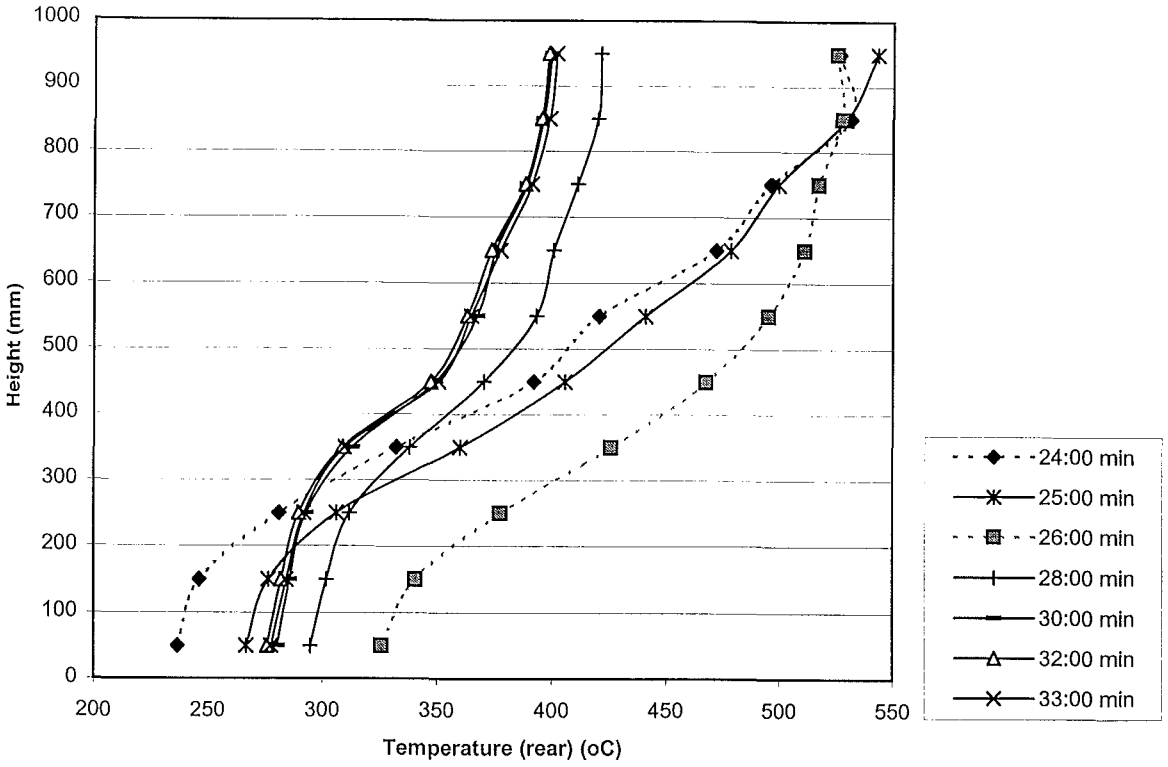

Figure 6.19 Upper Layer Position, Experiment 11- Stage V

Directly after the first explosion, grey smoke (similar to that produced during stage II) began discharging from the upper opening. This occurred for approximately 5 minutes and ended with the puffing phenomena characteristic of stage II. This occurrence is evident from Figure 6.10; the temperature increased directly after the explosion but decreased when the puffing began. Experiment 10 also went through the same process after the first explosion, although it occurred in a shorter time (refer Figure 6.9).

Prior to the second explosion the temperature in the upper layer decreased in a manner similar to that seen before the first explosion (refer Figure 6.10). This temperature drop is also present before the second explosion in experiment 10 (refer Figure 6.9), although it was slightly different to that observed in experiment 11. In experiment 10 the temperature decreased approximately 200°C over 10 minutes once smouldering started. It then increased 70°C over the next 10 minutes before the second explosion (refer Figure 6.9). The reason for this temperature increase is unknown.

No data exists for the concentrations of CO, CO_2, and O_2 during this period because the filter before the Servomex and Ultramat analysers became blocked, after which the analysers had to be switched off.

A comparison of Figures 6.14 and 6.19 shows that the temperature profiles before the first and the second explosions are very similar. Although before the second explosion the temperatures are almost 100°C higher than at the same point before the first explosion (refer Figure 6.10). The reason for this temperature increase is unknown, although some of it may be due to heat radiated from the internal walls and ceiling. The temperature of these surfaces increased as the experiment progressed.

Stage VI: Second Smoke Explosion (33:3 min)

The second smoke explosion depicted in Figure 6.20 was visually no different to the first; smoke and flames were emitted from each opening. However, the second explosion in experiment 11 was larger than the first. The peak pressure measured in the compartment during the second smoke explosion was greater than 2600 Pa, almost three times that produced during the first explosion in experiment 11 (refer Figure 6.21).

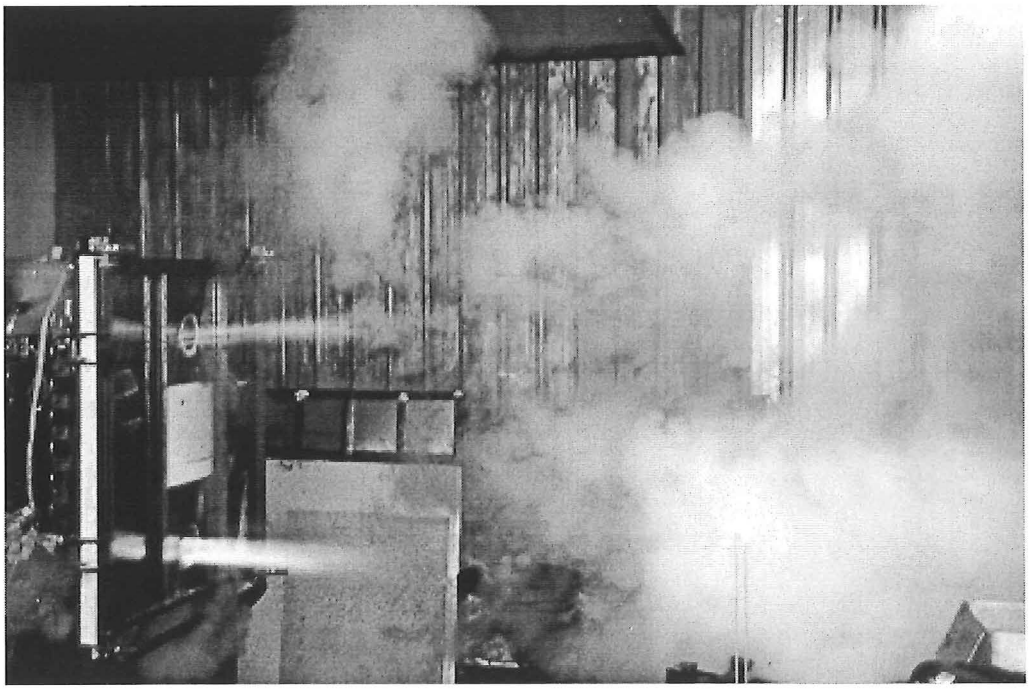

Figure 6.20 – Second Smoke Explosion, Experiment 11

The following chart shows the pressure spike in the compartment during the second smoke explosion. The vertical scale on this chart is in units of 500 mV, which represents 5 torr or 660 Pa.

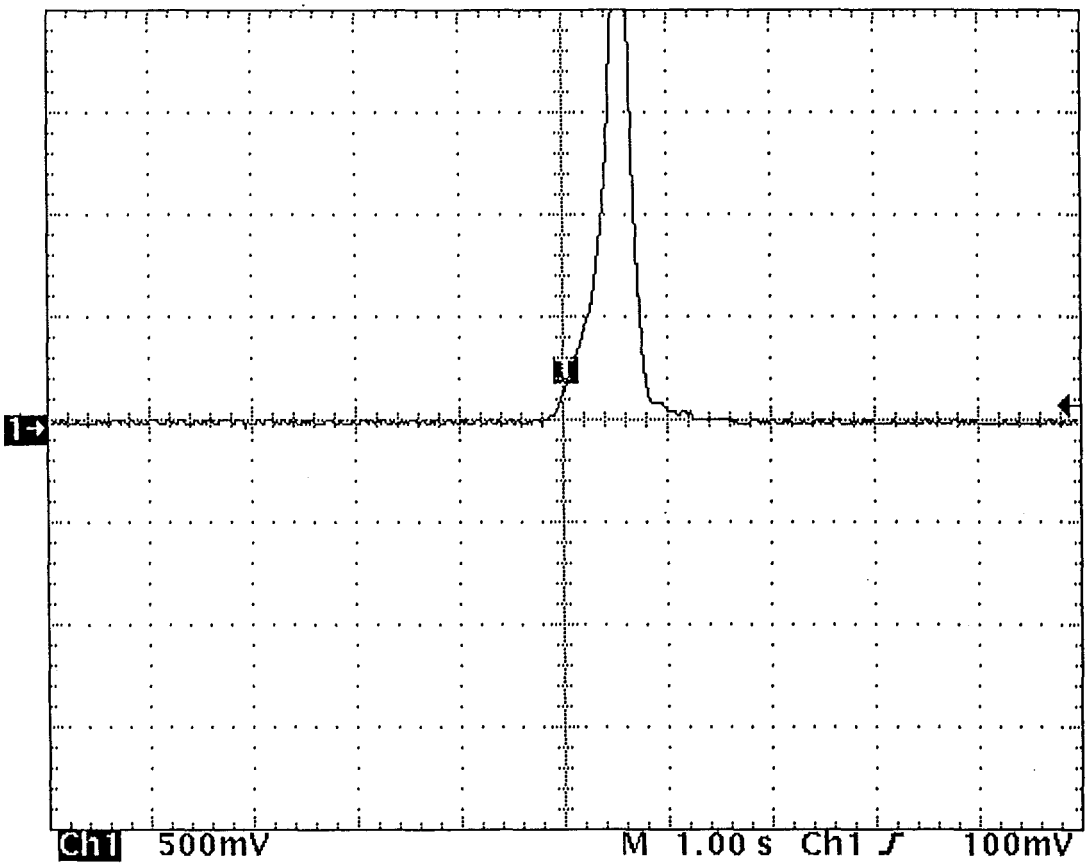

Figure 6.21 – Pressure in the Compartment (Elevation 850 mm, Front Corner) During the Second Smoke Explosion, Experiment 11

Stage VII: Second Smoke Explosion – Decay Period (33:4 min – Extinguishment)

This stage begins at the end of the second smoke explosion and ends when the compartment door is opened and the fire is extinguished.

The fire entered the decay phase after the second explosion in experiment 10, as did experiments 5 and 7 after their first explosion (refer Figures 6.7 and 6.8). However, this was not the case with experiment 11. Directly after the second explosion, smoke and flames were discharged from the lower opening every 30 seconds. This is seen in Figure 6.10 by the

pressure oscillations towards the end of the experiment. In some cases the flames and smoke discharged were as large as those produced during some of the smaller smoke explosions. The cause of these oscillations is unknown, although there are definite similarities to the puffing phenomena seen at the end of stage I, and after the second explosions in experiments 10 and 11.

6.3.3 Experiment 3

It is thought that a smoke explosion occurred during experiment 3, as there is the characteristic temperature drop wedged between two pressure spikes (refer 32 - 36 minutes, Figure 6.6). This trend was also seen before the smoke explosions in experiments 5, 7, 10 and 11.

However, there appears to be a number of other incidents that occurred during experiment 3, all of which have similarities to the smoke explosions produced in experiments 5, 7, 10 and 11. The first of these incidents occurred between 16.5 minutes and 21.2 minutes (refer Figure 6.6). During this time there was a large temperature drop of approximately 100°C, followed by a large temperature increase of approximately 150°C. No pressure spikes were recorded, but this may be due to the time averaging of the data.

The second incident occurred between 21.6 minutes and 24.0 minutes (refer Figure 6.6). This incident has more similarities to a smoke explosion than the first incident. As there is a definite temperature drop at the start of the period (100°C) and a very steep temperature rise at the end of the period (130°C). Associated with the temperature rise is a small spike in the pressures reading.

The third incident occurred between 26.5 minutes and 29.5 minutes (refer Figure 6.6). As with the other incidents there is a large temperature decrease followed by a steep temperature increase. A small pressure spike was also recorded with the temperature rise.

The fourth incident occurred between 30 minutes and 32.4 minutes (refer Figure 6.6). As with the other incidents there is the characteristic temperature drop, accompanied with pressure spikes at either end.

The last incident discussed in the opening paragraph has the strongest similarities to a smoke explosion of all the incidents (refer 32 minutes - 36 minutes, Figure 6.6). It has the characteristic temperature drop and the large pressure spikes at either end.

The cause of these incidents is unknown, none of the characteristic features of a smoke explosion were visually observed during the experiment (high velocity smoke and conical flames). Although it was suspected the compartment 'flashed over' during the experiment. The pressure spikes at the beginning of the last two incidents and the characteristic temperature drop during the last three incidents seems to indicate that a process very similar to a smoke explosion was the cause of these phenomenon. It is likely that the first few incidents were not explosions as defined in section 2.6, but more likely flash fires, although the last incident may have been a smoke explosion.

6.4 Unknown Gaseous Component

In all of the experiments the gas chromatograph (GC) showed the presence of an unknown gaseous component in the compartment. At times the concentration of this component was higher than the GC could measure. However, this does not always correspond to a high concentration. The output from the GC is displayed as a number of peaks, one peak per component. The concentration of each component is proportional to the area under its representative peak; some peaks are short and wide, and some are tall and skinny. Unfortunately the GC will not calculate the area of peak when the peak is above a certain height, as was sometimes the case with the unknown component. Furthermore, even when the GC calculated the area of the unknown component the concentration could not be calculated as the component was unknown (i.e. the chromatograph could not be calibrated with this component).

It is suspected that this unknown component may have been formaldehyde. This is a common product from wood pyrolysis and is also used as the glue in the manufacture of medium density fibreboard, so its presence would not be totally unexpected.

6.5 Chapter Summary

Out of eleven experiments conducted, four produced smoke explosions; the first two (experiments 5 and 7) burnt a 4 kg crib, and produced only a single smoke explosion each. Experiments 10 and 11 burnt an 8 kg crib and produced two smoke explosions each. All four experiments had upper and lower opening diameters of 100 mm. It is suspected that a smoke explosion occurred during experiment 3, which burnt a 4 kg crib with 75 mm openings. Investigation of the temperature and pressure profiles before each explosion revealed that there is a definite phenomenon responsible for forming an explosive atmosphere within the compartment, and then for ignition. Observations made before the explosions revealed that the crib fires had been extinguished, and the fires were smouldering. The cause of extinguishment was found to be the result of a phenomenon termed 'puffing'. More precisely, the puffs are detached burning towards the lower inlet, and the inflow after a large puff was observed to extinguish the fire.

The fuel for the explosions is definitely not carbon monoxide, and is undoubtedly of hydrocarbon nature.

Chapter 7.0 Proposed Mechanism

One of the aims of this research was to develop a mechanism for the occurrence of a smoke explosion. This may now be possible because of the eleven experiments conducted in this study, smoke explosions were produced in four. Even more astonishing is that each fire follows almost the same path before each smoke explosion. This suggests that there is a single process responsible for all the explosions.

The purpose of this chapter is to suggest the most likely mechanism responsible for the smoke explosions. It is probable that this mechanism will be unique to these smoke explosions. It should be noted that in all previous research the smoke explosions produced were the result of low temperature environments, and occurred over long periods (refer section 2.5). In this research smoke explosions, were produced in much shorter times and from high temperature environments.

Contained in Table 7.1 are the temperatures at the start and at the end of the first smouldering phase in experiments 5, 7, 10 and 11. Also contained in the table is the temperature rise due to the first smoke explosion (refer Figures 6.7 to 6.10). Temperatures are from the rear of the compartment, at an elevation of 950mm. The time duration shown in the table is the length of time from the start of the smouldering phase to the smoke explosion. The mass loss is the amount of fuel that has been vaporized before puffing; this does not include the white sprits. The temperatures, times and mass loss data pertain only to the first smoke explosions produced during experiments 5, 7, 10 and 11. Figure 7.1 contains the temperature profiles immediately before the first explosion in experiments 5, 7, 10, and 11. The temperatures are from the rear of the compartment, at an elevation of 950 mm.

Table 7.1 – Data from the Smouldering Period, First Smoke Explosion, Experiments 5, 7, 10 and 11.

Experiment	Crib Size	Mass loss	Temperature (°C)			Time Duration
		(kg)	Start	End	Rise	(min)
5	**4 kg**	2	616	360	201	4.88
7		2.5	664	362	276	5.22
10	**8 kg**	2.3	587	319	162	5.77
11		2.0	674	322	202	5.93

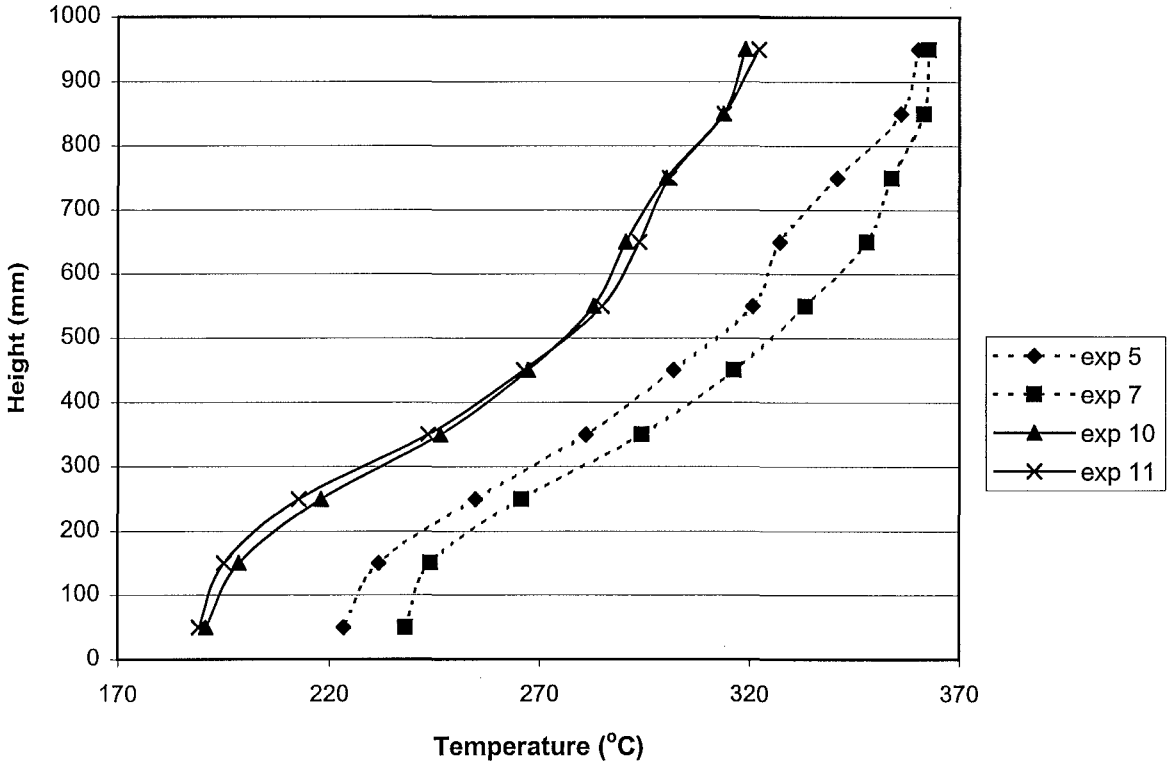

Figure 7.1 Temperature Profiles before the First Explosions.

The following table contains data similar to that contained in Table 7.1 but for experiments 6, 8 and 9. These experiments were setup identically to experiments 5 and 7 but they did not produce smoke explosions. The temperatures are from the 950 mm thermocouple in the rear of the compartment at 17 minutes. Seventeen minutes corresponds to when puffing occurred in experiments 5 and 7. Mass loss is the amount of fuel vaporization that has occurred 17 minutes after the door was closed.

Table 7.2 – Data from Experiments 6, 8 and 9.

Experiment	Crib Size	Mass Loss	Temperature
		(kg)	(°C)
6	4 kg	1.6	580
8	4 kg	1.8	580
9	4 kg	2.3	615

Smoke explosions were produced in experiments 5 and 7 but not in experiments 6, 8 and 9. The only other difference between the experiments is that on average, experiments 5 and 7 were at higher temperatures with faster pyrolysis (refer Tables 7.1 and 7.2). For puffing to occur and cause the extinguishment of an under-ventilated fire, it is likely that the rate of pyrolysis needs to be relatively high. The reason being that the main process of puffing is detached burning, which would require a high pyrolyzate concentration.

7.1 Mechanism

All the smoke explosions produced during this research are believed to follow this basic mechanism, but further experimental work is needed to confirm this mechanism.

1. Initially the cribs burn in an under-ventilated environment and the temperature of the compartment rises to approximately 600-700°C (refer Table 7.1).
2. A phenomenon defined as 'puffing' in section 6.3 extinguishes the fire and the crib smoulders vigorously. Puffing only occurs when the mix of temperature and ventilation is right.
3. Smouldering causes the combustion reactions to essentially stop. Although a small amount of combustion still occurs at the fuel surface (refer section 2.4). As there is no high temperature reaction-zone and the temperature of the layer is not hot enough, heat generation stops. However as the temperatures are still relatively high, pyrolysis continues.

4. Temperatures in the compartment ensure there is still flow in and out; consequently, the temperature drops as the compartment is slowly flushed with ambient air.
5. Flushing causes carbon monoxide and carbon dioxide levels to decrease whilst oxygen levels increase.
6. Pyrolysis is still occurring, and the concentration of pyrolyzates in the compartment increases.
7. When the right concentrations of oxygen and pyrolyzates exist in the compartment with an ignition source a smoke explosion occurs.

However, the mechanism is slightly more complicated than described above because there appears to be a definite triggering mechanism for the explosions. This is evident because:

1. The temperatures at the start of the smouldering phase are scattered between 587°C and 674°C; there are no similarities between the four temperatures (refer Table 7.1). This is not the case for the temperatures at the end of the smouldering phase (just before the explosion). For the identical experiments 5 and 7, the temperature profiles in the compartment are within 10°C at almost all locations measured (refer Figure 7.1). For identical experiments 10 and 11 the temperature profiles are almost identical at all locations (refer Figure 7.1).
2. In experiments 5 and 7 the smouldering phase lasted for 4.9 and 5.2 minutes respectively. In experiments 10 and 11 smouldering lasted for 5.8 and 5.9 minutes. In both cases the higher starting temperatures corresponded to a slightly longer duration, both reaching the same end temperature. This suggests a single identical step is responsible for the ignition of each smoke explosion.

The actual ignition source is undoubtedly the initiation of a flame from the smouldering crib. However, it will be one of the following four variables that will determine when ignition occurs.

- Temperature
- Layer height

- Fuel concentration
- Oxygen concentration

Although the temperatures are very similar before the explosions in experiments 5 and 7 and in experiments 10 and 11, it is very unlikely that temperature triggers the explosion. As during the smouldering phase the temperature decreases. Spontaneous ignition would be expected earlier when there were higher temperatures. This is basically the trigger that causes a flashover in a compartment fire.

In a hypothetical situation where high concentrations of fuel and oxygen are present in the upper-layer but the layer cannot be ignited until it descends to the ignition source. The layer height could be responsible for ignition. It is very unlikely that a descending layer triggered the explosions produced in this research, as:

1. The compartment is only one metre high. This sort of process would be expected from much higher compartments.
2. The layer height reaches it maximum depth 3 to 4 minutes before the explosion occurs. Most of the crib is fully submerged within the layer long before explosion occurs (refer Figures 6.14).

It is also unlikely that fuel concentration in the upper layer triggers the explosions. This is based upon the duration of the smouldering period; the period during which the concentration of fuel builds up in the upper layer. In experiments 5 and 7, this duration is smaller by approximately three-quarters of a minute than in experiments 10 and 11. If fuel concentration was the trigger, then the explosions should have occurred sooner during experiments 10 and 11 than in experiments 5 and 7. As in experiments 10 and 11 an 8 kg crib was burnt, compared with the 4 kg cribs burnt during experiments 5 and 7. The 8 kg crib has twice the surface area. This should therefore lead to a faster production of pyrolyzates and an explosion sooner.

The most likely trigger is the build up of oxygen in the upper layer. This explains the shorter duration of the smouldering phase in experiments 5 and 7. In these experiments the internal

pressures and temperatures are higher (refer Figures 6.6 to 6.7 and Figure 7.1). Therefore there would be a greater flowrate through the compartment. Greater flowrates would lead to a faster build up of oxygen in the upper layer and an explosion sooner, as seen in experiments 5 and 7, (refer Table 7.1). It is also occurs that the higher starting temperatures in experiments 5 and 7 and in experiments 10 and 11 correspond to slightly longer periods of smouldering (refer Table 7.1). It is suspected that the higher starting temperatures in experiments 7 and 11 correspond to lower initial oxygen concentrations in the compartment. A higher internal temperature indicates that there would be more combustion; therefore, there should be a lower oxygen concentration. If this were the case then the experiments with the higher initial temperatures (lower oxygen concentrations) would take longer to build up the required oxygen concentration to initiate flaming. This is thought to be the reason why there were slightly longer periods of smouldering in experiments 7 and 11.

Approximately a minute before the first explosion during experiment 11, the oxygen concentration plateaus at 15% (elevation 900 mm), not at the ambient concentration of 21%. There are two possible reasons for this plateau:

1. There is still combustion occurring at the fuel surface. The 15% O_2 might be the balance between what is expended during combustion (refer section 2.4) and what flows in and out of the compartment.
2. The other possible reason is that the filter became blocked at this point; it is definitely known that this filter was blocked shortly after this. This filter is fitted in-line before the Servomex and Ultramat analyser, so blocking this may cause an increase in the response time of the analysers. This would been seen as a plateau or a very sluggish response in Figure 6.8.

The Fire Research Station concluded after their study on the explosion at Chatham Dockyards that the ignition source was the development of the smouldering fire into a flaming fire (refer section 2.5). The same process is believed to have the caused ignition of the smoke explosions produced in experiments 5, 7, 10 and 11. It is suspected that ignition occurs after approximately the same time duration in each of the experiments (refer Table 7.1 and Figure 7.1) because the smouldering cribs are brought to flaming ignition when the oxygen reaches a

critical concentration. For experiment 11 this concentration was 15% (elevation 900 mm), for experiments 5, 7 and 10 the O_2 concentration was not measured continuously, and therefore it is unknown.

Chapter 8.0 Conclusions

The following is the suggested mechanism for the smoke explosions that occurred in this research:

1. Initially the cribs burn in an under-ventilated environment and the temperature of the compartment rises to approximately 600-700°C.
2. A phenomenon defined as 'puffing' extinguishes the fire and the crib smoulders vigorously.
3. Smouldering causes most of the combustion to stop, but because the temperatures are still relatively high, pyrolysis continues.
4. Temperatures in the compartment ensure there is still flow in and out; consequently, the temperature drops as the compartment is slowly flushed with ambient air.
5. Carbon monoxide and carbon dioxide levels decrease whilst oxygen levels increase.
6. Pyrolysis ensures that the concentration of pyrolyzates in the compartment increases.
7. When the concentration of oxygen in the compartment reaches a critical concentration, the smouldering fire is brought to flaming.
8. The high concentration of oxygen and pyrolyzates in the compartment and the ignition source generates a smoke explosion.

Carbon monoxide was not the major fuel source for the smoke explosions in this research. The fuel source is undoubtedly of hydrocarbon nature.

The smoke explosions produced in this research were the result of smouldering fires. A phenomenon referred to as 'puffing' is the process that extinguished of the under-ventilated fires, and initiated smouldering. It is suspected that puffing will only occur when the temperatures and the pyrolysis rate are high, as puffing is essentially detached burning requiring a high pyrolyzate concentration.

The smoke explosions produce in this research were the result of a vigorously smouldering fire. The Fire Research Station (Borehamwood, England) concluded that an explosion at Chatham Dockyards was the result of a slow smouldering foam mattress fire. It is a recommendation that all smouldering fires be treated with caution independent of the fire's level of activity and the temperature.

Chapter 9.0 Future Research

The completeness of this research was limited largely by time; as such there are many questions that remain unanswered and theories that require validation. Anyone attempting to undertake further research in this area may find the following list of recommendations useful.

- The puffing phenomena found to be responsible for the extinguishment of the fires and the development of smouldering is only barely understood. Questions that remain unanswered are:

    1. What is the process responsible and why does it only occur only with certain sized openings and at relatively high temperatures?
    2. Why is the air inflow after a puff large enough to extinguish a developed fire?

    If only one gas analyser is available for future research then during puffing this should be sampling from the same elevation as the base of the crib. This might lead to an indication of what causes puffing. If possible, an anslyser capable of measuring the hydrocarbon content would be ideal. A window installed in the side of the compartment might help explain exactly what occurs and why the inflow after the puffs have such an affect. Varying the size of the ventilation opening between 75 mm and 100 mm should be investigated; this could help further comprehend the process responsible.

- A mechanism was suggested from this research, it highlights the oxygen concentration as the trigger for the smoke explosions. It would be interesting to note whether this mechanism could be applied to situations like the Chatham Dockyard incident. To test this a slow smouldering fire would be required; this might be accomplished by severely limiting the ventilation at both the compartment and at the fuel.

- Experimenting with increasing amounts of fuel may allow a prediction of the pressures expected from a smoke explosion in an actual fire.

- Oxygen concentrations could not be properly validated as the trigger for the smoke explosions. Validating this should be possible if the hydrocarbon content was continually measured and a window was installed in the compartment.

Chapter 11.0 References

Beyler, C. L. (1986), "Major Species Production by Diffusion Flames in a Two-Layer Compartment Fire Environment", Fire Safety Journal, v10, 47-56.

Bryner, N. P., Johnsson, E. L. Pitts, W. M., (1994), "Carbon Monoxide Production in Compartment Fires – Reduced – Scale Enclosure Test Facility", National Institute of Standards and Technology, US, NISTIR 94-5568.

Chang R. (1998), "Chemistry", McGraw Hill, Sixth Edition, US.

Croft, W. M. (1980), "Fires Involving Explosions – A Literature Review", Fire Safety Journal, 3, 3-24.

de Nevers N. (1991), "Fluid Mechanics for Chemical Engineers", McGraw Hill, US.

Dosanjh, S. S., Pagni, P. J., Carlos Fernadez-Pello, A., (1987), "Forced Cocurrent Smoldering Combustion", Combustion and Flame, 68, 131-142.

"Fatal Mattress Store Fire at Chatham Dockyards", (1975), Fire, 67, 388.

Gottuk, D. T. (1992), "Generation of Carbon Monoxide in Compartment Fires", National Institute of Standards and Technology, US, NIST-GCR-92-619.

Gottuk, D. T., Roby, R. J., Beyler, C. L. (1995), "The Role of Temperature on Carbon Monoxide Production in Compartment Fires", Fire Safety Journal, 24, 315-31.

Gottuk, D. T., Roby, R. J., Peatross, M. J., Beyler, C. L. (1992), "Carbon Monoxide Production in Compartment Fires", Journal of Fire Protection Engineering, 4, 133-150.

Jost, W. (1946), "Explosions and Combustion Processes in Gases", McGraw-Hill Book Company, London, 1946.

Leonard, S., Mulholland, G. W., Puri, R., Santoro, R. J. (1994), "Generation of CO and Smoke During Underventilated Combustion", Combustion and Flame, 98, 20 –34.

Parkes A. R. (1996), "Under-Ventilated Compartment Fires - A Precursor to Smoke Explosions", Fire Engineering Research Report, University of Canterbury.

Pitts, W. M. (1997), "An Algorithm for Estimating Carbon Monoxide in Enclosure Fires", Fire Safety Science-Proceedings of the Fifth International Symposium, 535-546.

Pitts W. M. (1994), "Limitations of the Global Equivalence Ratio Concept for Predicting CO Formation in Room Fires", Fire Research Institute, Japan.

Pitts, W. M., Johnsson, E. L., Bryner, N. P. (1994), "Carbon Monoxide Formation in Fires by High Temperature Anaerobic Wood Pyrolysis", Twenty Fifth Symposium (International) on Combustion, The Combustion Institute, 1455-1462.

Rogers G. F. C. (1992), Mayhew Y. R., "Thermodynamic and Transport Properties of Fluids", Blackwell Publishers, US.

Russel, D. (1983), "Seven Fire Fighters Caught In Explosion", Fire Engineering, April, 22-23.

Servomex, (1994), "540A Oxygen Analyser Instruction Manual".

Siemens, (1997), "Instruction Manual for Ultramat 6E, Analyzers for IR – Absorbing Gases", Germany.

Society of Fire Protection Engineers, National Fire Protection Association, (1995) "The SFPE Handbook of Fire Protection Engineering", National Fire Protection Association, US.

Solomons G. (1992), "Organic Chemistry", Wiley, Fifth Edition, US.

Sugawa, O., Kawagoe, K., Oka, Y., Ogahara, I. (1989), "Burning Behaviour in a Poorly-Ventilated Compartment Fire – Ghosting Fire", Fire Science & Technology, 9, (2), 5-14.

Wiekema, B. J, (1984). "Vapour Cloud Explosions – an Analysis Based on Accidents", Journal of Hazardous Materials, 8, 295-329.

Wooley, W. D., and Ames, S. A. (1975), "The Explosive Risk of Stored Foamed Rubber", Building Research Establishment, Current Paper 36/75, Borehamwood, UK.

Appendices

A. Experimental Results, Experiments 1 – 11.

B. Burning Regimes of the 4 kg Crib and the 8 kg Crib.

Appendix A. Results from Experiments 1 to 11

A1. Fuel Vaporisation Rate, Temperatures and Pressures Profiles, Experiments 1 – 11.

A2. Compartment Temperature Profiles (Rear), Experiments 1 –11.

A3. Compartment Temperature Profiles (Front), Experiments 1 –11.

A4. Gas Composition of the Compartment (Elevation 900 mm), Experiments 6 and 11.

A5. Raw Data from the Gas Chromatograph, Experiments 1- 11.

A1. Fuel Vaporisation Rate, Temperature and Pressure Profiles.

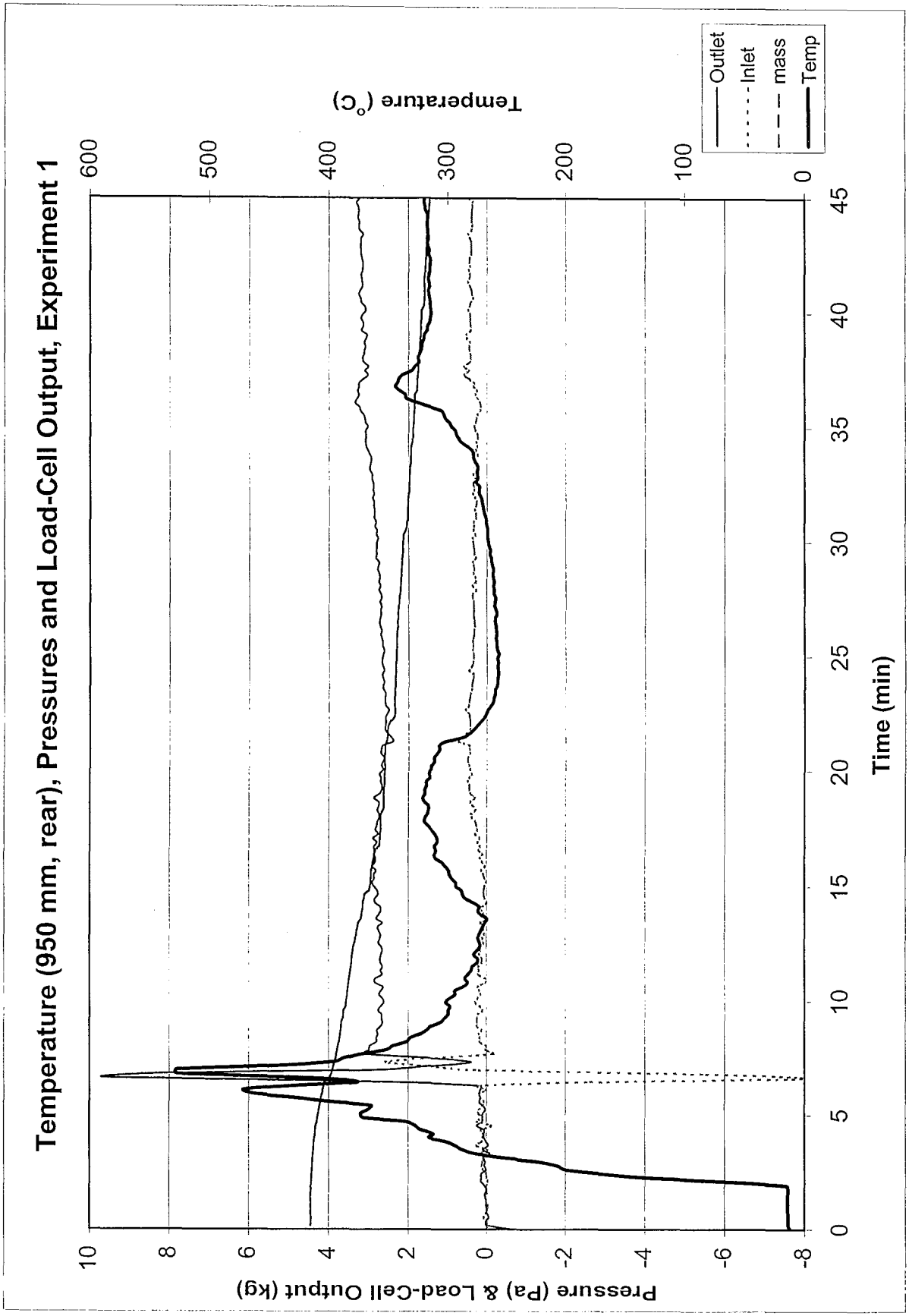

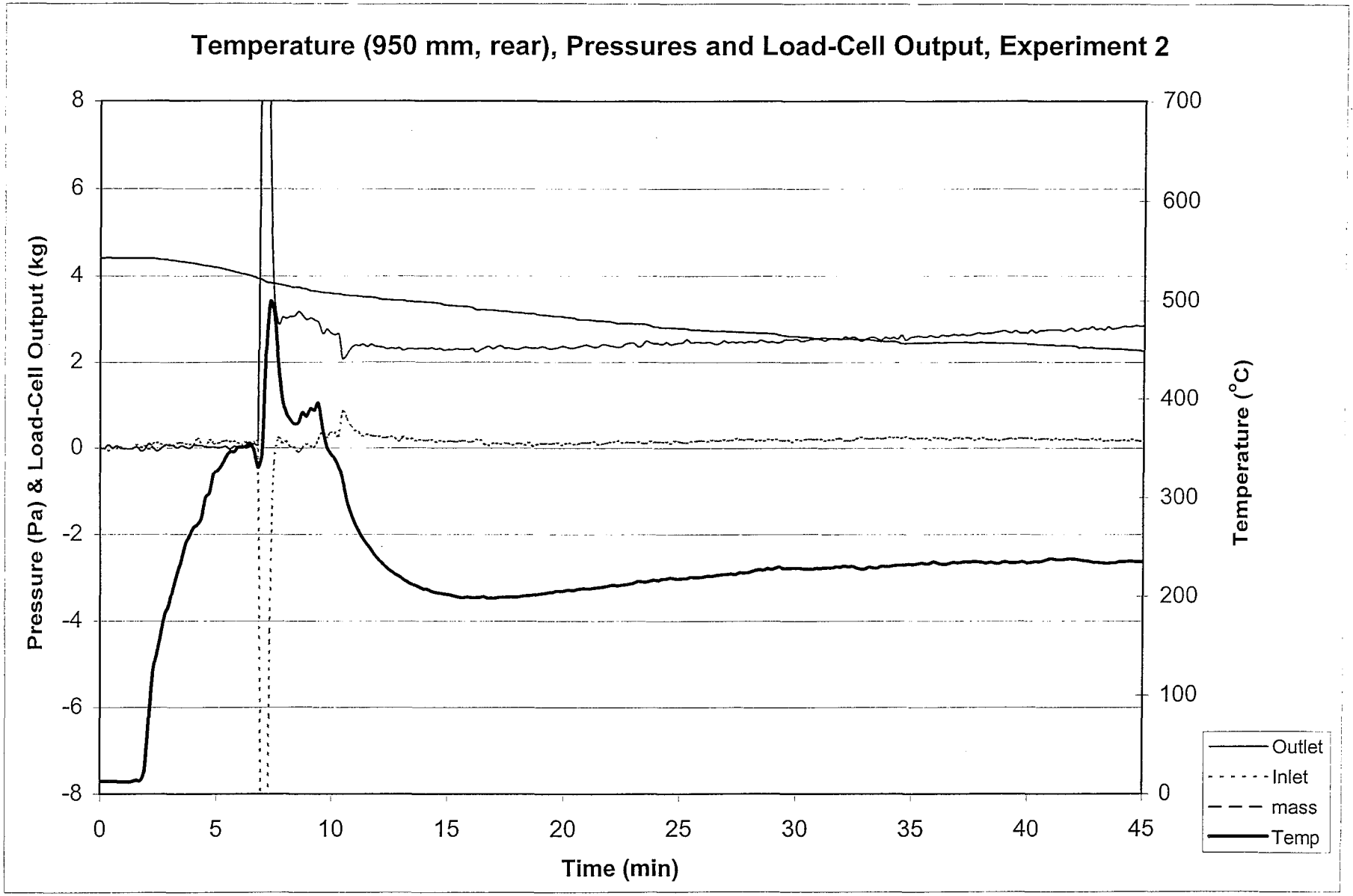
Temperature (950 mm, rear), Pressures and Load-Cell Output, Experiment 2
Pressure (Pa) & Load-Cell Output (kg)
Temperature (°C)
Time (min)
8
6
4
2
0
-2
-4
-6
-8
700
600
500
400
300
200
100
0
0
5
10
15
20
25
30
35
40
45
Outlet
Inlet
mass
Temp

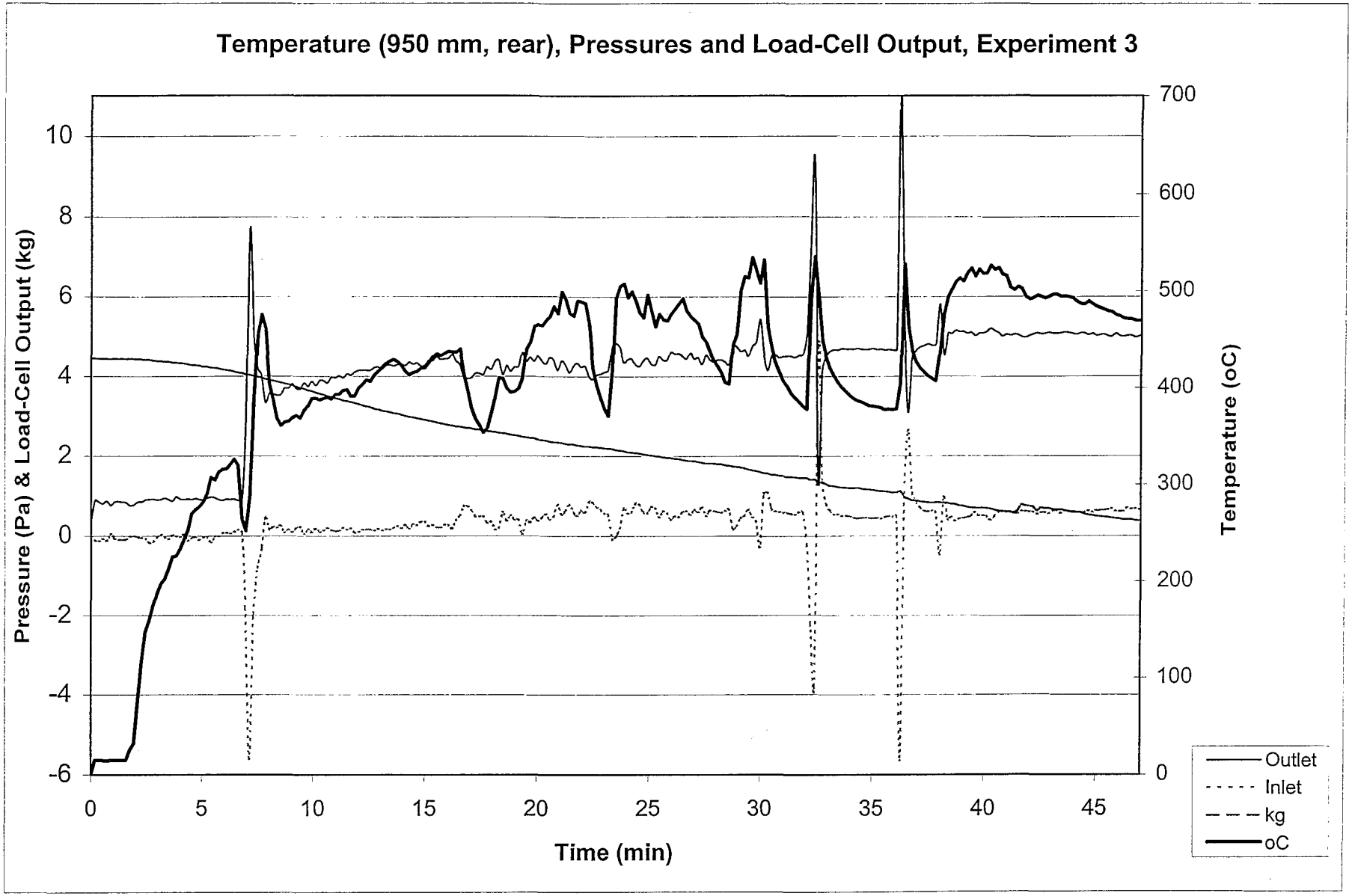
Temperature (950 mm, rear), Pressures and Load-Cell Output, Experiment 3
Pressure (Pa) & Load-Cell Output (kg)
Temperature (oC)
Time (min)
10
8
6
4
2
0
-2
-4
-6
700
600
500
400
300
200
100
0
0
5
10
15
20
25
30
35
40
45
Outlet
Inlet
kg
oC

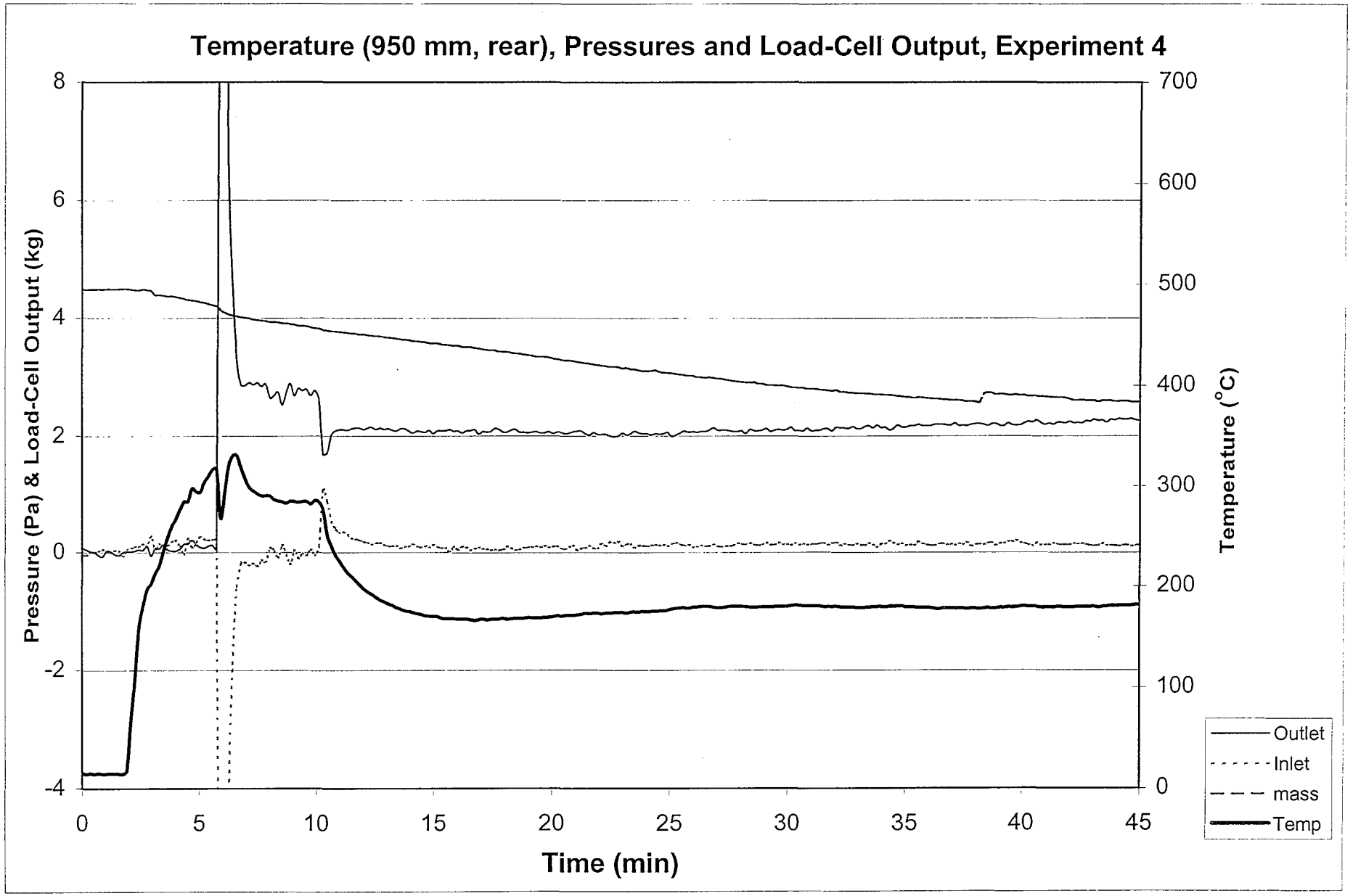
Temperature (950 mm, rear), Pressures and Load-Cell Output, Experiment 4
Pressure (Pa) & Load-Cell Output (kg)
Temperature (°C)
Time (min)
8
6
4
2
0
-2
-4
700
600
500
400
300
200
100
0
0
5
10
15
20
25
30
35
40
45
Outlet
Inlet
mass
Temp

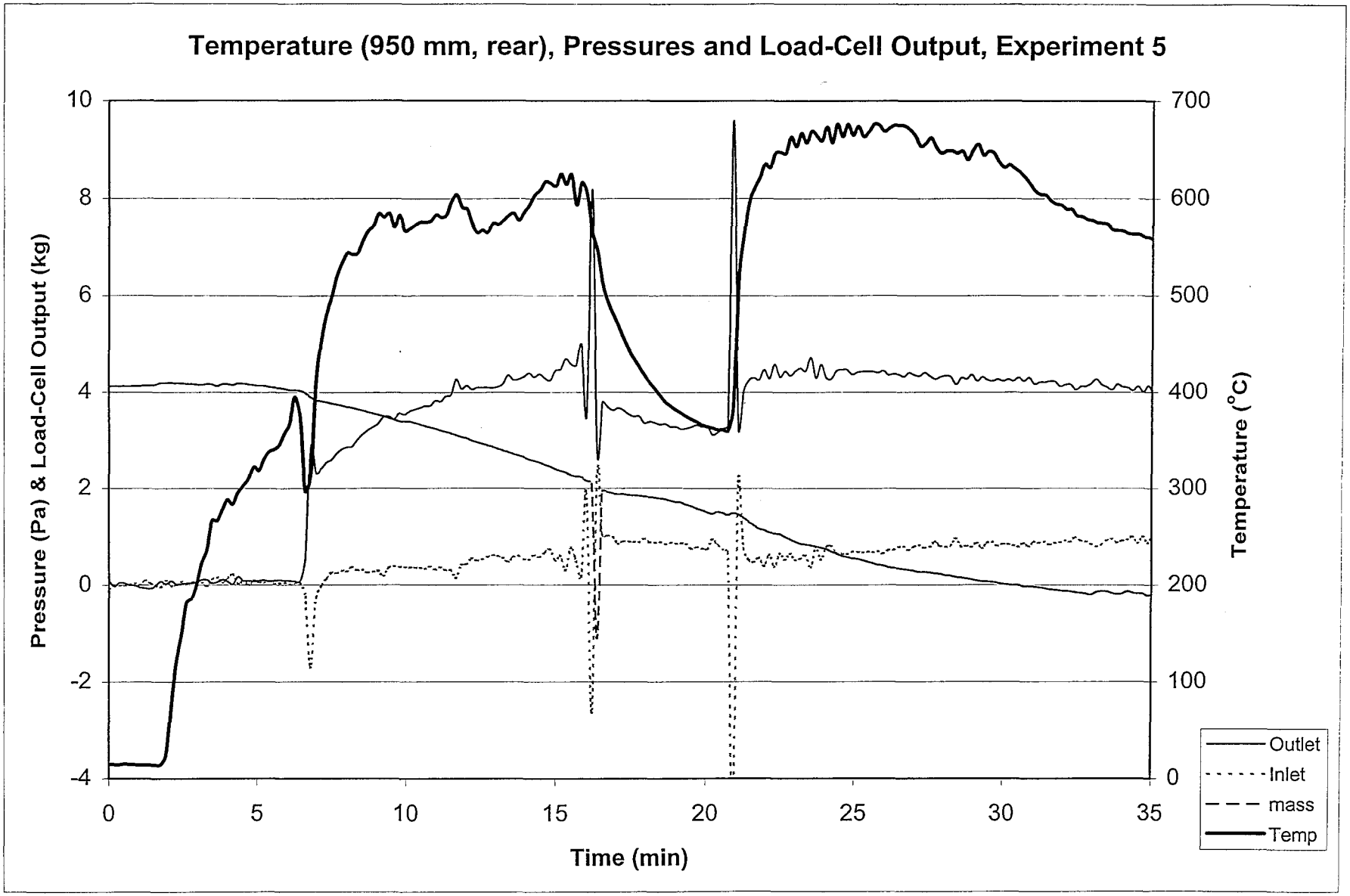
Temperature (950 mm, rear), Pressures and Load-Cell Output, Experiment 5
Pressure (Pa) & Load-Cell Output (kg)
Temperature (°C)
Time (min)
10
8
6
4
2
0
-2
-4
700
600
500
400
300
200
100
0
0
5
10
15
20
25
30
35
Outlet
Inlet
mass
Temp

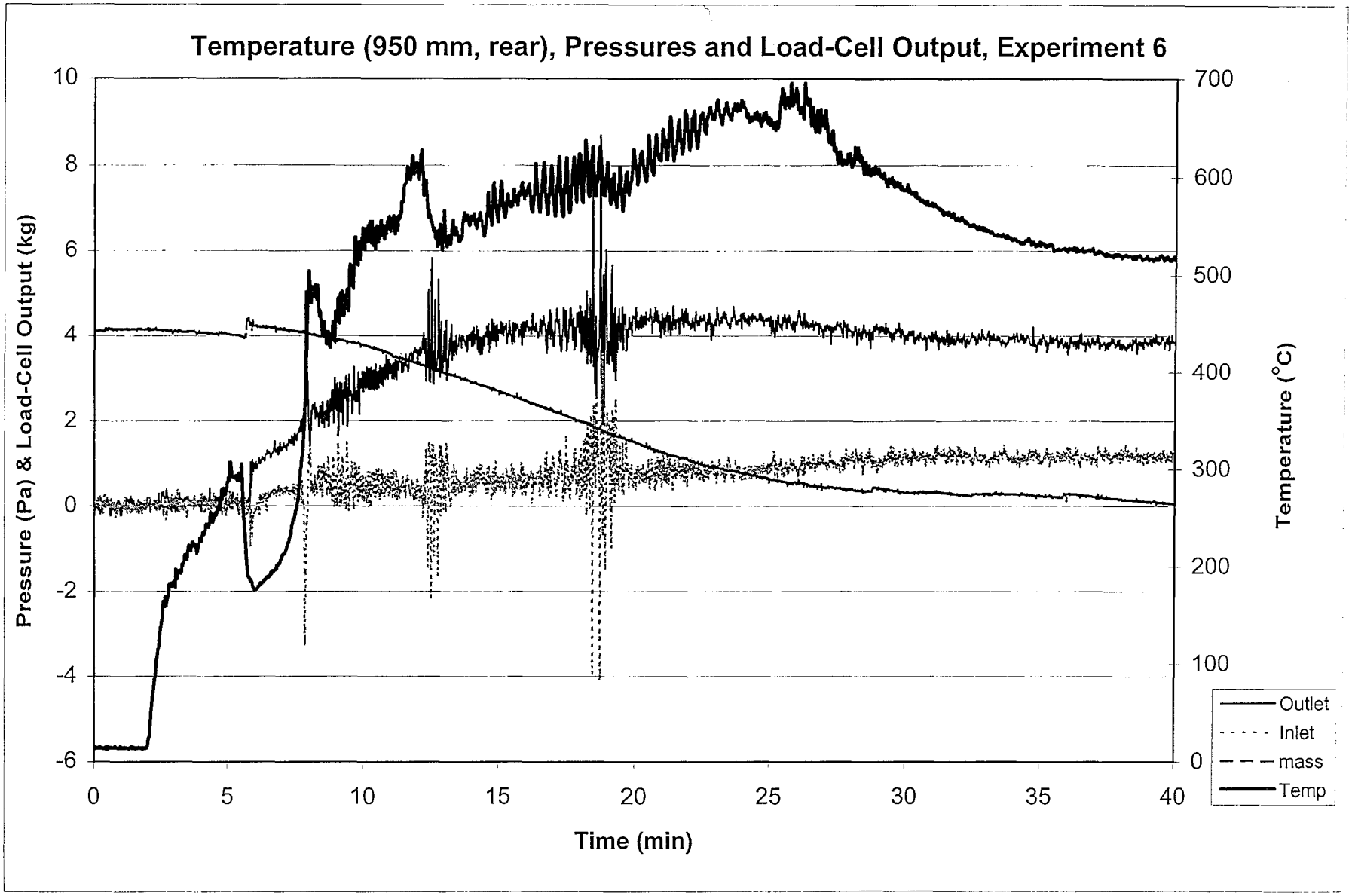
Temperature (950 mm, rear), Pressures and Load-Cell Output, Experiment 6
Pressure (Pa) & Load-Cell Output (kg)
Temperature (°C)
Time (min)
10
8
6
4
2
0
-2
-4
-6
700
600
500
400
300
200
100
0
0
5
10
15
20
25
30
35
40
Outlet
Inlet
mass
Temp

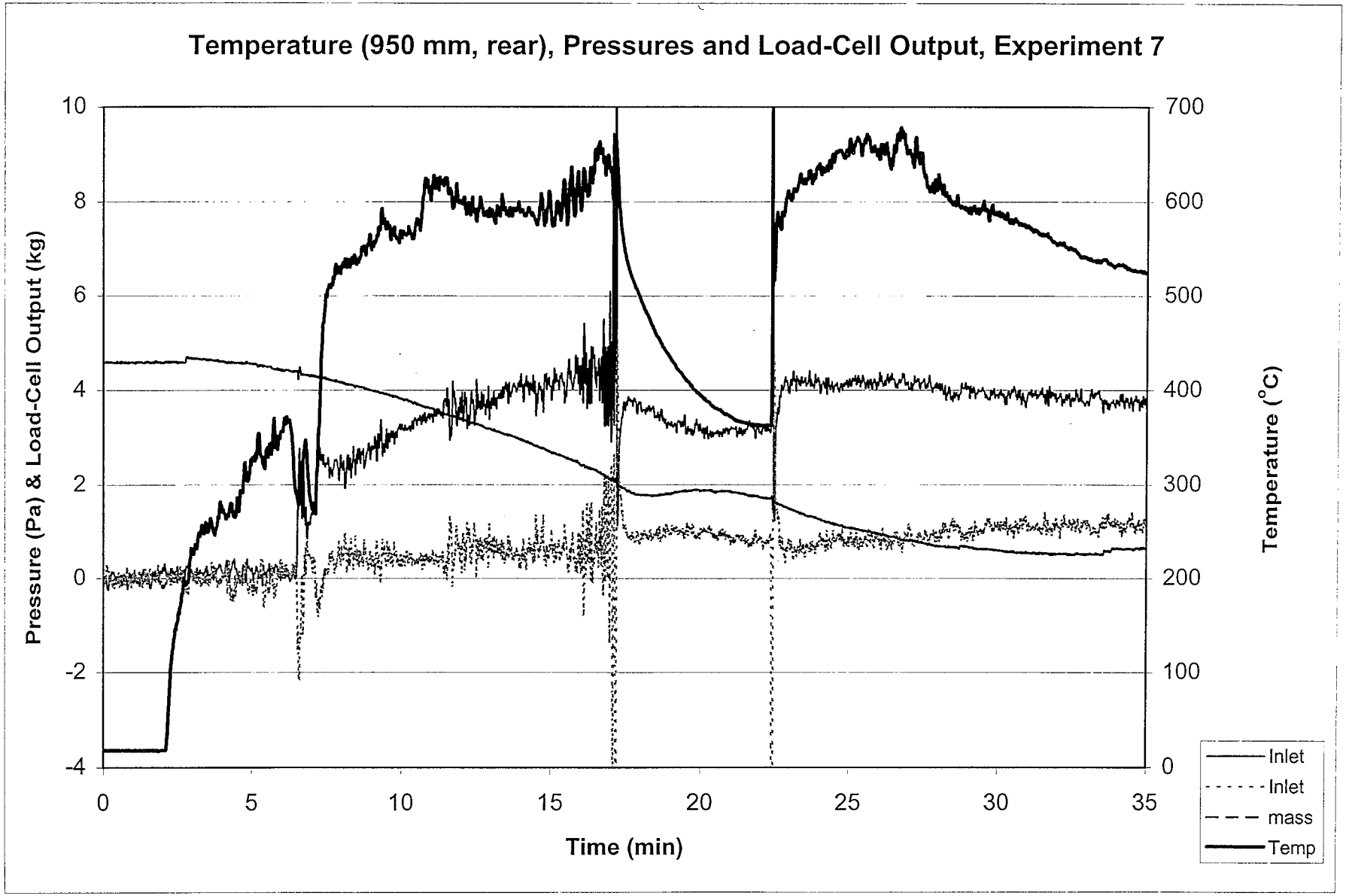
Temperature (950 mm, rear), Pressures and Load-Cell Output, Experiment 7
Pressure (Pa) & Load-Cell Output (kg)
Temperature (°C)
Time (min)
10
8
6
4
2
0
-2
-4
700
600
500
400
300
200
100
0
0
5
10
15
20
25
30
35
Inlet
Inlet
mass
Temp

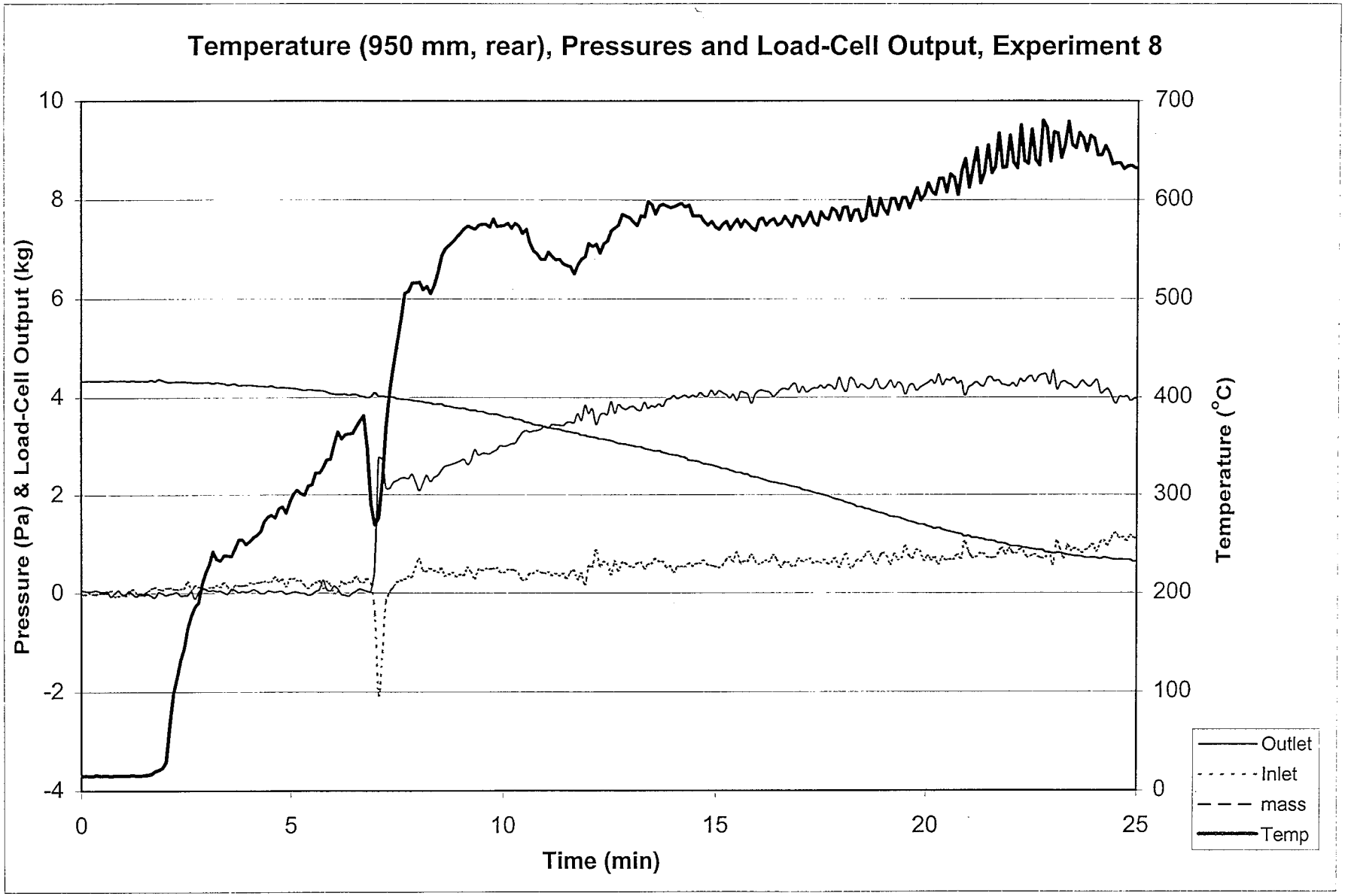
Temperature (950 mm, rear), Pressures and Load-Cell Output, Experiment 8
Pressure (Pa) & Load-Cell Output (kg)
Temperature (°C)
Time (min)
10
8
6
4
2
0
-2
-4
700
600
500
400
300
200
100
0
0
5
10
15
20
25
Outlet
Inlet
mass
Temp

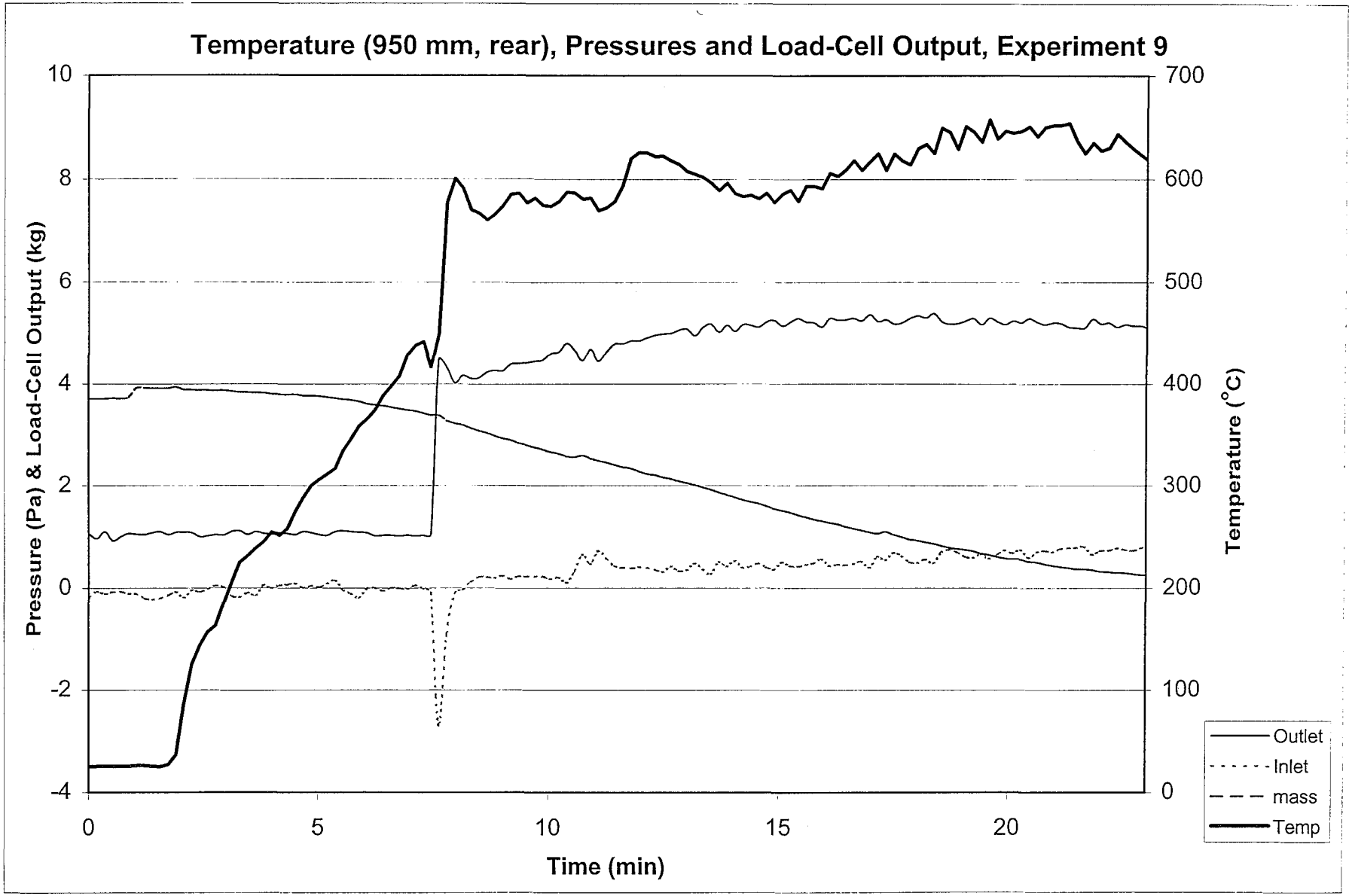
Temperature (950 mm, rear), Pressures and Load-Cell Output, Experiment 9
Pressure (Pa) & Load-Cell Output (kg)
Temperature (°C)
Time (min)
10
8
6
4
2
0
-2
-4
700
600
500
400
300
200
100
0
0
5
10
15
20
Outlet
Inlet
mass
Temp

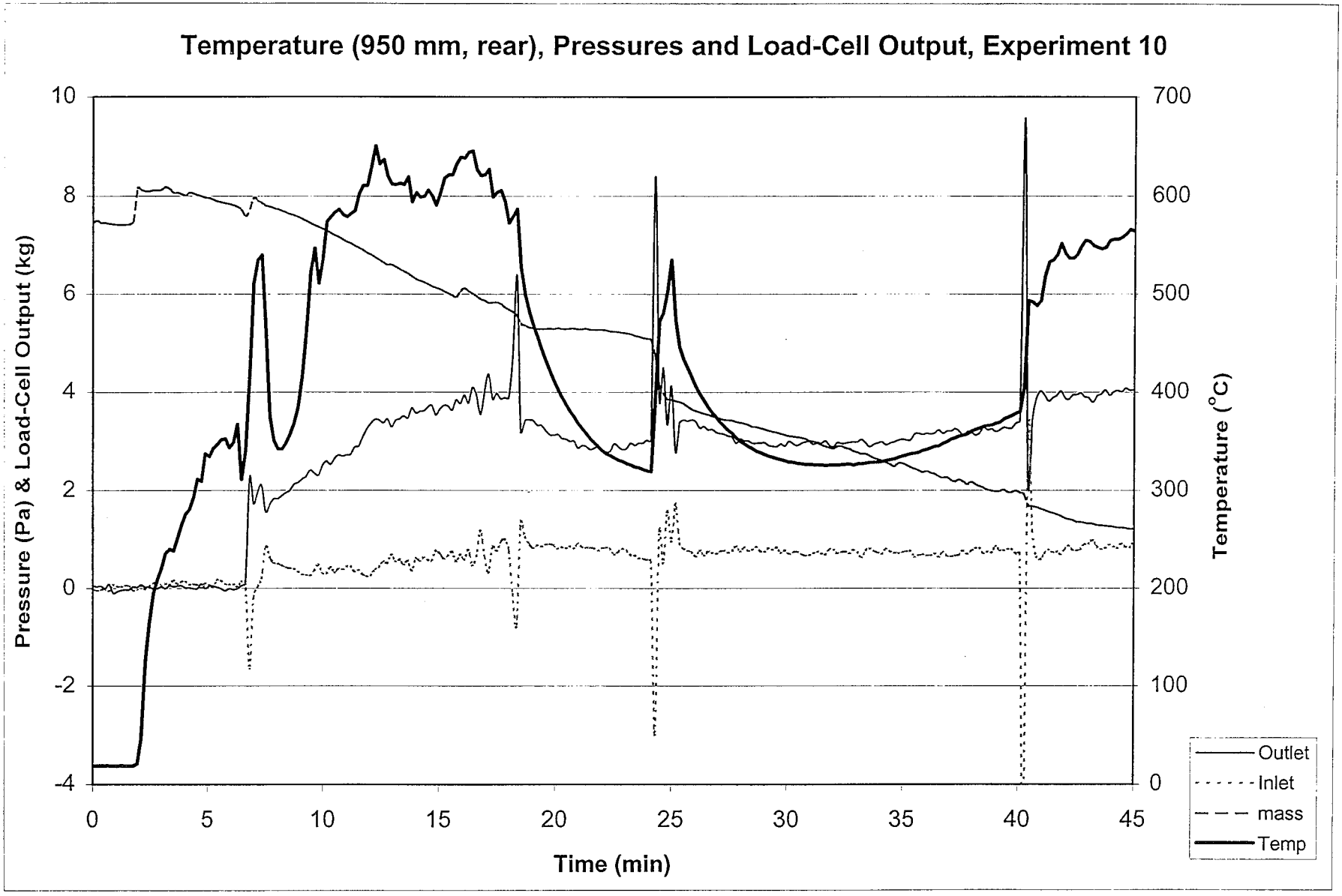
Temperature (950 mm, rear), Pressures and Load-Cell Output, Experiment 10
Pressure (Pa) & Load-Cell Output (kg)
Temperature (°C)
Time (min)
10
8
6
4
2
0
-2
-4
700
600
500
400
300
200
100
0
0
5
10
15
20
25
30
35
40
45
Outlet
Inlet
mass
Temp

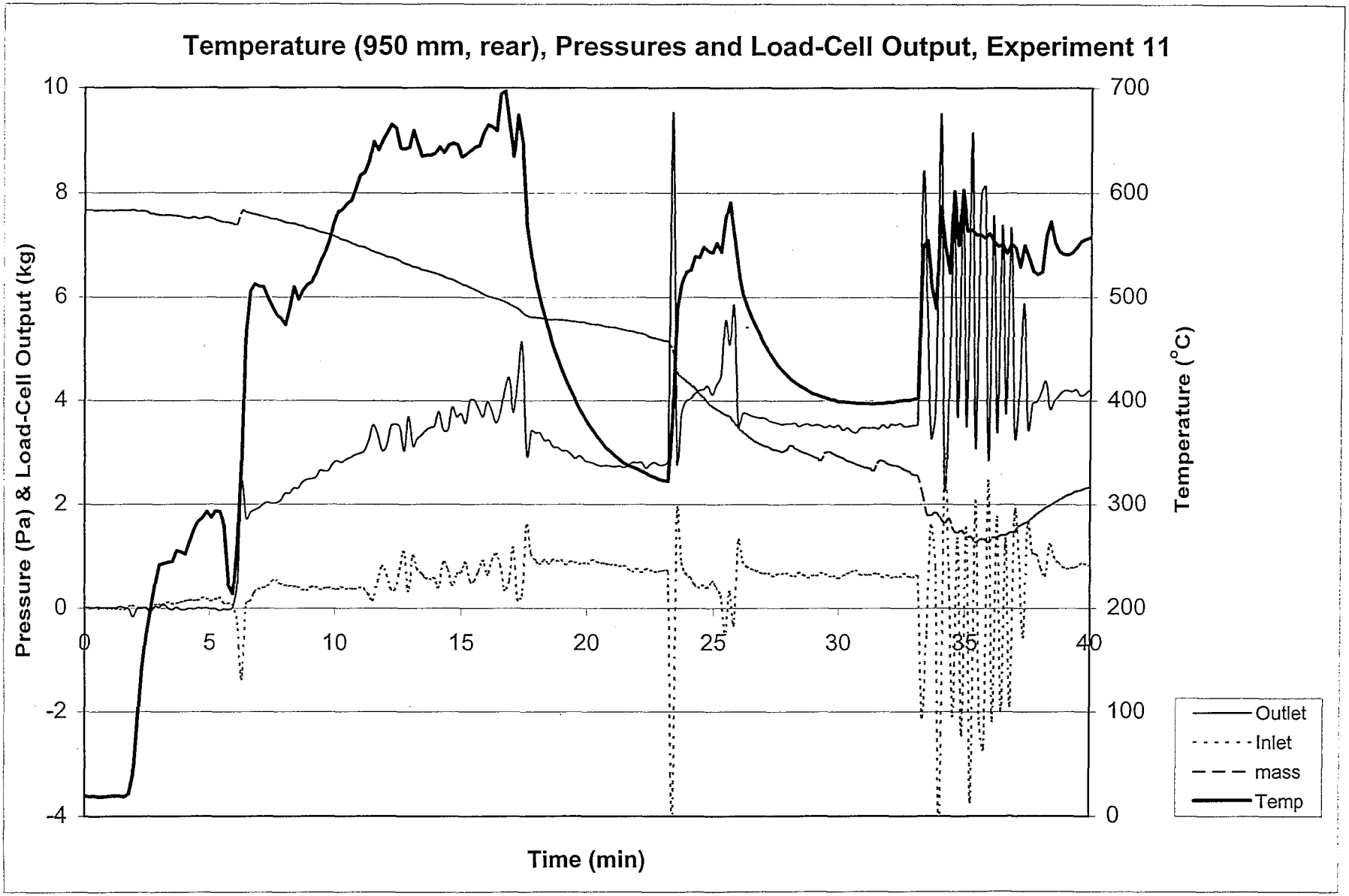
Temperature (950 mm, rear), Pressures and Load-Cell Output, Experiment 11
Pressure (Pa) & Load-Cell Output (kg)
Temperature (°C)
Time (min)
10
8
6
4
2
0
-2
-4
700
600
500
400
300
200
100
0
0
5
10
15
20
25
30
35
40
Outlet
Inlet
mass
Temp

A2. Compartment Temperature Profiles (Front), Experiments 1 –11.

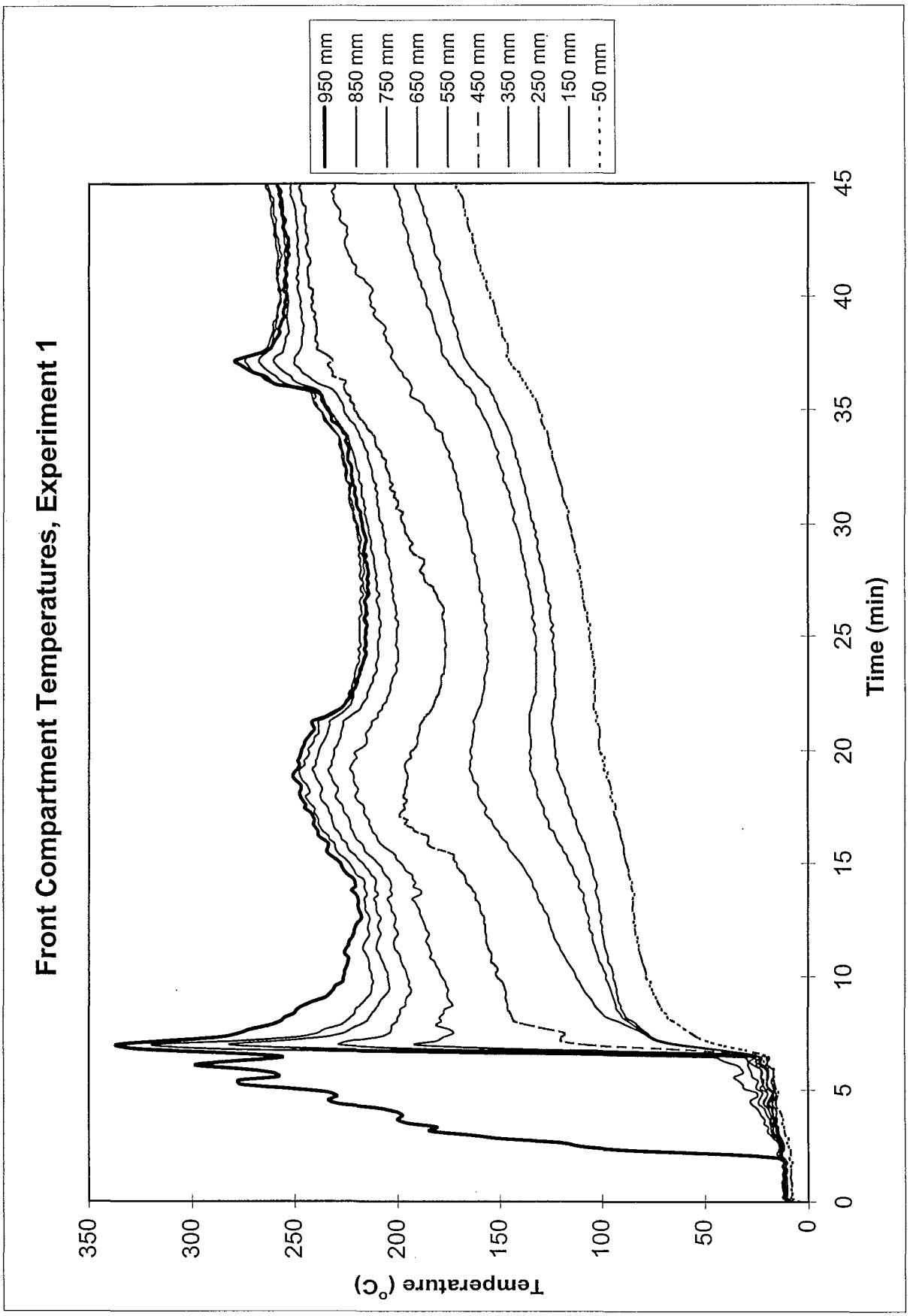

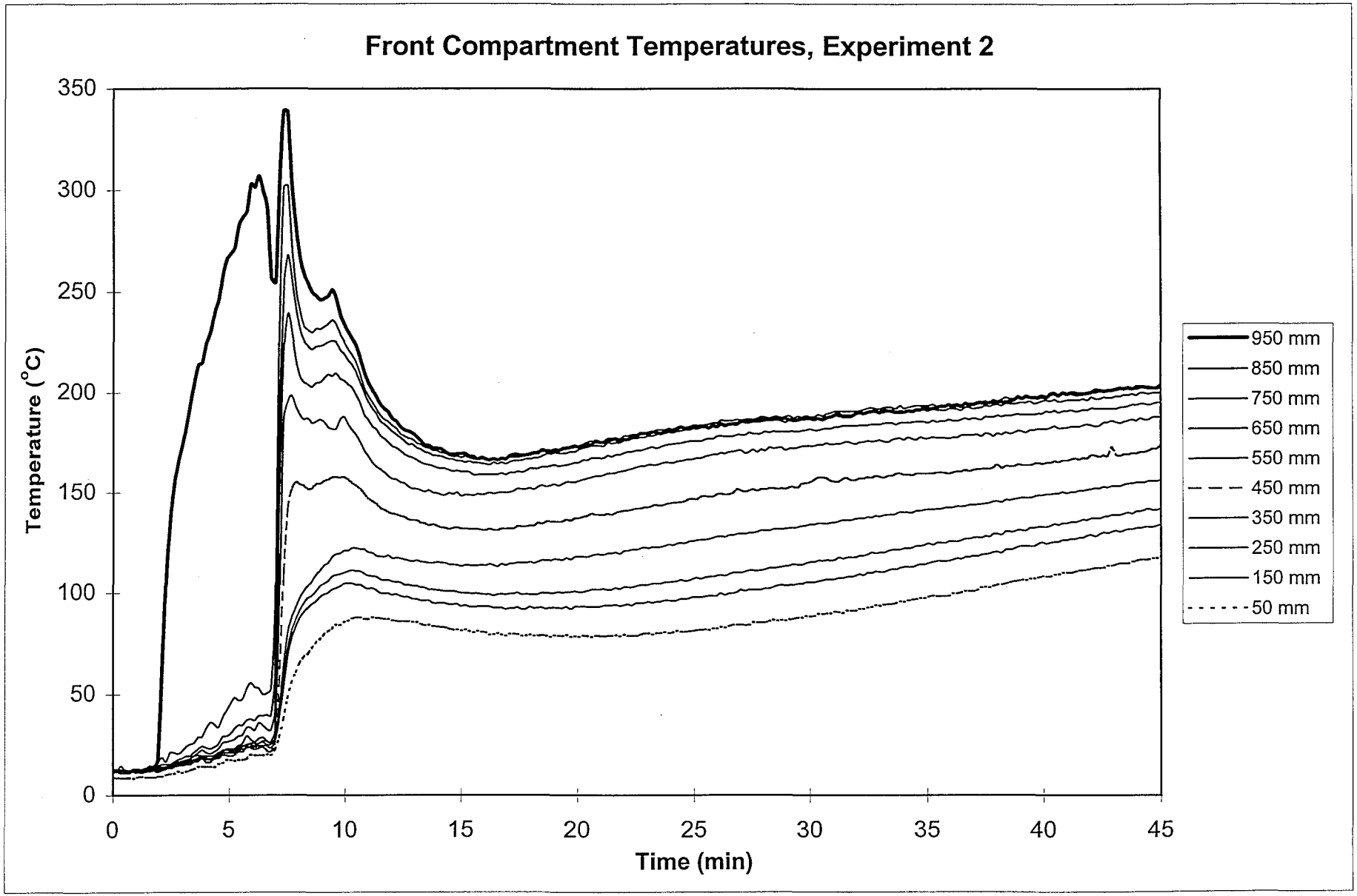
Front Compartment Temperatures, Experiment 2
Temperature (°C)
350
300
250
200
150
100
50
0
0
5
10
15
20
25
30
35
40
45
Time (min)
950 mm
850 mm
750 mm
650 mm
550 mm
450 mm
350 mm
250 mm
150 mm
50 mm

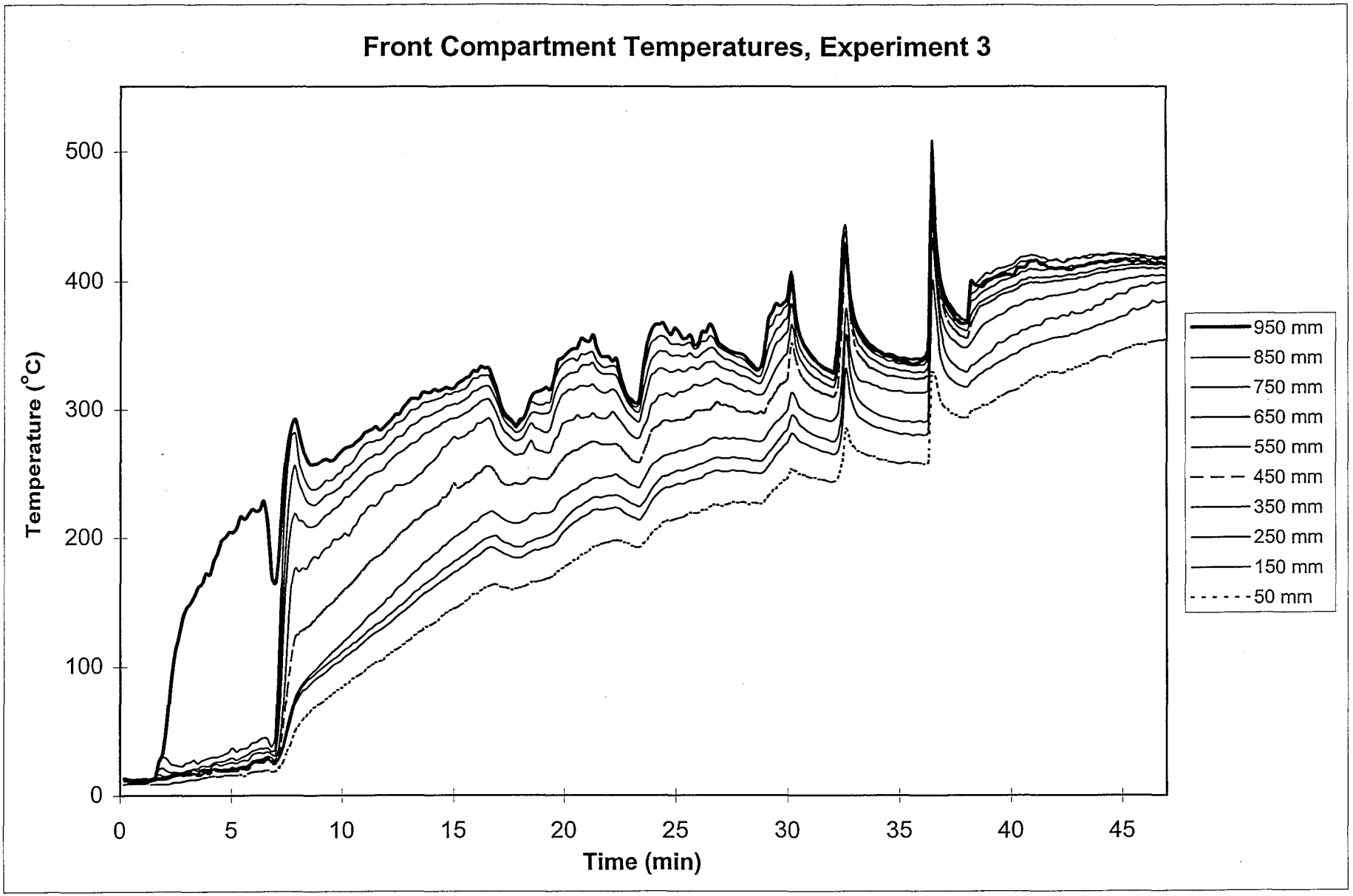
Front Compartment Temperatures, Experiment 3
Temperature (°C)
0
100
200
300
400
500
0
5
10
15
20
25
30
35
40
45
Time (min)
950 mm
850 mm
750 mm
650 mm
550 mm
450 mm
350 mm
250 mm
150 mm
50 mm

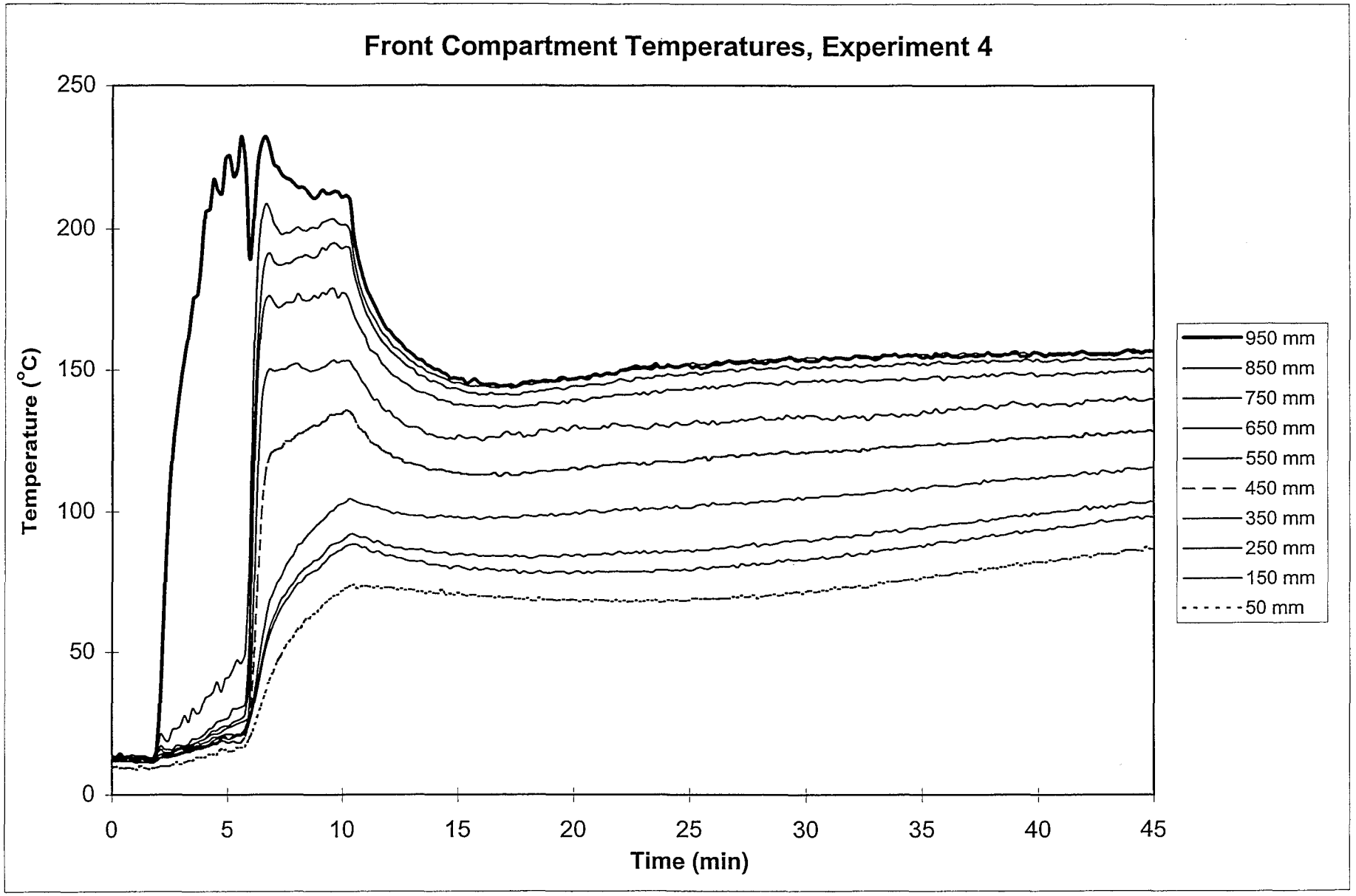
Front Compartment Temperatures, Experiment 4
Temperature (°C)
250
200
150
100
50
0
0
5
10
15
20
25
30
35
40
45
Time (min)
950 mm
850 mm
750 mm
650 mm
550 mm
450 mm
350 mm
250 mm
150 mm
50 mm

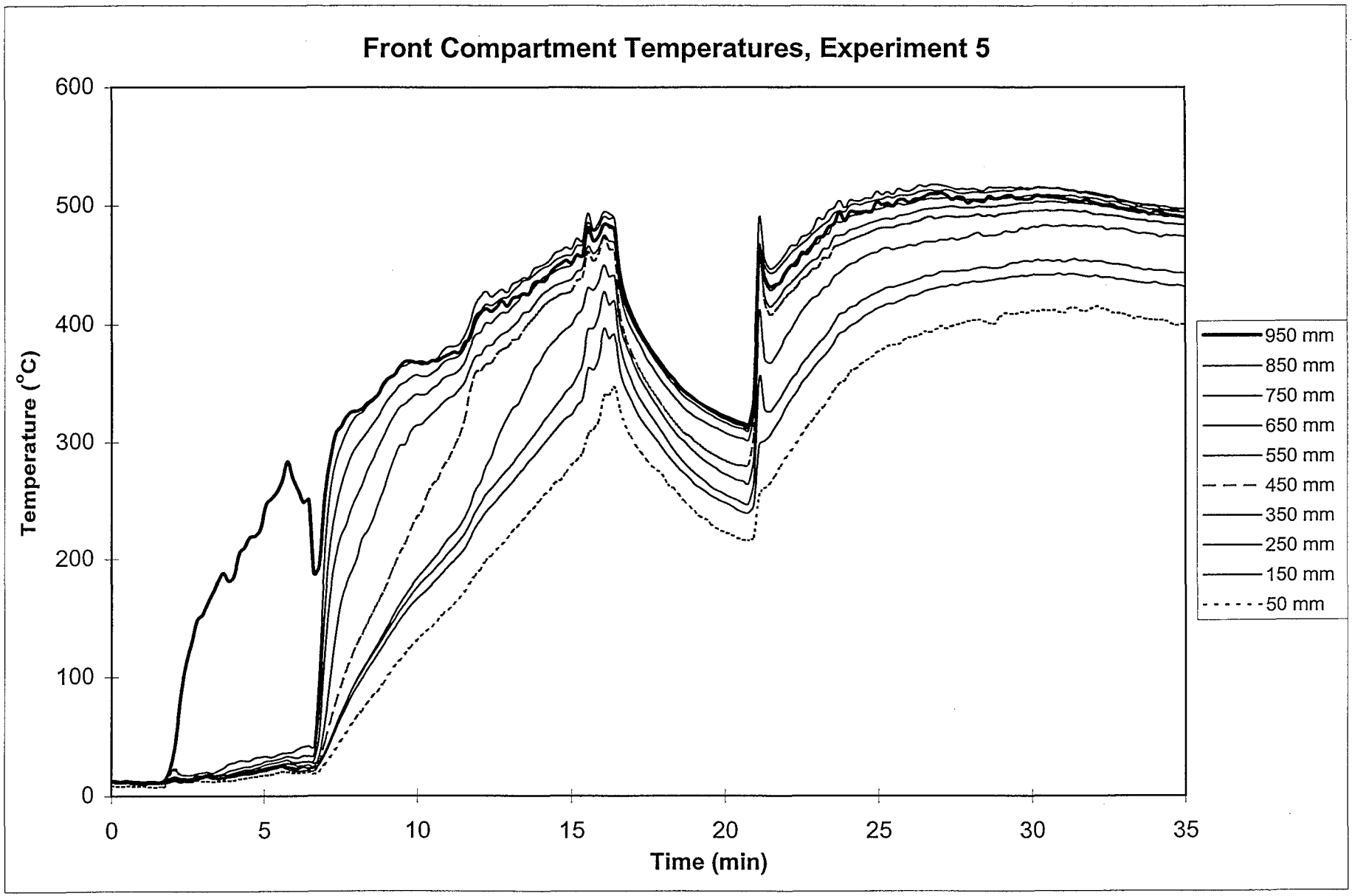
Front Compartment Temperatures, Experiment 5
Temperature (°C)
600
500
400
300
200
100
0
0
5
10
15
20
25
30
35
Time (min)
950 mm
850 mm
750 mm
650 mm
550 mm
450 mm
350 mm
250 mm
150 mm
50 mm

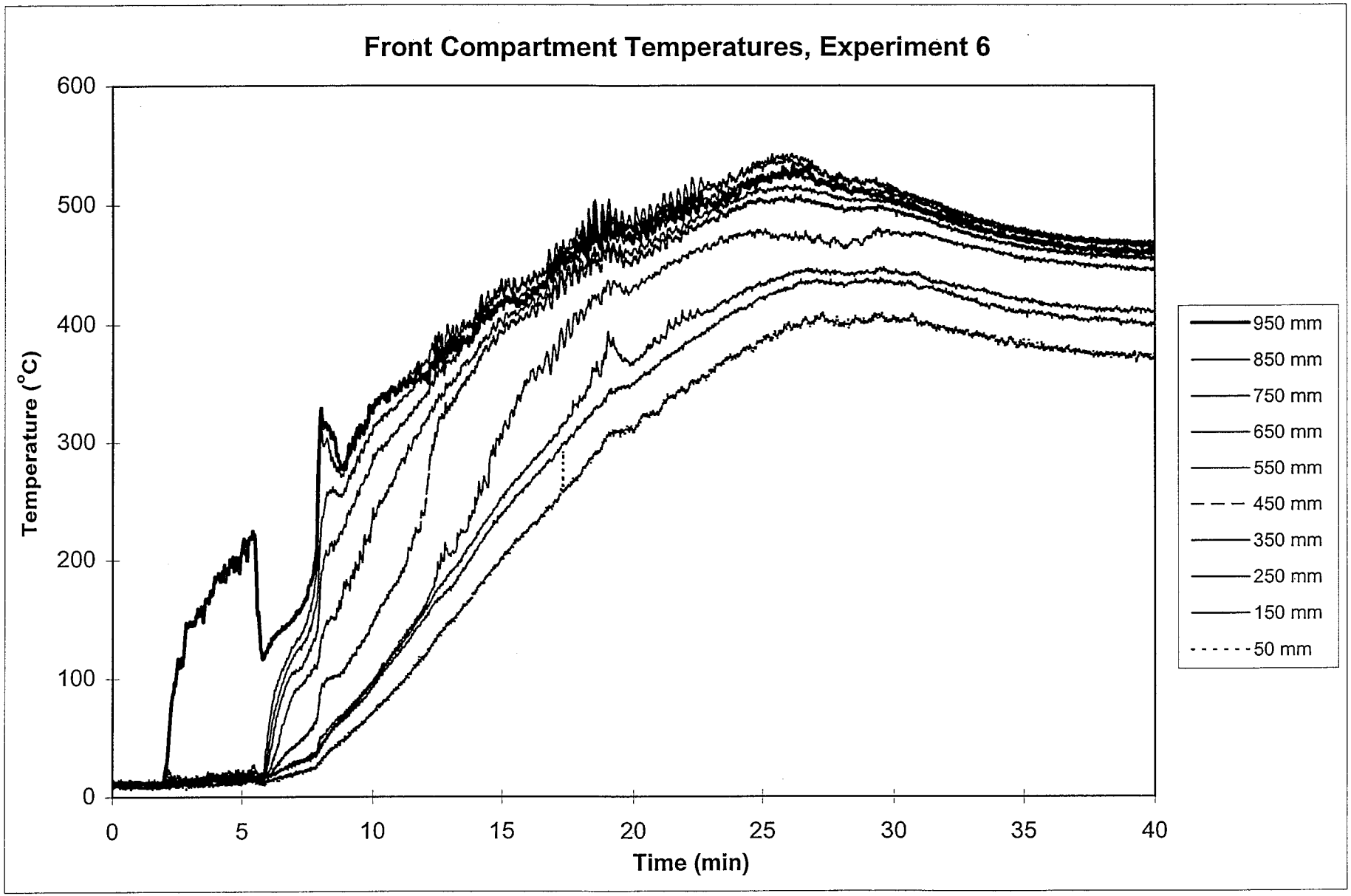
Front Compartment Temperatures, Experiment 6
Temperature (°C)
600
500
400
300
200
100
0
0
5
10
15
20
25
30
35
40
Time (min)
950 mm
850 mm
750 mm
650 mm
550 mm
450 mm
350 mm
250 mm
150 mm
50 mm

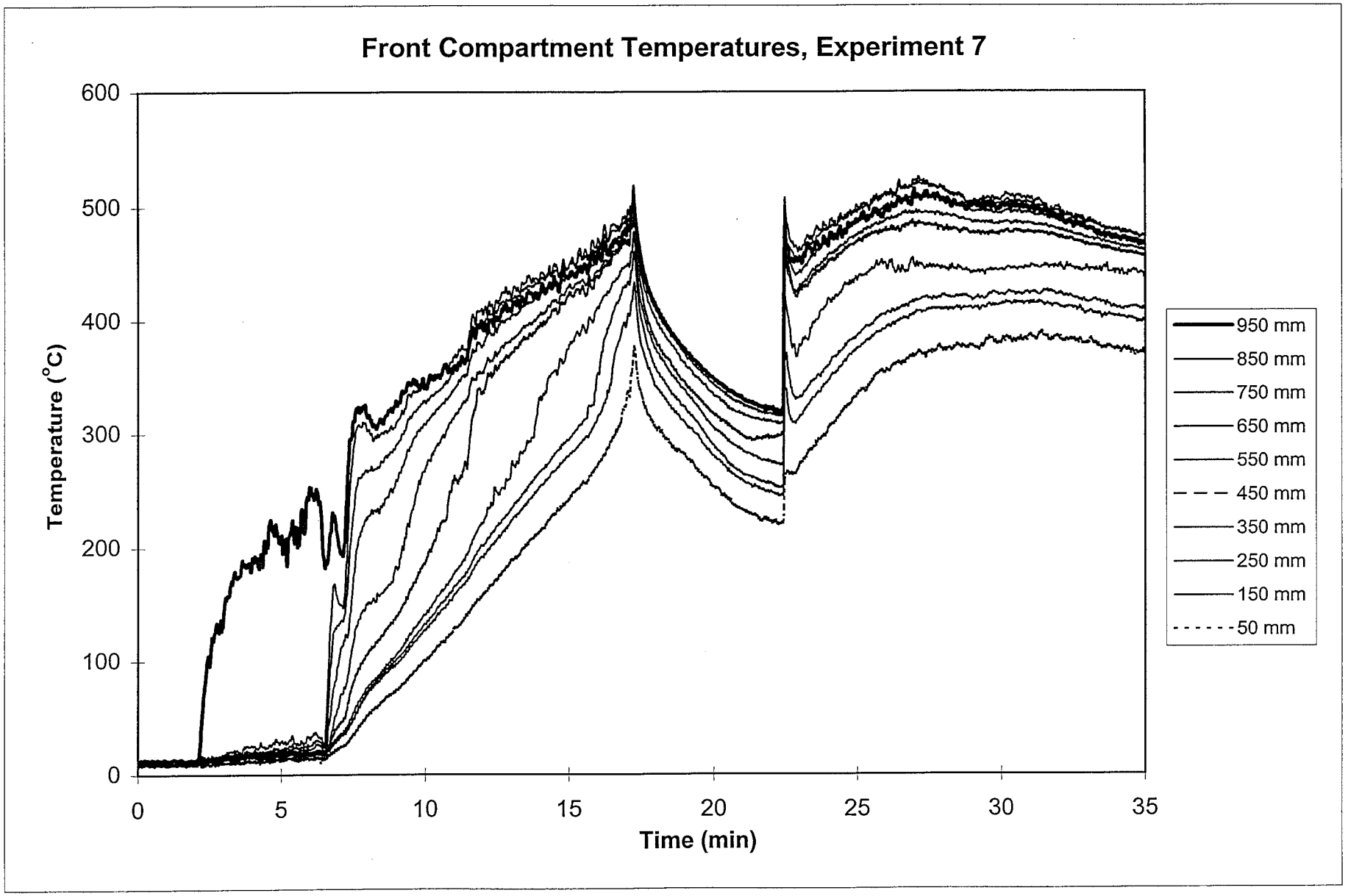
Front Compartment Temperatures, Experiment 7
Temperature (°C)
600
500
400
300
200
100
0
0
5
10
15
20
25
30
35
Time (min)
950 mm
850 mm
750 mm
650 mm
550 mm
450 mm
350 mm
250 mm
150 mm
50 mm

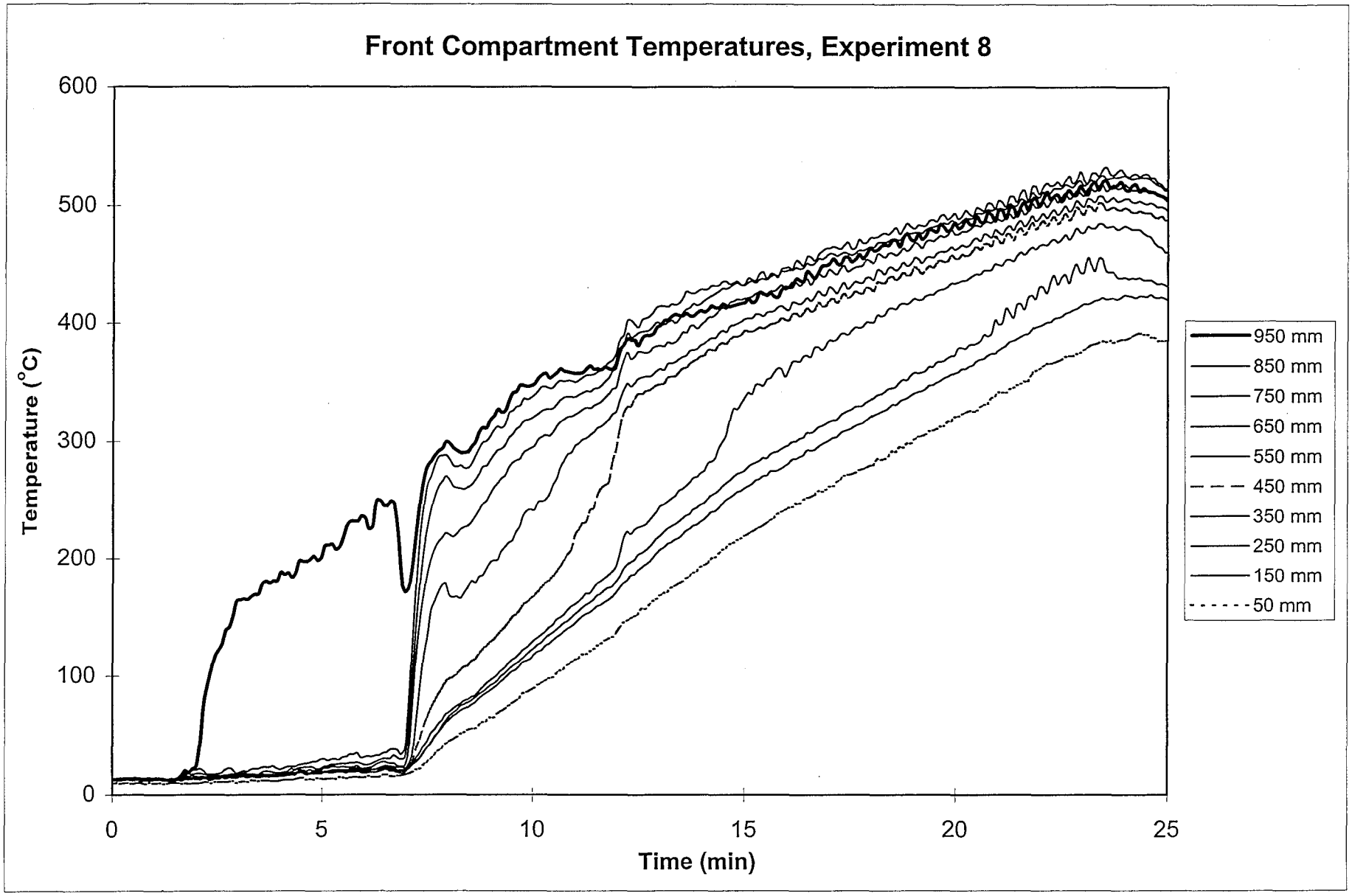
Front Compartment Temperatures, Experiment 8
Temperature (°C)
600
500
400
300
200
100
0
0
5
10
15
20
25
Time (min)
950 mm
850 mm
750 mm
650 mm
550 mm
450 mm
350 mm
250 mm
150 mm
50 mm

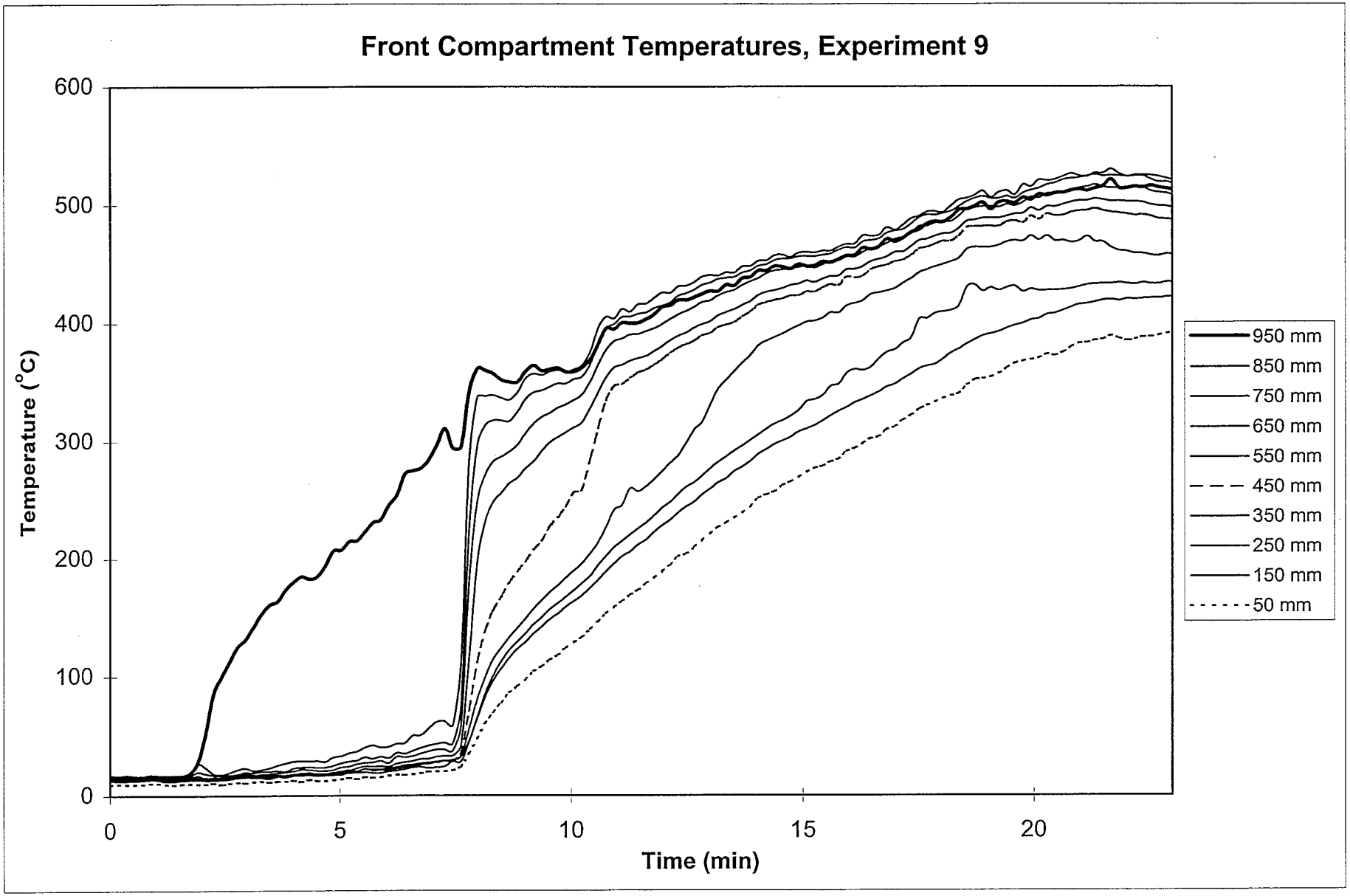
Front Compartment Temperatures, Experiment 9
Temperature (°C)
600
500
400
300
200
100
0
0
5
10
15
20
Time (min)
950 mm
850 mm
750 mm
650 mm
550 mm
450 mm
350 mm
250 mm
150 mm
50 mm

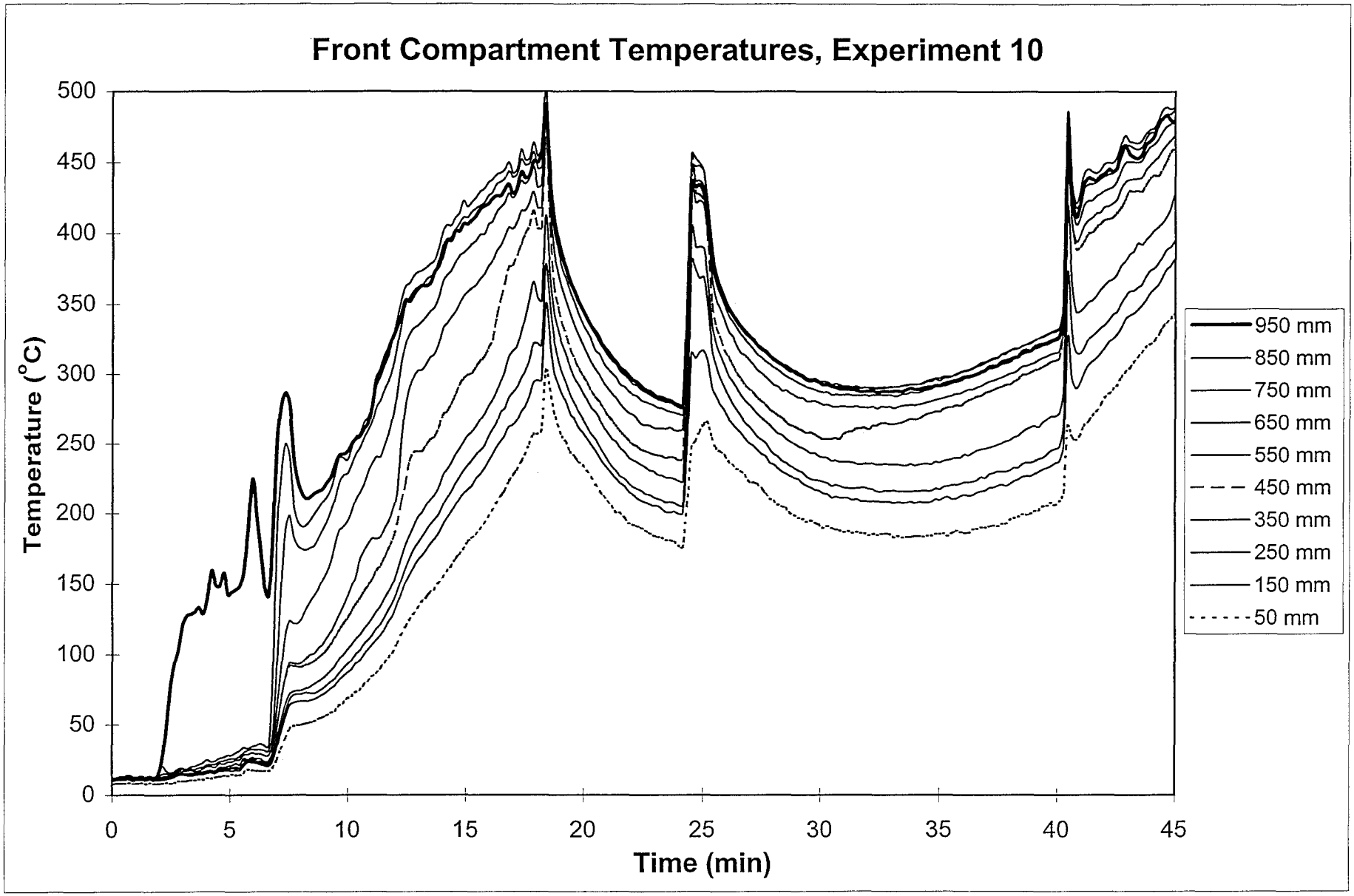
Front Compartment Temperatures, Experiment 10
Temperature (°C)
500
450
400
350
300
250
200
150
100
50
0
0
5
10
15
20
25
30
35
40
45
Time (min)
950 mm
850 mm
750 mm
650 mm
550 mm
450 mm
350 mm
250 mm
150 mm
50 mm

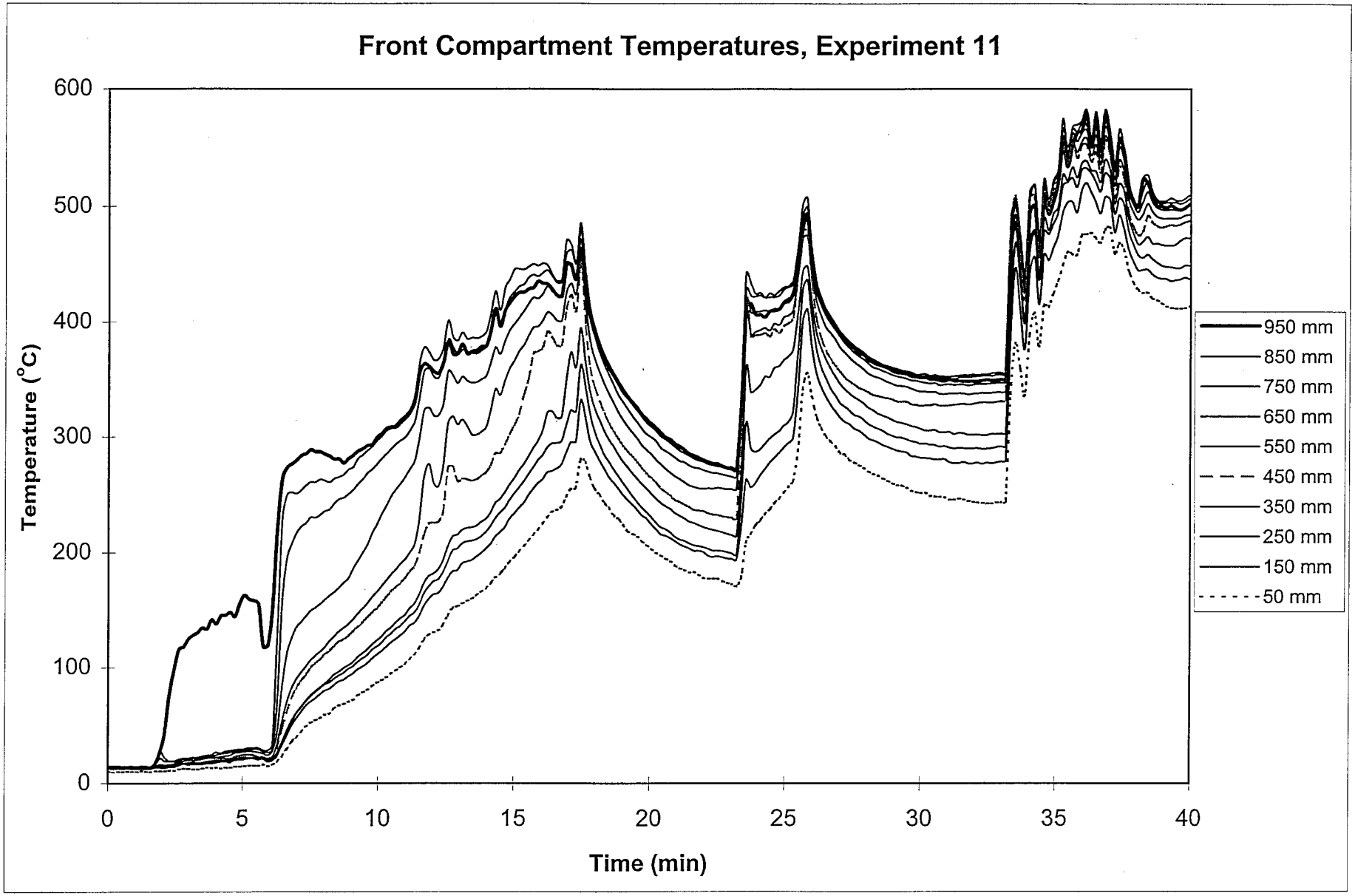
Front Compartment Temperatures, Experiment 11
Temperature (°C)
600
500
400
300
200
100
0
0
5
10
15
20
25
30
35
40
Time (min)
950 mm
850 mm
750 mm
650 mm
550 mm
450 mm
350 mm
250 mm
150 mm
50 mm

A3. Compartment Temperature Profiles (Rear), Experiments 1 –11.

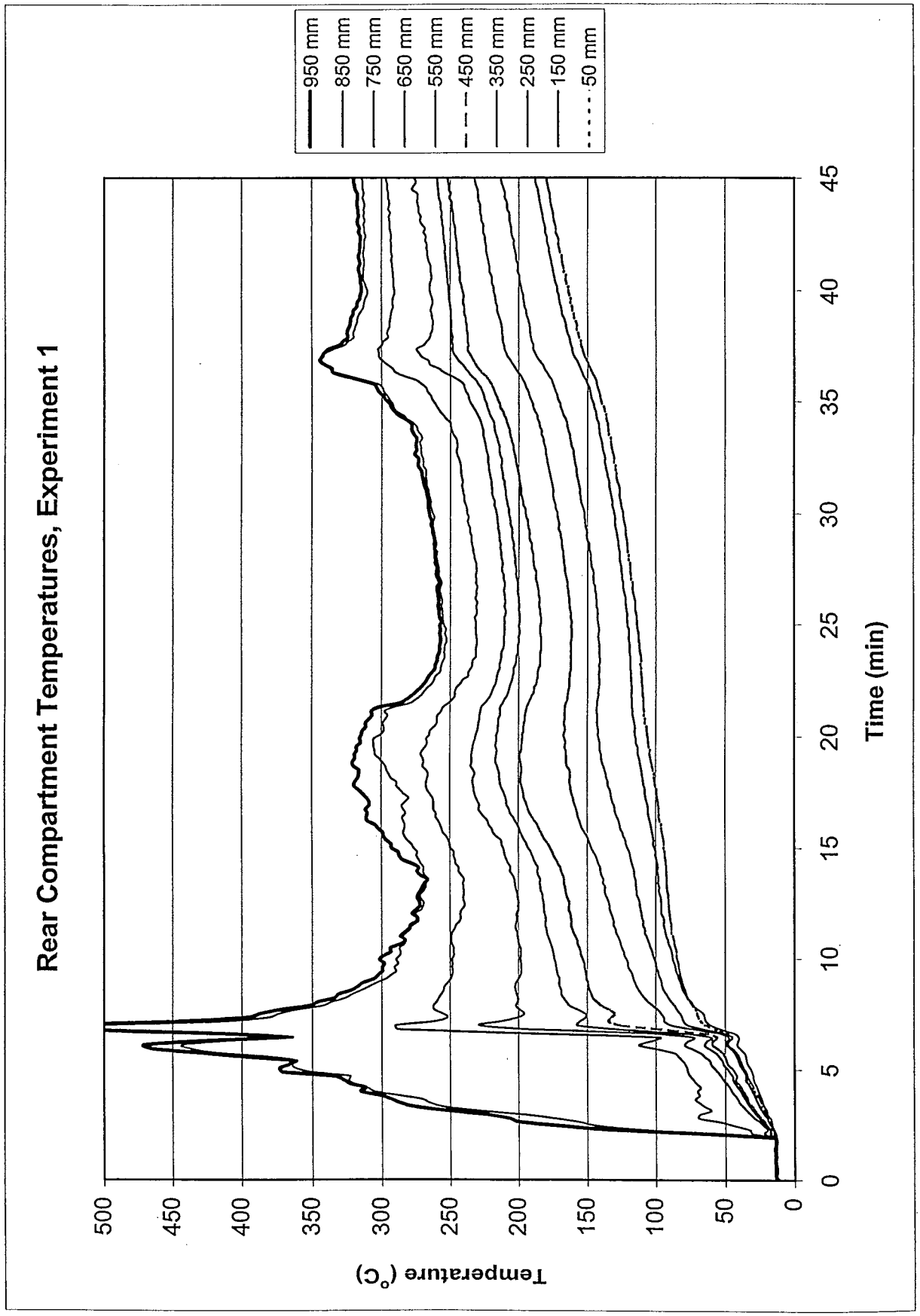

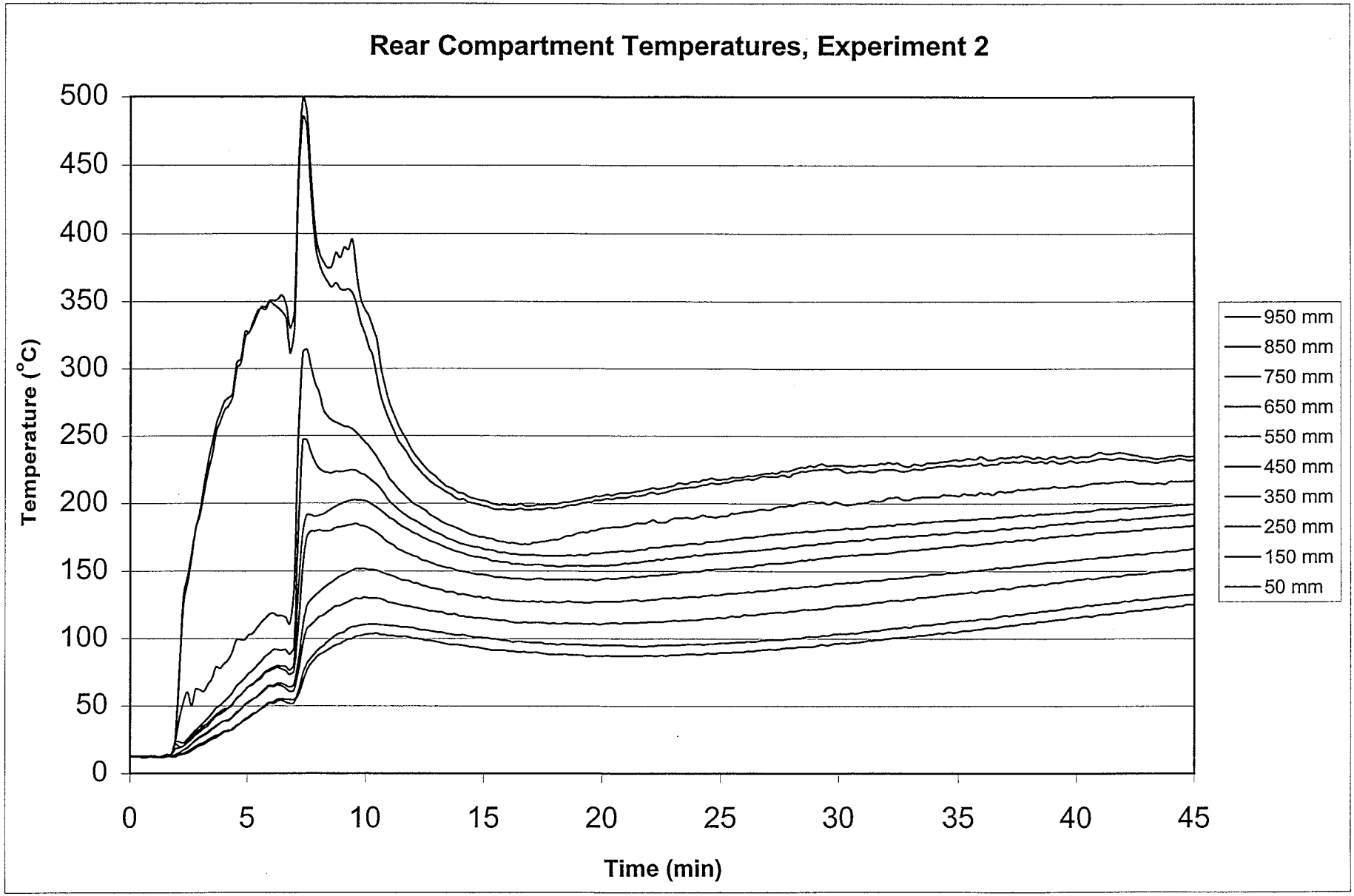
Rear Compartment Temperatures, Experiment 2
Temperature (°C)
500
450
400
350
300
250
200
150
100
50
0
0
5
10
15
20
25
30
35
40
45
Time (min)
950 mm
850 mm
750 mm
650 mm
550 mm
450 mm
350 mm
250 mm
150 mm
50 mm

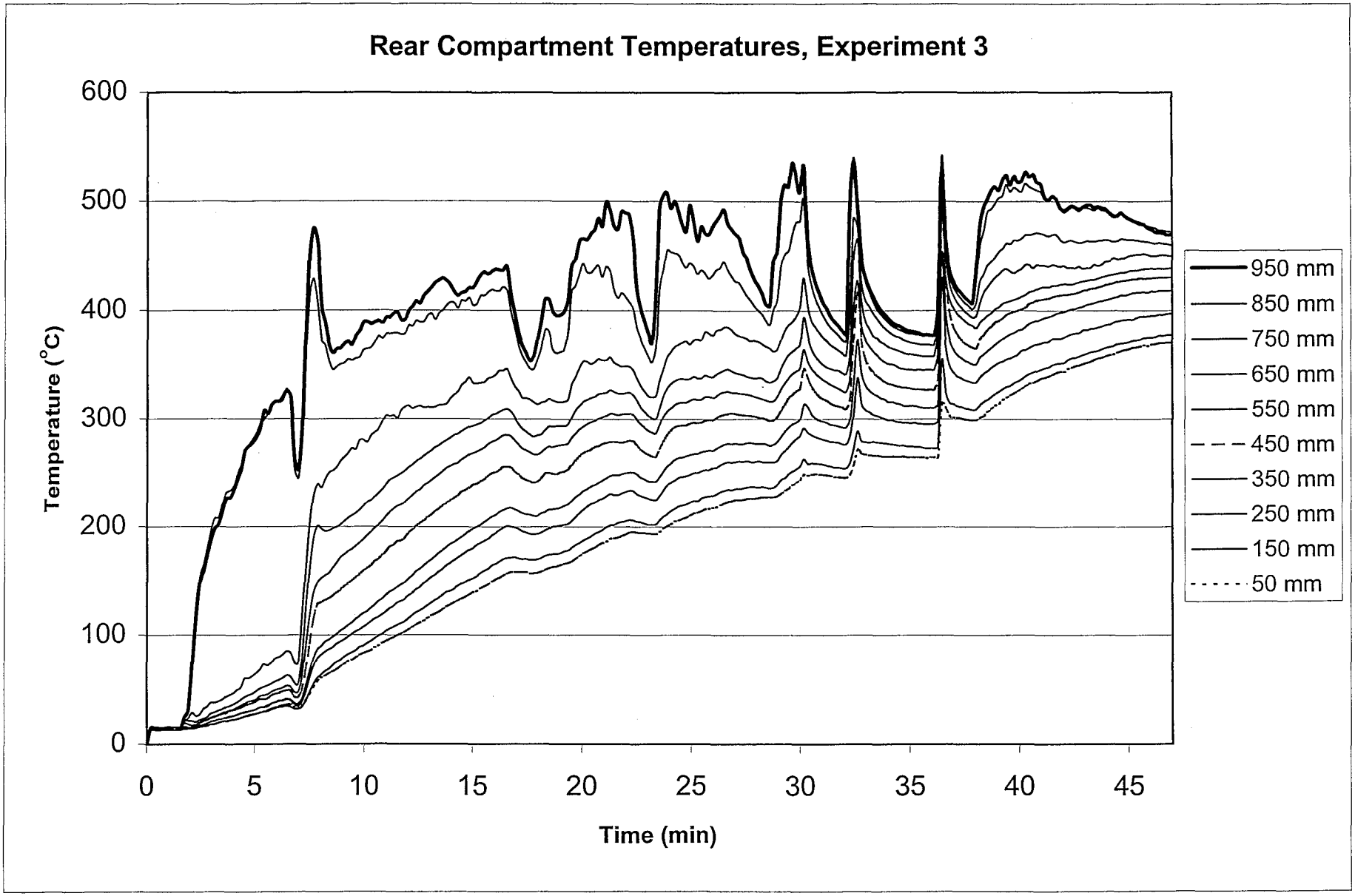
Rear Compartment Temperatures, Experiment 3
Temperature (°C)
600
500
400
300
200
100
0
0
5
10
15
20
25
30
35
40
45
Time (min)
950 mm
850 mm
750 mm
650 mm
550 mm
450 mm
350 mm
250 mm
150 mm
50 mm

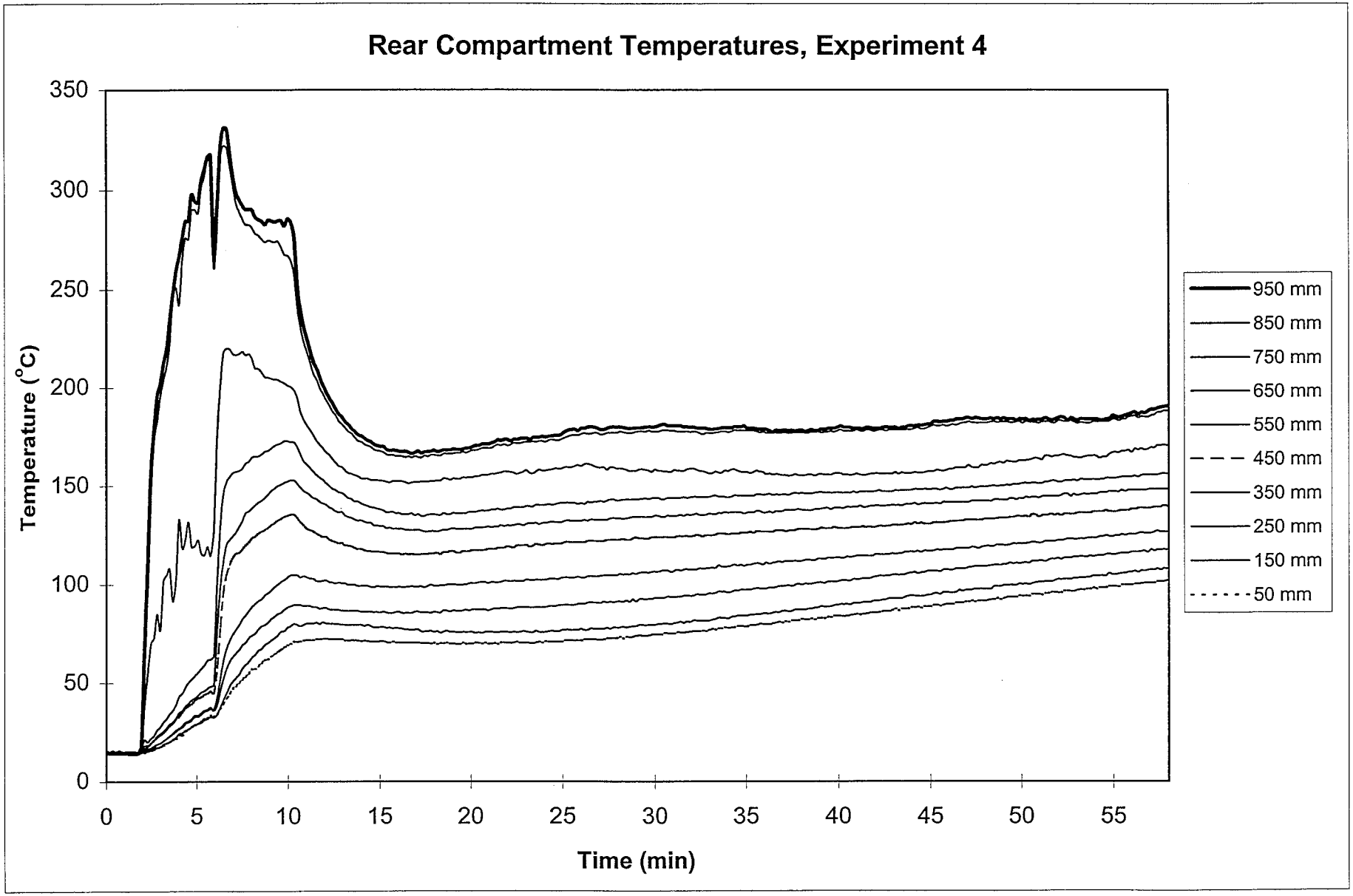
Rear Compartment Temperatures, Experiment 4
Temperature (°C)
350
300
250
200
150
100
50
0
0
5
10
15
20
25
30
35
40
45
50
55
Time (min)
950 mm
850 mm
750 mm
650 mm
550 mm
450 mm
350 mm
250 mm
150 mm
50 mm

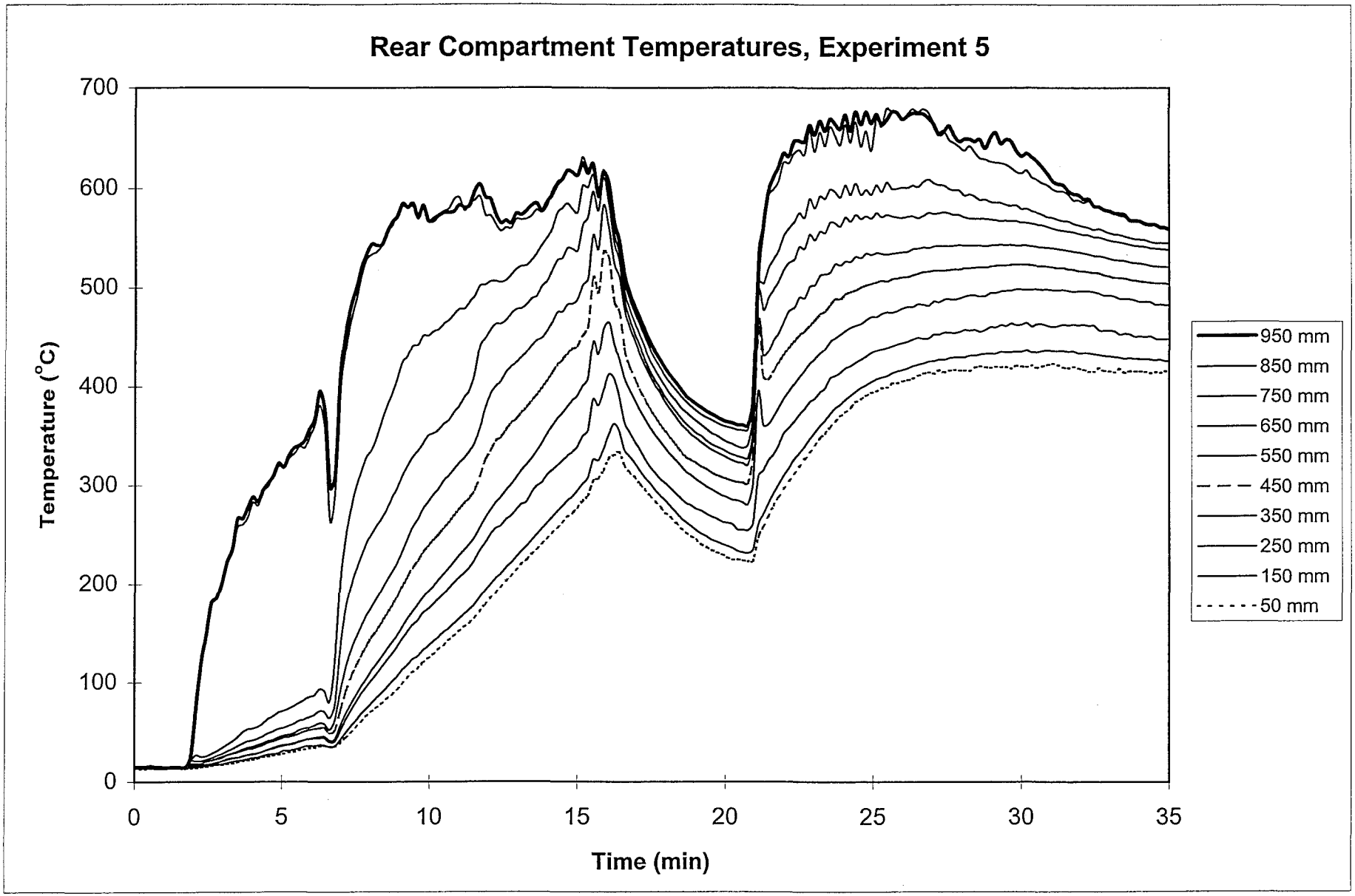
Rear Compartment Temperatures, Experiment 5
Temperature (°C)
700
600
500
400
300
200
100
0
0
5
10
15
20
25
30
35
Time (min)
950 mm
850 mm
750 mm
650 mm
550 mm
450 mm
350 mm
250 mm
150 mm
50 mm

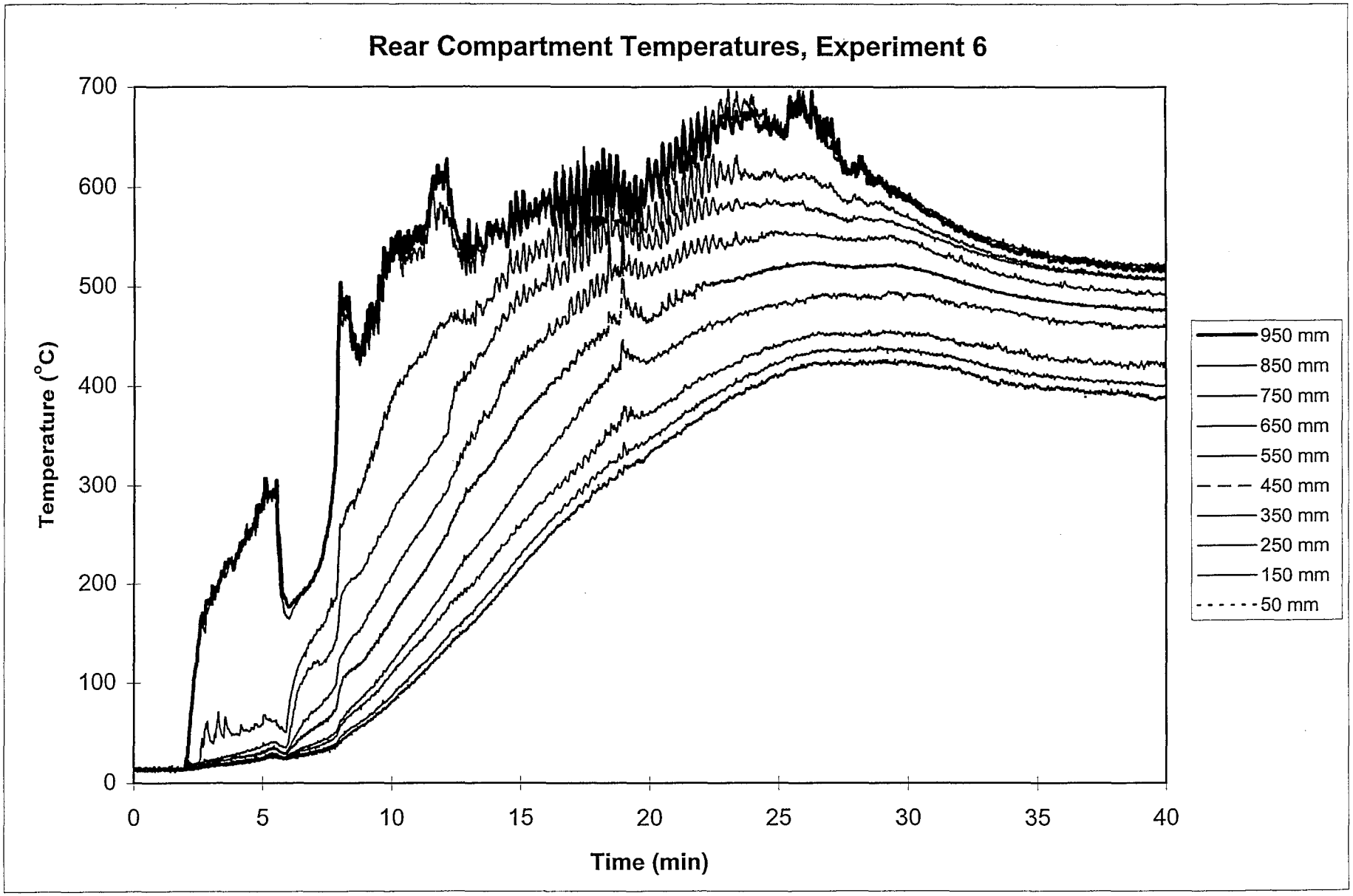
Rear Compartment Temperatures, Experiment 6
Temperature (°C)
700
600
500
400
300
200
100
0
0
5
10
15
20
25
30
35
40
Time (min)
950 mm
850 mm
750 mm
650 mm
550 mm
450 mm
350 mm
250 mm
150 mm
50 mm

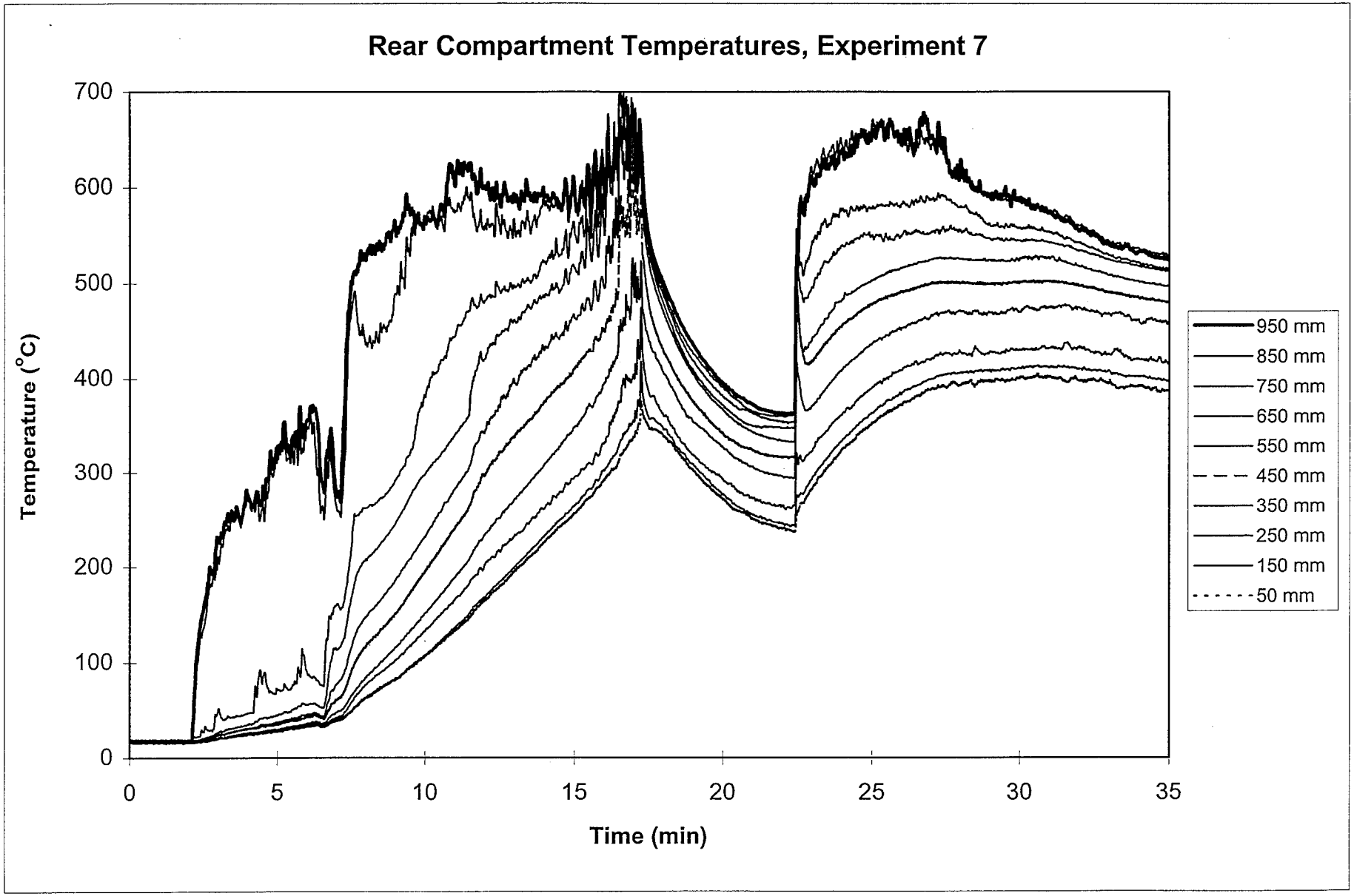
Rear Compartment Temperatures, Experiment 7
Temperature (°C)
700
600
500
400
300
200
100
0
0
5
10
15
20
25
30
35
Time (min)
950 mm
850 mm
750 mm
650 mm
550 mm
450 mm
350 mm
250 mm
150 mm
50 mm

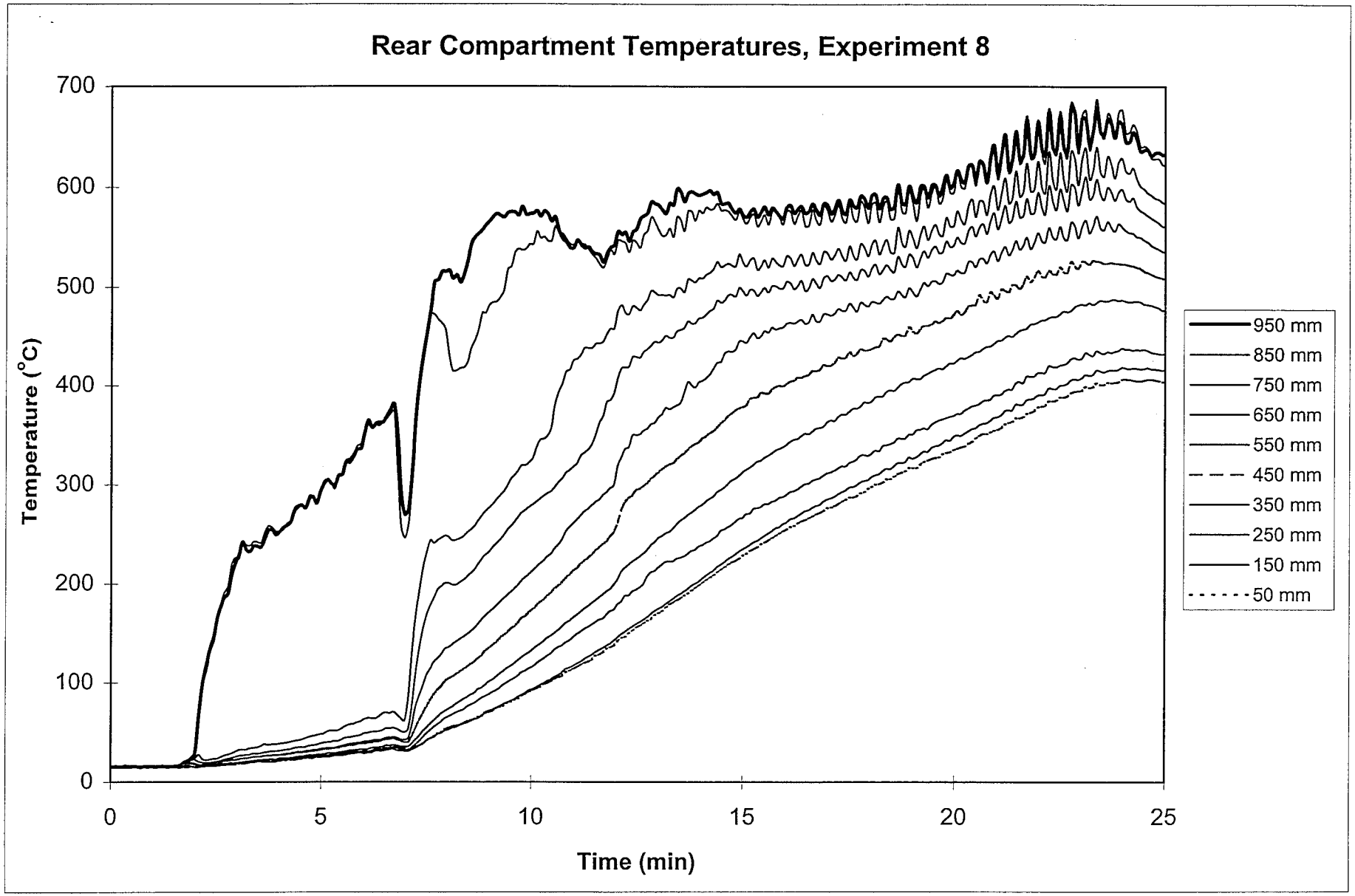
Rear Compartment Temperatures, Experiment 8
Temperature (°C)
700
600
500
400
300
200
100
0
0
5
10
15
20
25
Time (min)
950 mm
850 mm
750 mm
650 mm
550 mm
450 mm
350 mm
250 mm
150 mm
50 mm

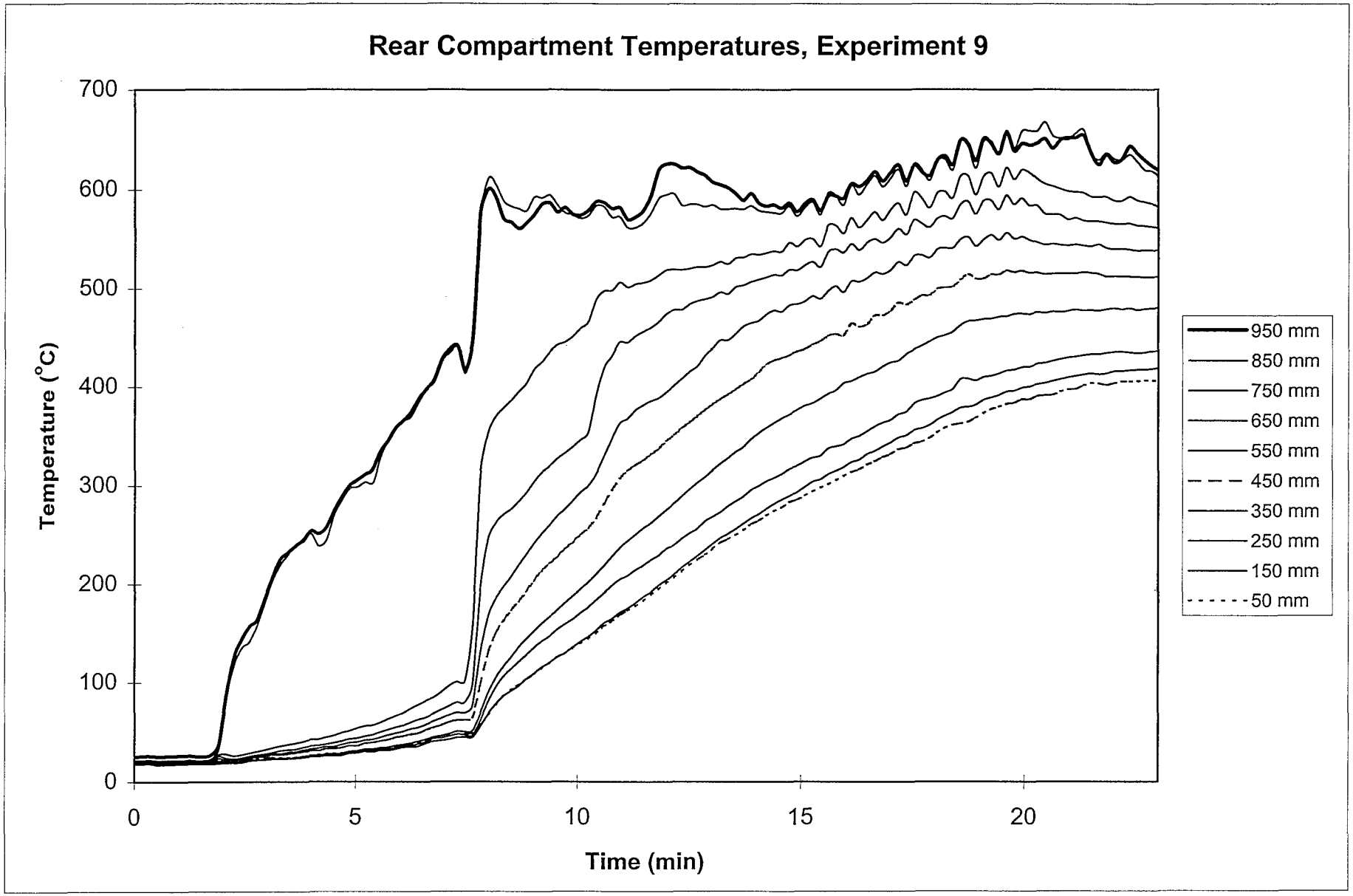
Rear Compartment Temperatures, Experiment 9
Temperature (°C)
700
600
500
400
300
200
100
0
0
5
10
15
20
Time (min)
950 mm
850 mm
750 mm
650 mm
550 mm
450 mm
350 mm
250 mm
150 mm
50 mm

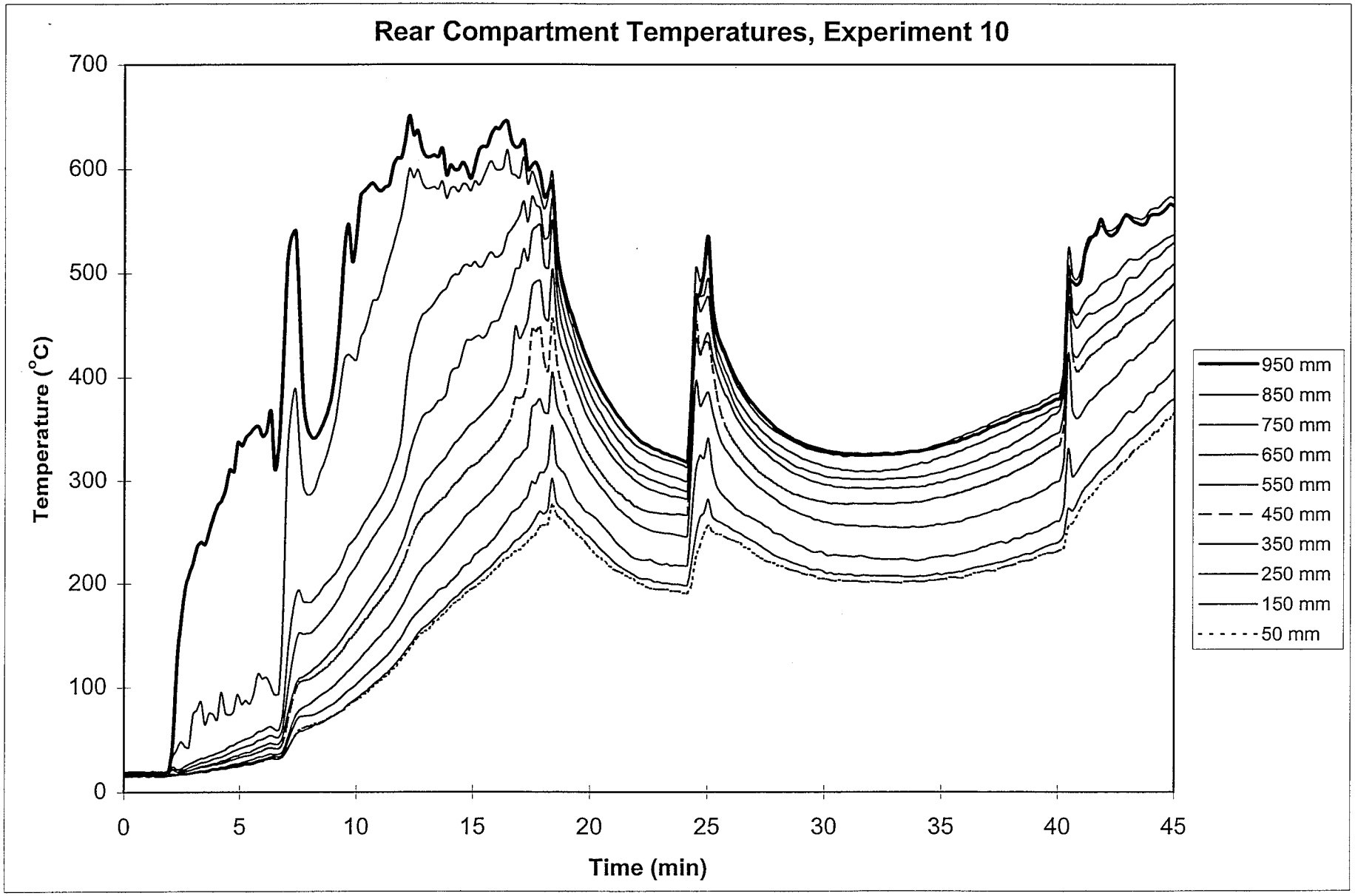
Rear Compartment Temperatures, Experiment 10
Temperature (°C)
700
600
500
400
300
200
100
0
0
5
10
15
20
25
30
35
40
45
Time (min)
950 mm
850 mm
750 mm
650 mm
550 mm
450 mm
350 mm
250 mm
150 mm
50 mm

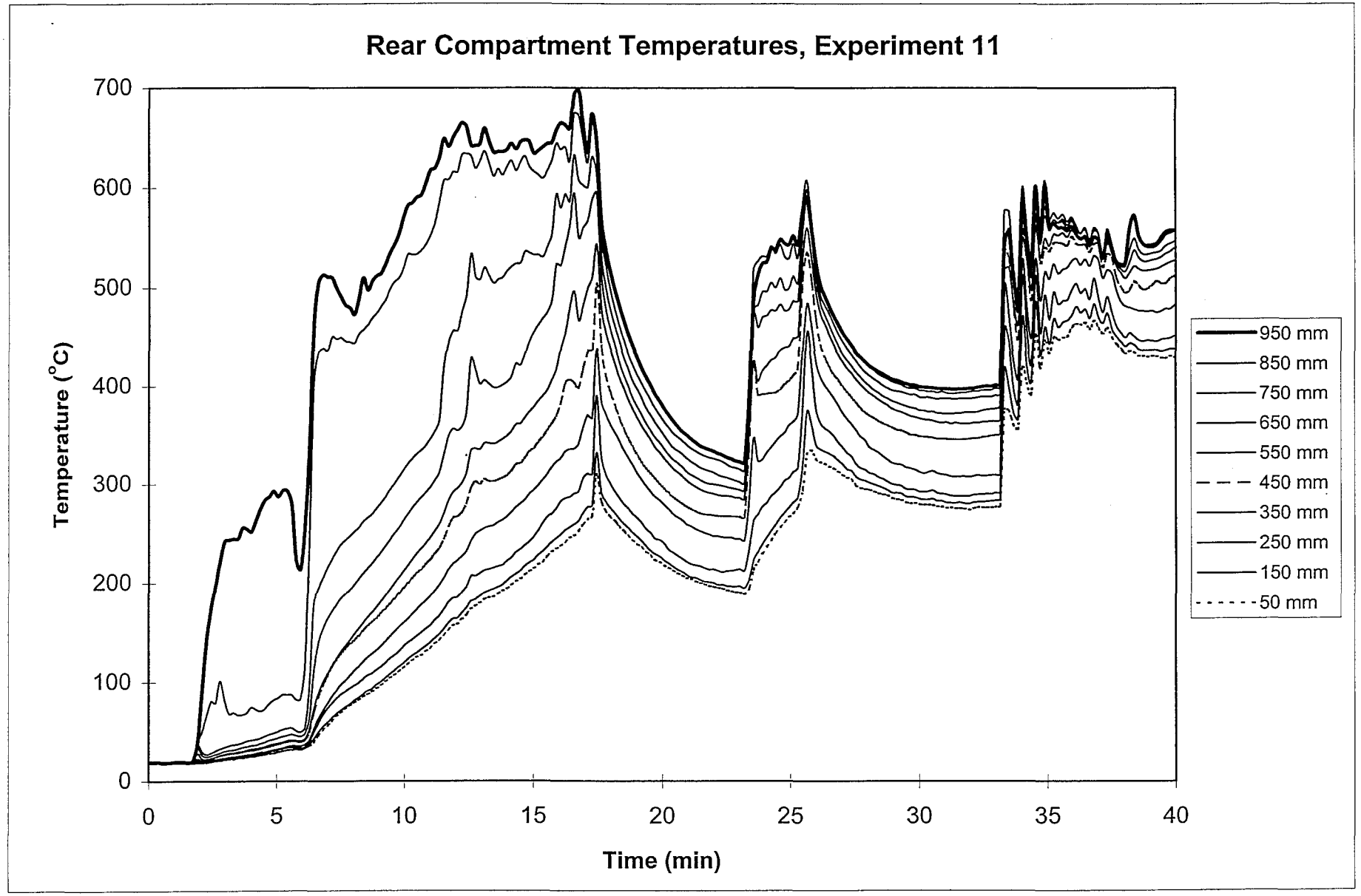
Rear Compartment Temperatures, Experiment 11
Temperature (°C)
700
600
500
400
300
200
100
0
0
5
10
15
20
25
30
35
40
Time (min)
950 mm
850 mm
750 mm
650 mm
550 mm
450 mm
350 mm
250 mm
150 mm
50 mm

A4. Gas Compositions, Elevation 900 mm, Experiments 6 and 11.

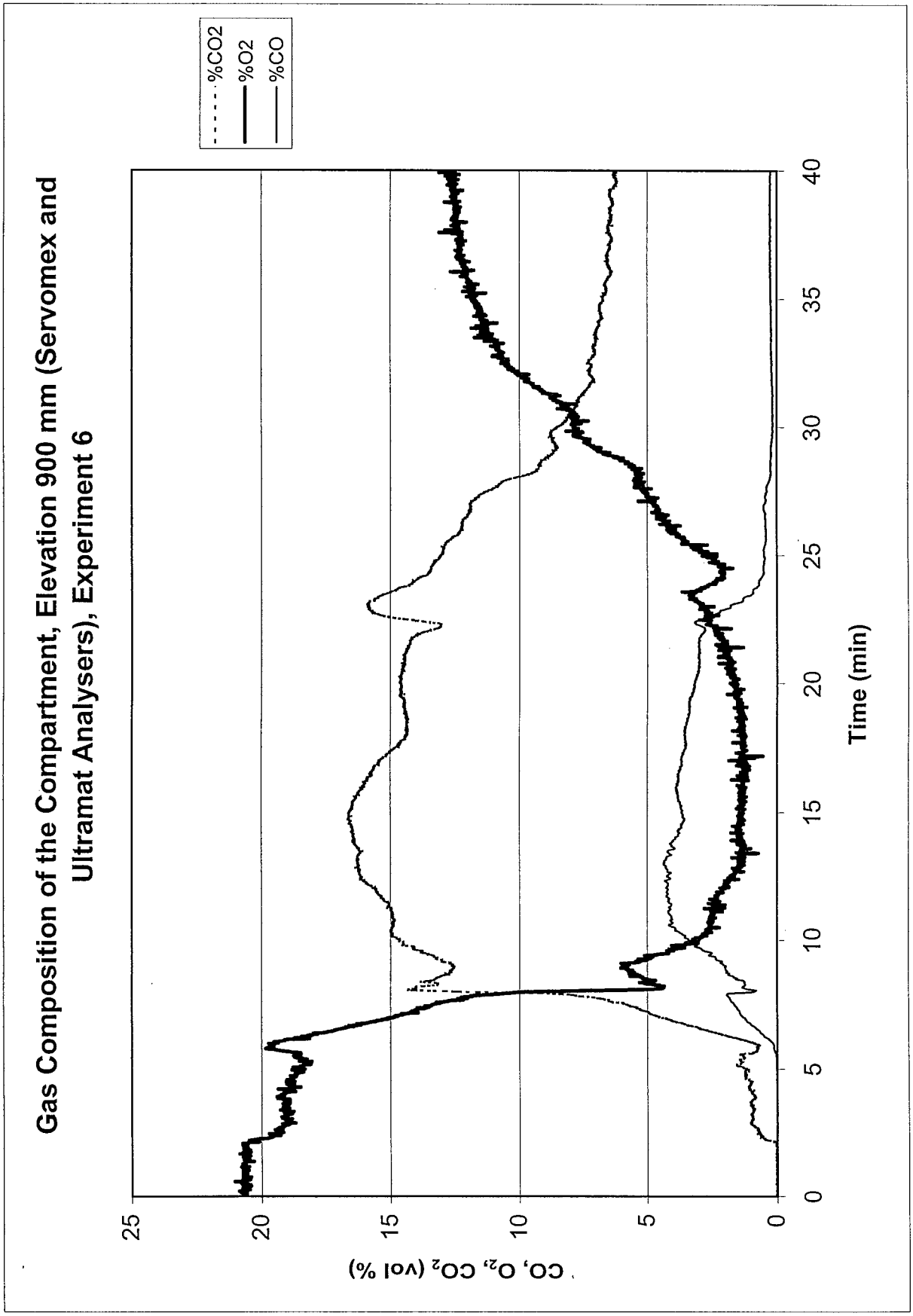

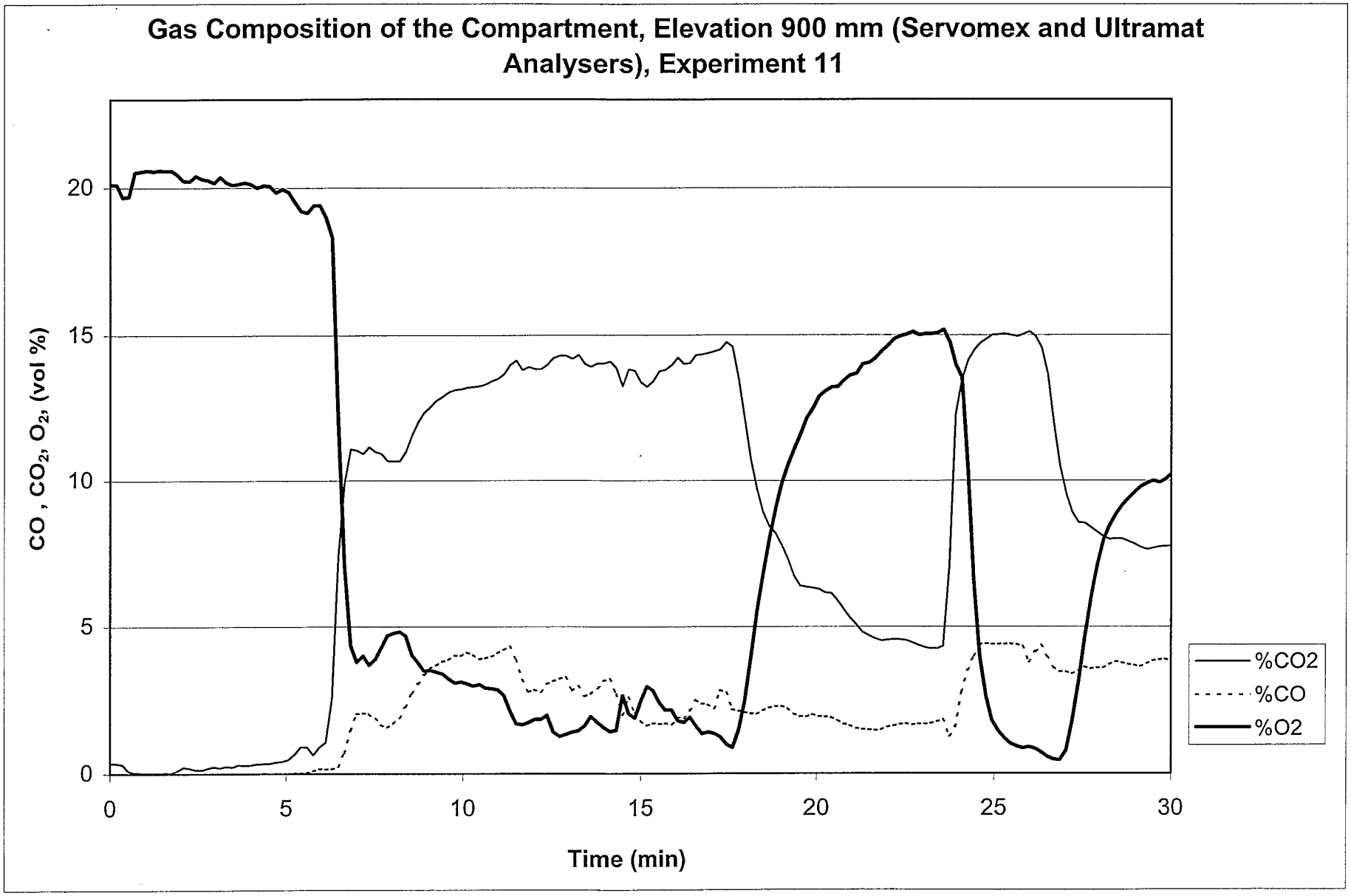
Gas Composition of the Compartment, Elevation 900 mm (Servomex and Ultramat Analysers), Experiment 11
CO , CO2, O2, (vol %)
20
15
10
5
0
0
5
10
15
20
25
30
Time (min)
%CO2
%CO
%O2

A5. Raw Data from the Gas Chromatograph

The following Appendix contains all the data that was collected from the gas chromatograph for experiments 1 through 11.

GC Results, Experiment 1

Time	O_2	N_2	CH_4	CO	CO_2	H_2O
(min)	vol (%)	vol (%)	vol (%)	vol (%)	vol (%)	vol (%)
10.3	6.2	63.8	0.6	3.8	11.9	11.9
25.1	5.1	62.6	1.0	4.7	13.4	13.4
36.1	3.8	64.6	0.1	4.8	11.7	11.7
49.8	4.6	66.4	0.5	4.1	12.3	12.3
66.0	3.4	67.7	0.25	3.1	11.5	11.5
81.0	3.1	68.5	0	3.4	11.9	11.9

GC Results, Experiment 2

Time	O_2	N_2	CH_4	CO	CO_2	H_2O
(min)	vol (%)	vol (%)	vol (%)	vol (%)	vol (%)	vol (%)
10.3	6.7	66.0	0.3	2.8	12.0	12.0
24.0	6.3	62.4	0.8	4.5	14.5	14.5
36.3	4.4	62.0	0.7	4.7	14.6	14.6
49.0	4.9	64.2	0.6	4.5	12.6	12.6
65.1	5.2	66.9	0.6	4.4	12.1	12.1

GC Results, Experiment 3

Time	O_2	N_2	CH_4	CO	CO_2	H_2O
(min)	vol (%)	vol (%)	vol (%)	vol (%)	vol (%)	vol (%)
12.0	3.4	64.1	0.7	4.6	13.6	13.6
24.2	2.0	66.8	0.3	3.2	13.8	13.8
36.4	5.3	62.9	0.8	4.6	13.5	13.5
51.2	4.4	67.6	0	1.8	13.7	13.7
66.9	4.8	67.6	0	1.7	14.2	14.2

GC Results, Experiment 4

Time	O_2	N_2	CH_4	CO	CO_2	H_2O
(min)	vol (%)	vol (%)	vol (%)	vol (%)	vol (%)	vol (%)
11.0	9.6	71.2	0.3	2.5	-	-

GC Results, Experiment 5

Time	**O_2**	**N_2**	**CH_4**	**CO**	**CO_2**	**H_2O**
(min)	vol (%)	vol (%)	vol (%)	vol (%)	vol (%)	vol (%)
10.3	0.6	55.4	1.0	5.6	16.7	16.7
18.5	11.6	61.9	0.6	2.9	11.2	11.2
25.1	0.9	59.6	1.0	3.4	16.6	16.6
31.8	0.9	60.2	1.0	4.0	16.8	16.8

GC Results, Experiment 6

Time	**O_2**	**N_2**	**CH_4**	**CO**	**CO_2**	**H_2O**
(min)	vol (%)	vol (%)	vol (%)	vol (%)	vol (%)	vol (%)
11.0	1.7	60.4	0.6	4.8	14.6	14.6
18.3	5.6	63.3	0.7	3.0	15.1	15.1
27.0	3.6	65.0	1.0	2.0	13.1	13.1

GC Results, Experiment 7

Time	**O_2**	**N_2**	**CH_4**	**CO**	**CO_2**	**H_2O**
(min)	vol (%)	vol (%)	vol (%)	vol (%)	vol (%)	vol (%)
11.1	0.4	60.0	0.4	2.7	16.4	16.4
18.4	6.2	63.2	0.5	3,3	13.6	13.6
29.0	3.8	68.0	0.9	1.7	12.4	12.4

GC Results, Experiment 8

Time	**O_2**	**N_2**	**CH_4**	**CO**	**CO_2**	**H_2O**
(min)	vol (%)	vol (%)	vol (%)	vol (%)	vol (%)	vol (%)
11.0	0.6	55.9	0.7	4.5	15.7	15.7
19.0	7.2	62.5	0.6	2.8	12.8	12.8

GC Results, Experiment 9

Time	**O_2**	**N_2**	**CH_4**	**CO**	**CO_2**	**H_2O**
(min)	vol (%)	vol (%)	vol (%)	vol (%)	vol (%)	vol (%)
13.0	9.9	66.5	0.1	0.9	10.5	10.5
16.3	10.0	65.0	0.5	2.4	10.3	10.3
21.1	9.6	70.0	0.2	0.6	10.2	10.2

GC Results, Experiment 10

Time	**O_2**	**N_2**	**CH_4**	**CO**	**CO_2**	**H_2O**
(min)	vol (%)	vol (%)	vol (%)	vol (%)	vol (%)	vol (%)
11.4	1.7	62.0	0.6	4.4	14.3	14.3
16.5	1.3	63.0	0.13	1.6	16.3	16.3
21.2	11.2	59.4	0.16	1.4	13.6	13.6
24.1	14.8	64.0	0.14	1.3	8.7	8.7
32.0	14.3	66.3	0.48	2.5	6.6	6.6
36.6	13.7	68.2	0.74	3.2	6.5	6.5

GC Readings, Experiment 11

Time	**O_2**	**N_2**	**CH_4**	**CO**	**CO_2**	**H_2O**
(min)	vol (%)	vol (%)	vol (%)	vol (%)	vol (%)	vol (%)
12.2	0.5	58.8	0.41	2.9	16.3	16.3
16.9	3.4	58.6	0.2	2.2	13.4	13.4
31.1	9.7	57.3	0.84	3.6	8.7	8.7

Appendix B. Limiting Condition for a Crib Fire

B1. Burning Regimes of the 4 and 8 kg Cribs.

B1. Burning Regimes of the 4 and 8 kg cribs.

The following spreadsheet was used to calculate whether a 8 kg crib will have a fuel controlled burning rate or a porosity controlled burning rate.

Fuel Surface Controlled $$\dot{m} = \frac{4}{D} m_o v_p \left(1 - \frac{2 v_p t}{D}\right)$$ Eqn. 4, SFPE 3-6

Crib Porosity Controlled $$\dot{m} = 0.0004 \left(\frac{S}{h_c}\right)\left(\frac{m}{D}\right)$$ Eqn. 5 SFPE 3-6

V_p	$0.0000022(D)^{-0.6}$	Fuel surface regression velocity, Table 3-1.3, SFPE 3-4.
m_o		Initial mass of the crib, kg
S		Stick spacing, m
h_c		Crib height, m
D		Stick thickness, m

Physical Dimensions

Density of particle board is 675 kg/m^3

Crib	
Width	0.3 m
Height	0.3 m
Length	0.3 m

Sticks	
Width	0.018 m
Height	0.018 m
Stick Spacing	0.018 m

Number of sticks	
wide	8.8
High	16.7
Total	147

Crib mass 9.7 kg

$\mathbf{m_{fuel}}$ 0.05260 kg/s

$\mathbf{m_{porosity}}$ 0.01417 kg/s

The smallest value of two burning rates dictates the burning regime.

A 8 kg crib will have its burning limited by ventilation.

The following spreadsheet was used to calculate whether a 4 kg crib will have a fuel controlled burning rate or a porosity controlled burning rate.

Fuel Surface Controlled $$\dot{m} = \frac{4}{D} m_o v_p \left(1 - \frac{2 v_p t}{D}\right)$$ Eqn. 4, SFPE 3-6

Crib Porosity Controlled $$\dot{m} = 0.0004 \left(\frac{S}{h_c}\right)\left(\frac{m}{D}\right)$$ Eqn. 5 SFPE 3-6

V_p	$0.0000022(D)^{-0.6}$	Fuel surface regression velocity, Table 3-1.3, SFPE 3-4.
m_o		Initial mass of the crib, kg
S		Stick spacing, m
h_c		Crib height, m
D		Stick thickness, m

Physical Dimensions

Density of particle board is 675 kg/m^3

Crib	
Width	0.3 m
Height	0.15 m
Length	0.3 m

Sticks	
Width	0.018 m
Height	0.018 m
Stick Spacing	0.018 m

Number of sticks	
wide	8.8
High	8.3
Total	74

Crib mass 4.8 kg

A 300 x 300 $\dot{m}_{fuel}$ 0.02630 kg/s

$\dot{m}_{porosity}$ 0.01417 kg/s

The smallest value of two burning rates dictates the burning regime.

A 4 kg crib will have its burning limited by ventilation.

FIRE ENGINEERING RESEARCH REPORTS

95/1	Full Residential Scale Backdraft	I B Bolliger
95/2	A Study of Full Scale Room Fire Experiments	P A Enright
95/3	Design of Load-bearing Light Steel Frame Walls for Fire Resistance	J T Gerlich
95/4	Full Scale Limited Ventilation Fire Experiments	D J Millar
95/5	An Analysis of Domestic Sprinkler Systems for Use in New Zealand	F Rahmanian
96/1	The Influence of Non-Uniform Electric Fields on Combustion Processes	M A Belsham
96/2	Mixing in Fire Induced Doorway Flows	J M Clements
96/3	Fire Design of Single Storey Industrial Buildings	B W Cosgrove
96/4	Modelling Smoke Flow Using Computational Fluid Dynamics	T N Kardos
96/5	Under-Ventilated Compartment Fires - A Precursor to Smoke Explosions	A R Parkes
96/6	An Investigation of the Effects of Sprinklers on Compartment Fires	M W Radford
97/1	Sprinkler Trade Off Clauses in the Approved Documents	G J Barnes
97/2	Risk Ranking of Buildings for Life Safety	J W Boyes
97/3	Improving the Waking Effectiveness of Fire Alarms in Residential Areas	T Grace
97/4	Study of Evacuation Movement through Different Building Components	P Holmberg
97/5	Domestic Fire Hazard in New Zealand	KDJ Irwin
97/6	An Appraisal of Existing Room-Corner Fire Models	D C Robertson
97/7	Fire Resistance of Light Timber Framed Walls and Floors	G C Thomas
97/8	Uncertainty Analysis of Zone Fire Models	A M Walker
97/9	New Zealand Building Regulations Five Years Later	T M Pastore
98/1	The Impact of Post-Earthquake Fire on the Built Urban Environment	R Botting
98/2	Full Scale Testing of Fire Suppression Agents on Unshielded Fires	M J Dunn
98/3	Full Scale Testing of Fire Suppression Agents on Shielded Fires	N Gravestock
98/4	Predicting Ignition Time Under Transient Heat Flux Using Results from Constant Flux Experiments	A Henderson
98/5	Comparison Studies of Zone and CFD Fire Simulations	A Lovatt
98/6	Bench Scale Testing of Light Timber Frame Walls	P Olsson
98/7	Exploratory Salt Water Experiments of Balcony Spill Plume Using Laser Induced Fluorescence Technique	E Y Yii
99/1	Fire Safety and Security in Schools	R A Carter
99/2	A Review of the Building Separation Requirements of the New Zealand Building Code Acceptable Solutions	J M Clarke
99/3	Effect of Safety Factors in Timed Human Egress Simulations	K M Crawford
99/4	Fire Response of HVAC Systems in Multistorey Buildings: An Examination of the NZBC Acceptable Solutions	M Dixon
99/5	The Effectiveness of the Domestic Smoke Alarm Signal	C Duncan

99/6	Post-flashover Design Fires	R Feasey
99/7	An Analysis of Furniture Heat Release Rates by the Nordtest	J Firestone
99/8	Design for Escape from Fire	I J Garrett
99/9	Class A Foam Water Sprinkler Systems	D B Hipkins
99/10	Review of the New Zealand Standard for Concrete Structures (NZS 3101) for High Strength and Lightweight Concrete Exposed to Fire	M J Inwood
99/11	Simple Empirical Method for Load-Bearing Light Timber Framed Walls at Elevated Temperatures	K H Liew
99/12	An Analytical Model for Vertical Flame Spread on Solids: An Initial Investigation	G A North
99/13	Should Bedroom Doors be Open or Closed While People are Sleeping? - A Probabilistic Risk Assessment	D L Palmer
99/14	Peoples Awareness of Fire	S J Rusbridge
99/15	Smoke Explosions	B J Sutherland
99/16	Reliability of Structural Fire Design	JKS Wong

School of Engineering
University of Canterbury
Private Bag 4800, Christchurch, New Zealand

Phone 643 364-2250
Fax 643 364-2758